

The University of Adelaide  
School of Agriculture, Food and Wine  
**Faculty of Sciences**



# Defining the impact of flavour interactions in protein based food matrices

A thesis submitted for the degree of Master of Philosophy

Jessica Sanderson  
August, 2016



## Table of Contents

Abstract.....	iii
Declaration.....	v
Acknowledgements.....	vi
List of Abbreviations.....	vii
List of Figures.....	viii
List of Tables.....	x
Chapter 1 Introduction and literature review.....	1
1.1 Food flavour.....	1
1.2 Flavour perception.....	2
1.3 Volatile release from food matrices.....	4
1.4 Flavour-ingredient interactions.....	6
1.4.1 Flavour-protein interactions.....	8
1.5 Methods for measuring flavour interactions.....	10
1.5.1 Instrumental analysis.....	10
1.5.2 Direct sampling.....	13
1.5.3 Descriptive sensory analysis techniques.....	14
1.6 Summary and thesis objectives.....	15
Chapter 2 Development of methodology to quantify interactions between flavour volatiles and meat proteins.....	17
2.1 Protein extraction and quantitation.....	17
2.1.1 Phosphate buffer preparation.....	18
2.1.2 Preparation of pork muscle homogenate.....	19
2.1.3 Extraction of myofibrillar protein.....	20
2.1.4 Quantitation of homogenate using BCA assay.....	23
2.2 Instrumental analysis of flavour-protein interactions.....	29
2.2.1 Volatile selection.....	30
2.2.2 Development of SHA-GCMS methodology for volatile analyses.....	32
2.2.3 Application of PRV techniques to measure flavour interactions.....	41
2.3 Optimised methods summary.....	51
2.3.1 Myofibrillar protein extraction and quantitation from pork muscle.....	51
2.3.2 Static headspace analysis of flavour compounds using GCMS.....	51
2.3.3 Calculation of partition coefficients using GCFID with the PRV method.....	52
Chapter 3 Measuring the impact of myofibrillar proteins on volatile partitioning using the PRV method.....	53
3.1 Preface.....	53
Chapter 4 Conclusions and future directions.....	91

4.1 Conclusion .....	91
4.2 Future directions .....	93
Appendices .....	95
Appendix 1 Optimised GCMS instrument configuration .....	96
Appendix 2 Preliminary PRV study using hexanal .....	102
Appendix 3 PRV calculation summary for hexanal.....	103
Appendix 4 Reduction in peak areas post MSD maintenance .....	104
References.....	107

## Abstract

Flavour is widely accepted as a major determinant of consumer satisfaction, so factors that influence flavour quality are of great interest to both food scientists and the manufacturing industry globally. Volatile organic compounds (VOC) play an important role in characterising the unique flavour profile of foods. However non-volatile matrix solutes are capable of selectively binding these compounds and modifying their availability for perception during consumption.

The impact of carbohydrates and lipids has been extensively studied which has led to a comprehensive understanding of the principles governing their interaction with flavour volatiles. Proteins, in comparison, remain poorly understood. This is due mainly to their structural diversity and resulting range of available binding mechanisms which can change in response to environmental conditions such as those encountered during food processing.

Myofibrillar proteins are compositionally significant components of skeletal muscle tissue and play a critical role in defining the textural properties of processed meat products including burgers and sausages. To determine their influence on flavour, a series of model solutions were analysed and partition coefficients  $K_{g-m}$  calculated to enable changes in compound volatility to be measured.

Eleven different flavour volatiles were evaluated, including a number of plant derived bioactive compounds not previously considered in binding studies. Partition coefficients were measured using static headspace-gas chromatography (SH-GC) methods partnered with indirect phase ratio variation (PRV) techniques. The retention effect of myofibrillar proteins was quantified by reporting the percentage change in  $K_{g-m}$  following the introduction of protein extract into the system.

Myofibrillar proteins were obtained from a series of extractions of pork loin fillet with sodium phosphate buffer. The process yielded 58.6 mg/g of muscle which accounted for an approximate recovery rate of 60% of total available proteins. Subsequent instrumental analysis confirmed that at 35°C, a 2 mg/mL protein extract was capable of binding all volatile compounds, to various degrees, reducing their volatility, or headspace concentration, and therefore the availability of each compound for sensory perception.

The greatest effect was recorded for isomers citral and neral, with 55.9% and 59.1% retention reported respectively, followed by ethyl hexanoate which gave 36.7% retention. Thymol and carvacrol followed closely, with 28.6% and 33.7% retention respectively. Data collected

throughout the study strongly indicates that myofibrillar proteins interact predominantly via weak reversible associations that are enhanced with increasing levels of flavour compound hydrophobicity.

Both SH-GC and PRV are commonly utilised in flavour interaction investigations and are known to have areas of limitation that must be considered throughout application. During instrumental method development however, a significant obstacle was encountered which had not been documented previously. After considerable method development, it was concluded that mass spectrometer (MS) detectors are not suitable for use in PRV trials due to the repeated injection of headspace water vapour into the system. This damaged MS components and limited the ionisation of analytes required for their detection.

## Declaration

I certify that this work contains no material which has been accepted for the award of any other degree or diploma in my name, in any university or other tertiary institution and, to the best of my knowledge and belief, contains no material previously published or written by another person, except where due reference has been made in the text. In addition, I certify that no part of this work will, in the future, be used in a submission in my name, for any other degree or diploma in any university or other tertiary institution without the prior approval of the University of Adelaide and where applicable, any partner institution responsible for the joint-award of this degree.

I give consent to this copy of my thesis when deposited in the University Library, being made available for loan and photocopying, subject to the provisions of the Copyright Act 1968.

The author acknowledges that copyright of published works contained within this thesis resides with the copyright holder(s) of those works.

I also give permission for the digital version of my thesis to be made available on the web, via the University's digital research repository, the Library Search and also through web search engines, unless permission has been granted by the University to restrict access for a period of time.

Signed: .....

Date: .....

## Acknowledgements

I wish to sincerely thank my principal supervisor Assoc Prof Kerry Wilkinson for all her encouragement, guidance and support throughout the duration of my Masters studies. I would also like to acknowledge the tremendous amount of direction and technical input provided by my co-supervisor Dr Heather Smyth in the field of instrumental flavour analysis, and co-supervisor Dr Yasmina Sultanbawa for her expertise in meat science and protein extraction methodology.

A special thank you as well to my former colleague Steve Fuller who showed enormous generosity with his time and efforts in providing hands-on technical assistance throughout the development, and application, of static headspace techniques within the Queensland Department of Agriculture and Fisheries' flavour chemistry laboratories.

Finally my greatest gratitude is extended to my family and friends for their enduring love, encouragement and support which was fundamental in enabling me to undertake further studies.

## List of Abbreviations

%R	percent retention
A	chromatographic peak area
BCA	bicinchoninic acid assay
BSA	bovine serum albumin
$C_g$	gas phase concentration
$C_m$	matrix concentration
$C_o$	initial matrix concentration
$C_p$	product concentration
$f_i$	proportional factor
FID	flame ionisation detector
GC	gas chromatography
GCMS	gas chromatography mass spectrometry
K	partition coefficient
$K_{g-m}$	gas-matrix partition coefficient
$K_{matrix}$	gas-matrix coefficient
$K_{water}$	gas-water coefficient
MS/MDS	mass spectrometer detector
PRV	phase ratio variation
SHA	static headspace analysis
SH-GC	static headspace gas chromatography
$V_g$	gas phase volume
VOC	volatile organic compound
$V_s$	solution/matrix volume
$\beta$	vial phase ratio

## List of Figures

Figure 1.1	Main stages and factors influencing flavour perception.....	3
Figure 1.2	Flavour release in vivo and subsequent transport to the receptors in the nose and mouth.....	4
Figure 1.3	Effect of fat on equilibrium headspace distribution of flavour compounds above an aqueous solution.....	7
Figure 1.4	Techniques used for (a) static and (b) dynamic headspace analysis.....	11
Figure 2.1	Separation of muscle homogenate using a phosphate buffer.....	21
Figure 2.2	Removal of insoluble connective tissue by screening.....	21
Figure 2.3	Overview of process for the extraction myofibrillar proteins.....	23
Figure 2.4	Overview of the two-step bicinchoninic acid assay.....	24
Figure 2.5	Colour development of BSA standards and samples, indicative of protein concentration (6 replicates for each preparation).....	26
Figure 2.6	Standard curve for bovine serum albumin (20 – 20,000 $\mu\text{L}/\text{mL}$ ) showing absorbance of 5%, 10% and 20% (left to right) sample preparations used to interpolate protein concentration (n= 6 replicates).....	28
Figure 2.7	Headspace vial configuration for static headspace gas chromatography.....	33
Figure 2.8	Evolution of headspace graphs at 35°C showing improved results when comparing peak areas from (a) the initial trial with (b) those obtained following modified sample preparation techniques to limit volatile loss during vial filling.....	38
Figure 2.9	Reproducibility of optimised SHA-GCMS method for use in partitioning trials for measuring $K_{g-m}$ .....	40
Figure 2.10	Influence of sample volume in vial on headspace concentration depicting saturation at higher levels of filling.....	43
Figure 2.11	Average peak areas of PRV replicates showing magnitude decreases with successive trials.....	45
Figure 2.12	Ethyl hexanote peak from chromatogram showing strong agreement between triplicate samples but a continuous reduction in recorded areas for successive PRV replicates which equated to large variations in calculated partition coefficients.....	46
Figure 2.13	Chromatographic overlay and graphical representation of PRV data confirmed that stable peak areas were obtained using GC-FID instrumentation.....	49

Figure 2.14	Effect of reducing limonene $\beta$ values to address the known limitations of applying PRV methodology to highly volatile compounds.....	50
Figure 1.	Graphical comparison of PRV calculations used to verify that eucalyptol displayed the properties of an ideal solution when evaluated individually (a) within a water matrix and (b) in a composite solution at 35°C, and that the conditions of linearity were met.....	82
Figure 2.	Relationship between increasing vial volume and resulting peak area for hexanal, with the chosen $\beta$ values illustrating the plateau effect at higher volumes where the headspace concentration eventually becomes independent of matrix volume.....	83
Figure 3.	Effect of working solution temperature during the filling of headspace vials on the peak areas obtained for anethole in replicate PRV trials.....	84
Figure 4.	Retention of aroma compounds by a phosphate buffer containing 0.5 M NaCl salt as compared to water at 35°C.....	85
Figure 5.	Retention of aroma compounds by myofibrillar protein at 2 mg/mL in solution as compared to a phosphate buffer control containing salt at 35°C.....	86
Figure 6.	Comparison of measured $K_{g-m}$ values between all matrices.....	87

## List of Tables

Table 1.1	Examples of different model food systems used in flavour interaction studies.....	5
Table 2.1	Experimental data used to construct a standard curve and generate a regression equation for the calculation of sample protein concentration.....	27
Table 2.2	Physicochemical properties and grouping of volatile flavour compounds selected for protein interaction studies.....	31
Table 2.3	SHA-GC retention times and selected MS ions for SIM acquisition and quantitation.....	37
Table 1.	Physicochemical properties and attributes of flavour volatiles.....	88
Table 2.	PRV calculations used to determine the partition coefficient (K) of thymol, hexanal and ethyl hexanoate in water at 35°C.....	89
Table 3.	Gas-matrix partition coefficients ( $K_{g-m} \times 10^3$ ) of volatiles in different matrices at 35°C compared to published values.....	90

## Chapter 1 Introduction and literature review

Flavour is considered one of the most important factors determining the quality perception and overall acceptance of food by consumers.<sup>1</sup> It also plays a key role in the commercial success of processed or reformulated products such as those reduced in fat or salt.<sup>2</sup> As a result, understanding the mechanisms of flavour perception and factors affecting appreciation is of great interest to the food industry; in particular the influence of ingredient interactions and the physical structure of food on flavour release.

The food matrix performs a critical function in controlling flavour release at each step of food preparation and consumption.<sup>3</sup> Thus many methods have been developed to study the physicochemical interactions between volatile aroma compounds and other non-volatile food constituents.<sup>4,5</sup> These techniques have been applied to compositionally diverse model food systems to elucidate matrix effects on the release of an extensive range of volatiles belonging to different chemical classes with varied physical properties (e.g. volatility and solubility). Effects are typically identified, quantified and compared using the thermodynamic and kinetic parameters that govern flavour partitioning and release.

The following chapter summarises the fundamental principles of food matrix-flavour interactions with a particular emphasis on the role that proteins play as major components of many food products. It also details the methods adopted by food scientists to study flavour interactions and measure the subsequent impact on flavour release, delivery and perception by consumers.

### 1.1 Food flavour

Foods are compositionally diverse systems composed of volatile and non-volatile components. Non-volatile components such as carbohydrates, proteins and lipids account for the bulk of the matrix, while volatile compounds are present at significantly lower levels.<sup>6</sup> Components from both classes contribute to flavour perception during consumption, but differ in the way in which they stimulate the human sensory system. The volatility of flavour active compounds determines the mechanism by which they are detected.

Volatile compounds are responsible for aroma perceived by the olfactory system, while non-volatiles are detected in the mouth as taste and contribute to mouthfeel.<sup>4</sup> The sum of these two stimuli is perceived as flavour, although aroma is considered to be the more important element

because of its function in characterising flavour profiles.<sup>7</sup> In addition, volatile compounds are more amenable to instrumental analysis (e.g. by gas chromatography-mass spectrometry) and consequently are the focal point of modern methods for flavour analysis.<sup>8</sup>

The aroma component of flavour is due to a complex mixture of volatile organic compounds representing a range of organic chemical classes including aldehydes, ketones, esters and alcohols.<sup>9</sup> These volatiles exhibit a range of physical and chemical properties that combined are referred to as physicochemical characteristics.

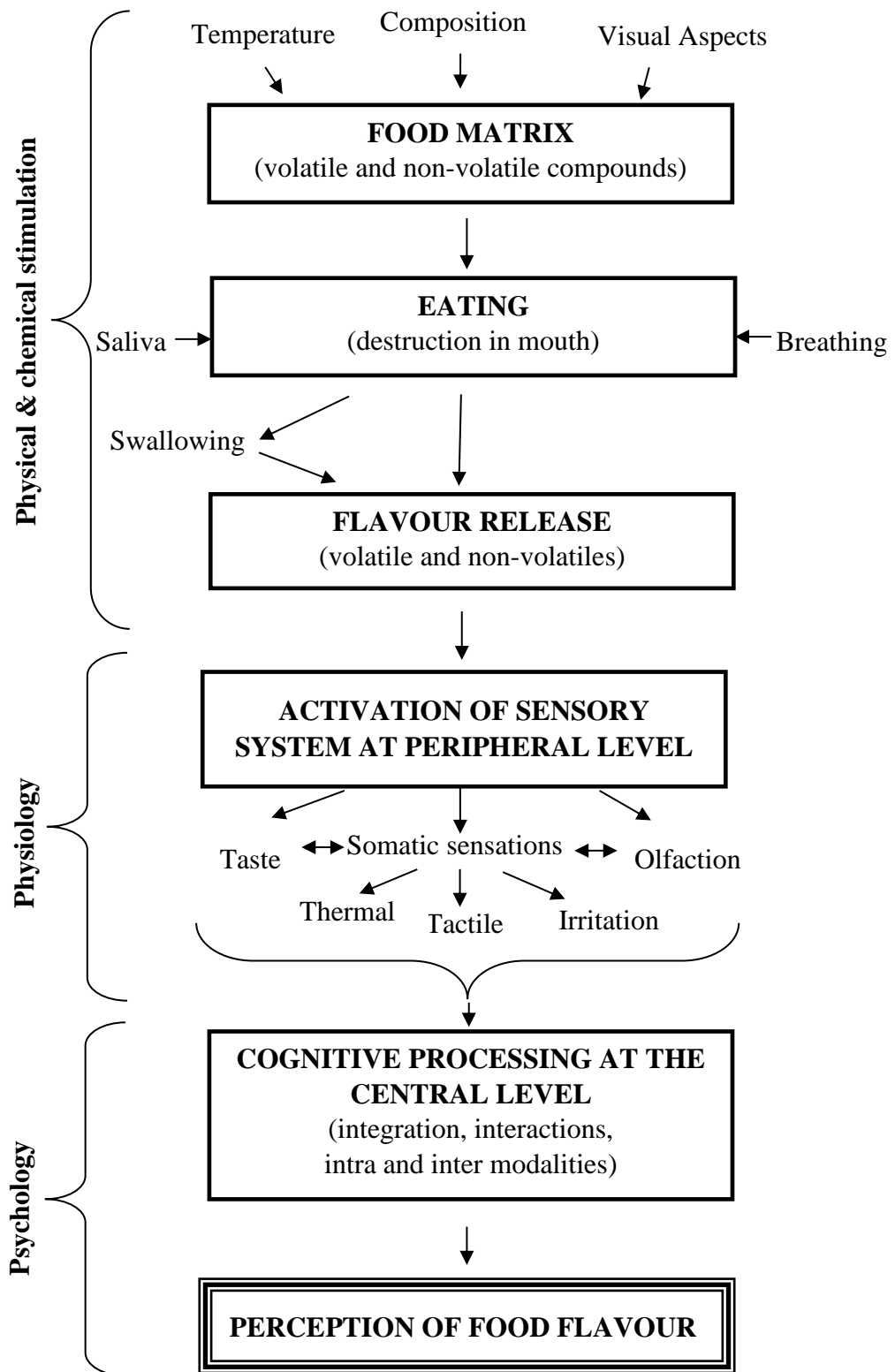
Foods differ in the number and nature of volatile aroma compounds present. For example, 'strawberry' is derived from approximately 350 different volatile constituents,<sup>10</sup> whereas the more complex aromas such as 'chocolate' may comprise up to 1,000 constituents.<sup>11</sup> In all cases, however, only a limited number are considered to be flavour active and critical for characterisation of the unique aroma of a food.<sup>12</sup>

Flavour represents a major component of organoleptic quality and its perception is understood to play a significant role in consumer appreciation and acceptability of food. Perception is heavily influenced by three factors: the ratio of volatile to non-volatile components in the food matrix; the availability and release of these components to the sensory systems; and the mechanisms of perception.<sup>13</sup>

## 1.2 Flavour perception

Sensory assessment of flavour is a complex and dynamic process involving multiple modalities. Flavour perception has been defined as the sensation arising from the integration or interplay of signals produced as a consequence of sensing smell, taste and irritation stimuli from a food or beverage.<sup>14</sup> Physical and chemical interactions with the food matrix together with physiological, cognitive and psychological aspects all influence perceived flavour quality of foods (Figure 1.1). Although flavour perception is a multimodal phenomenon, aroma and taste are considered to play prominent roles.<sup>15</sup>

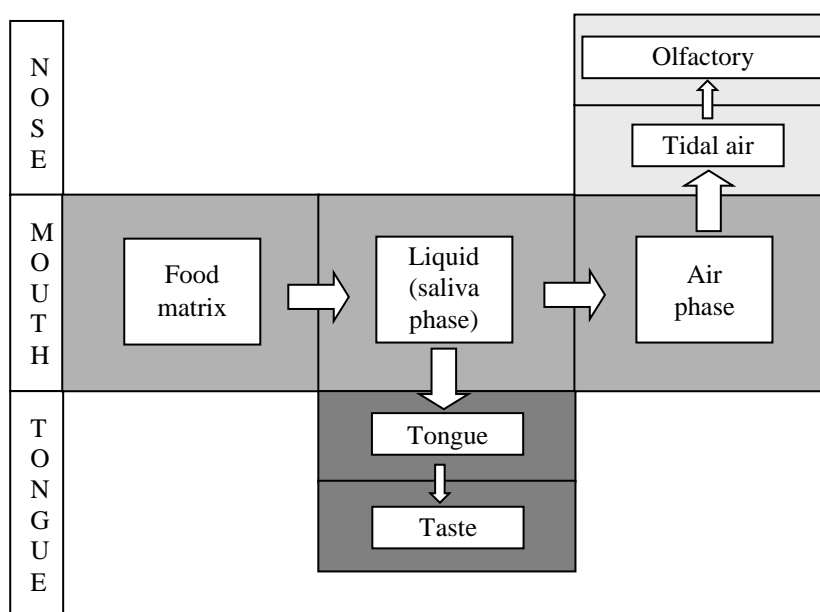
During consumption of foods, a variety of chemical stimuli are released and come into contact with receptor cells in the nose and mouth cavities.<sup>4</sup> Non-volatile constituents are detected on the tongue and limited to sensations of sweetness, sourness, saltiness, bitterness and umami.<sup>17</sup> In contrast, volatile compounds generate a much broader range of sensations and create unique aroma profiles recognised for individual foods.



Source: adapted from (Salles, 2006)<sup>15</sup> and (Keast et al., 2004)<sup>16</sup>

**Figure 1.1 The main stages and factors influencing flavour perception**

On release in the mouth, volatiles travel via the retronasal passage to the olfactory epithelium, where odour reception is mediated by receptor cells connected to the olfactory bulb in the brain.<sup>13</sup> Volatiles can also be delivered via the nose (orthonasally) by inhalation prior to ingestion when food is smelled or as food is placed in the mouth. An overview of flavour release is shown in Figure 1.2.



Source: (Taylor, 2002)<sup>18</sup>

**Figure 1.2 Flavour release in vivo and subsequent transport to the receptors in the nose and mouth**

In order to stimulate the olfactory system and elicit aroma recognition, sufficiently high concentrations of flavour molecules must be released from the food matrix and transported to the receptors. Flavour delivery depends on the availability of compounds in the gas phase and therefore the affinity of the flavour compounds for the food matrix.<sup>17</sup> Such interactions are governed predominantly by the physicochemical properties of the volatiles and the nature of the food matrix in terms of composition and structural arrangement.<sup>19</sup>

### 1.3 Volatile release from food matrices

Interactions impacting volatile release can occur on a number of levels. The importance of physical and chemical interactions between food matrix components have long been established, and as a consequence have been studied in a range of model food systems since the late 1970s<sup>20</sup> (Table 1.1). In many of these investigations, instrumental methods were adopted

to first identify physicochemical interactions, after which sensory techniques assessed the impact of modified release on perceived taste,<sup>21</sup> flavour intensity<sup>22</sup> or profile.<sup>23</sup>

**Table 1.1 Examples of different model food systems used in flavour interaction studies**

Model food system	Matrix component/s studied	Aroma compounds studied	Reference
cheese	fat	blue cheese flavour (diacetyl, ethyl hexanoate, heptan-2-one)	24
	fat and protein	ethyl hexanoate, 3-octanone, 2-nonanone, 2-heptanone	25
custard	fat	commercial strawberry flavour	26
	fat and starch	commercial strawberry flavour	27
yoghurt	starch, pectin, locust bean gum	15 key strawberry flavour compounds	28
	fat	13 key strawberry flavour compounds	29
water-based beverage	sugar and acid	citrus flavour (limonene and citral)	22
dairy dessert	starch, carrageenan	commercial strawberry flavour	30
sausage	fat	10 compounds of varying hydrophobicity	31

Flavour-matrix interactions can be attractive or repulsive in nature. Attraction involves the fixation of volatiles on food components reducing the extent of release whereas repulsive interactions increase the concentration in the vapour phase above the food surface.<sup>17</sup> The determination of relevant thermodynamic and kinetic parameters such as gas/matrix partition coefficients ( $K_{g-m}$ ), and diffusion or mass transfer coefficients are used by researchers to express the impact of both product composition and structure on aroma mobility.<sup>32</sup>

Methods for measuring interactions between aroma compounds and other food constituents are based on their physicochemical properties.<sup>33</sup> Historically, many studies have been carried out using simple binary (water-aroma) or ternary (water-solute-aroma) systems at low viscosity. Solutes are chosen due to their inherent status as major food matrix components of functional importance (e.g. nutritional or technical qualities), and in most cases are carbohydrate, protein or lipid ingredients. Commercial flavours or tailored laboratory blends containing multiple volatile compounds are then added as the aroma fraction.

Preliminary experimentation studying single compounds of varying individual physicochemical properties are often conducted to gain fundamental insight into the effect of molecular size, functional group, geometric shape and/or volatility on binding interactions. This is particularly important as selective interactions that alter the characteristic balance of key

volatile compounds in food flavours have been reported to considerably modify overall flavour profiles.<sup>34</sup>

Complete foods, however, are typically complex multi-phasic systems and the effects of structure and texture on flavour must also be taken into account. Articles published in the late 1990s<sup>5,35</sup> and early 2000s<sup>2,36</sup> criticised the focus on simple liquid systems and resulting lack of commercially relevant information pertaining to 'real foods'. This catalysed a shift in experimental approach and publication of a review outlining the effects of texture and microstructure on flavour release and retention.<sup>33</sup>

As a consequence, researchers began including more complete model foods into their studies, to take into account differences in structural arrangement and phase organisation, in addition to composition. An example is reported by Guth and Rusu<sup>3</sup> who used static headspace methods to investigate the release of lactones, esters and alcohols in both a series of model emulsions and prepared custards. By adopting this approach, they were able to determine how texture and composition affected volatile partitioning individually, as well as their overall effects, in a real food system.

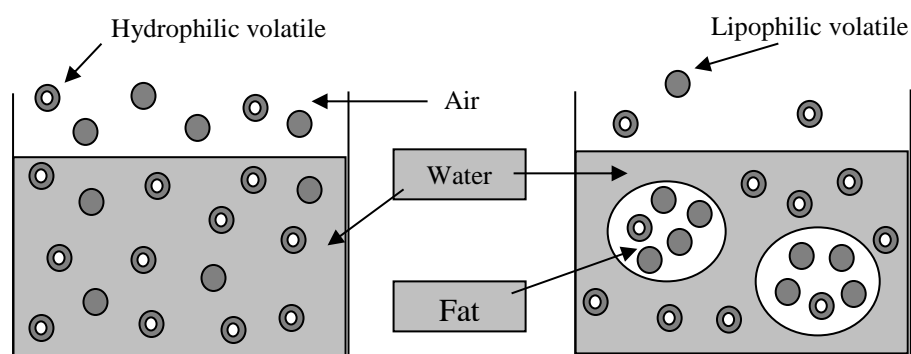
#### 1.4 Flavour-ingredient interactions

Matrix components control volatile release through chemical (irreversible) and physicochemical (reversible) binding as well as by creating physical barriers that limit aroma movement.<sup>11</sup> Chemical fixation is achieved via covalent bonding, while physicochemical binding may involve Van der Waals forces, hydrogen bonding, hydrophobic interactions and/or ionic bonding.<sup>17</sup>

The type and extent of interactions are determined by both the nature of volatile compounds and the matrix composition. Among the major food components, lipids, carbohydrates and proteins are known to bind flavours and in general, their presence reduces the volatility of an aroma compound, relative to its volatility in pure water.<sup>5</sup> Each component uses different mechanisms, so the overall effect in multi-component foods is the net balance of individual food constituents upon each flavour molecule.

Lipid ingredients have the greatest influence on aroma partitioning between the food and atmosphere phases when compared to that of other major food constituents of carbohydrate or protein origin. For example, the addition of 0.5% miglyol (triglyceride of caprylic and capric acids) to water results in a greater volatility decrease of 2-nonanone, compared with the addition of 3% of the protein  $\beta$ -lactoglobulin.<sup>37</sup> This significant retention effect has been demonstrated

repeatedly and is explained by the hydrophobic interaction mechanism by which lipids modify partitioning (Figure 1.3). Quite simply, most aroma compounds are non-polar and so thermodynamic partition coefficients dictate that they will be associated with the lipid phase at equilibrium.



Source: (Reineccius, 2006)<sup>11</sup>

**Figure 1.3 Effect of fat on equilibrium headspace distribution of flavour compounds above an aqueous solution**

Even small changes in lipid content have been shown to induce significant effects on the vapour pressure of hydrophobic flavour compounds.<sup>2</sup> This particular phenomenon, partnered with increasing consumer pressure for healthier low-fat foods, has established lipid-aroma interactions as the most thoroughly investigated area in matrix studies.

Carbohydrates have also been a focus for researchers because of their status as major food components and extensive application as texture modifying agents. Ranging from simple sugars to complex polysaccharides, carbohydrate ingredients such as starches and hydrocolloid gums (e.g. xanthan and gelatin) are capable of modifying aroma volatility using a wider range of mechanisms than lipids.<sup>11</sup> Any interactions are ultimately dependant on carbohydrate size, structure and side chains but can include both chemical binding and the creation of physical barriers to mass transfer within the food system due to viscosity increase.<sup>38</sup>

In general, complex carbohydrates reduce aroma volatility due to increased viscosity and the formation of inclusion complexes based on hydrophobic associations.<sup>11</sup> Simple sugars in contrast can have varied effects as observed by Friel and colleagues,<sup>39</sup> who studied the release of 40 aroma volatiles from aqueous sucrose solutions. This selective release and retention is explained as resulting from different interaction mechanisms that are made possible by the

varied physicochemical properties of individual volatile aroma compounds, together with the ranging sucrose concentrations.

Despite some of the earliest research into flavour interactions involving plant proteins, with the aim of limiting the development of off flavours and occurrence of taints,<sup>11,20</sup> research into the role of protein in flavour release in a broader sense, lags far behind that undertaken for lipids and carbohydrates. Current trends towards low-fat, low-carbohydrate diets, together with an increasing dependence on protein derived ingredients of functional importance in food processing has generated a renewed interest in understanding how proteins influence flavour.

#### 1.4.1 Flavour-protein interactions

Protein ingredients are widely used in food processing for their functional properties, which include emulsification, gelation and stabilisation of lipid dispersed food systems. Although their direct flavour contribution is minimal, their influence on flavour perception is considerable, due to their ability to bind and trap aroma compounds.<sup>40</sup>

A diverse range of binding mechanisms can occur between proteins and volatiles because of the extensive range of chemical structures available for interaction (e.g. amino acid side chains, terminal ends and hydrophobic pockets). Additionally, their use as texturising agents influences aroma release through increased resistance to mass transfer as demonstrated in model gelatin systems.<sup>41,42</sup> Flavour-protein interactions are highly specific and largely dependent on the three dimensional (3D) structure, which ultimately determines the availability of binding sites.

Protein 3D structure is a function of pH, temperature and ionic strength, and as such, aroma binding is modified by the addition of ingredients that alter these environmental conditions. Processing operations that cause proteins to change from their native state to a denatured state will also modify aroma binding.<sup>43</sup> Denaturation tends to increase aroma interactions, as the resulting structure is more open, with greater accessibility to potential binding sites.<sup>11</sup>

Protein-aroma interactions occur via weak, reversible physical adsorption mechanisms (Van der Waals or hydrophobic interactions) as well as stronger ionic effects and irreversible covalent bonding.<sup>44</sup> Although covalent bonding, such as that between aldehydes and the amino (NH<sub>2</sub>) and thiol (SH) functional groups of proteins are possible, in most cases interactions take place via reversible hydrophobic and hydrogen bonding.<sup>45</sup> Flavour retention is dependent on the type and amount of protein with the degree of interaction commonly expressed and compared in terms of gas-matrix partitioning ( $K_{g-m}$ ), binding ( $K_a$ ), or global affinity constants

(nK<sub>a</sub>). The partitioning coefficient is also described as the air-product partition coefficient, in some cases with related changes to the abbreviation.

Lactoglobulin, albumin, casein and soy based ingredients have all been studied in terms of their interaction with flavour components. Of these, the globular milk protein  $\beta$ -lactoglobulin is the most extensively investigated; primarily due to its status as the most well characterised whey protein and the important functional role it performs as a food emulsifier.<sup>46</sup> Limited research has been conducted on the influence of other animal proteins and their derivatives, particularly those from muscle tissue, on volatile release. In such cases, available information is largely restricted to pork proteins where the effects of different salts,<sup>47</sup> and protein conformation<sup>48</sup> on volatile binding with different extracts, has been published.

Sarcoplasmic, myofibrillar and stromal proteins constitute the main proteins in skeletal muscle.<sup>49</sup> Actin and myosin together represent approximately 63% of myofibrillar proteins and combine during muscle contraction to form the complex actomyosin.<sup>48</sup> Actomyosin is a much larger and more structurally complex protein than the thoroughly investigated  $\beta$ -lactoglobulin, which consists of only 162 amino acid residues and has a molecular weight (MW) of 18.4 kilodaltons (kDa).<sup>43</sup>

Myosin, in comparison is a highly asymmetrical protein, approximately 520 kDa in size, which consists of two globular heads and a double  $\alpha$ -helical tail. Each molecule is comprised of two 220 kDa heavy chains and two pairs of light chains, with the amino acid sequence and MW of the light chains varying between 15 and 22 kDa, depending on muscle type and species.<sup>50</sup> Actin is relatively conserved between species with little variation observed between different sources. In skeletal muscles, actin exists as double helical filaments composed of polymerised 43kDa globular monomers.<sup>51</sup>

In addition to its important physiological role, actomyosin is valued for its functional properties in processed meat products including water holding, emulsifying capacity, binding ability and gelation.<sup>52</sup> Perez-Juan and colleagues measured the ability of porcine actomyosin to interact with a series of volatiles that contribute to the typical flavour profile of cured ham using static headspace techniques.<sup>48,52</sup> Results confirmed the protein was able to bind all compounds, although interactions were highly affected by prior freezing, as well as the concentration and configuration of the actomyosin. Retention effects were also reported in an earlier study designed to evaluate the ability of fish actomyosin to bind undesirable lipid oxidation products.<sup>53</sup> In this case, interactions were reportedly affected by salt concentration and temperature.

## 1.5 Methods for measuring flavour interactions

The binding of aroma compounds has been studied using a variety of different approaches. *In-vitro* instrumental methods<sup>54</sup> descriptive sensory techniques<sup>55</sup> and direct sampling from subjects during consumption,<sup>56</sup> have all been used to describe matrix effects on the release of endogenous and added flavours. Instrumental methods generate information on how binding occurs and affects the extent and release rates of individual aroma compounds, while sensory techniques reveal how interactions influence overall flavour perception. The direct sampling of volatiles released during consumption has allowed simultaneous chemical and sensory analysis to correlate modifications in aroma release with changes in flavour perception.<sup>42</sup>

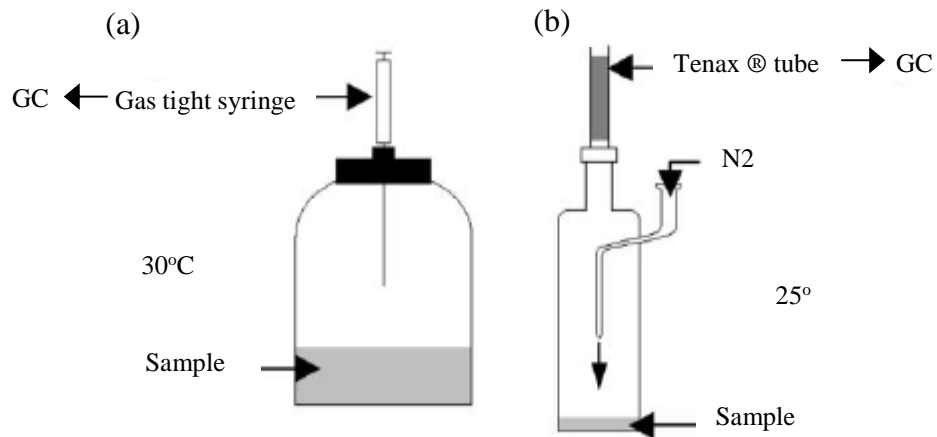
Each of the above approaches has been optimised for protein studies, and successfully used to obtain information on how individual proteins<sup>46</sup> as well as manufacturing grade protein-based ingredients,<sup>56</sup> affect food flavour.

### 1.5.1 Instrumental analysis

Most instrumental methods for measuring flavour reactions are chromatography based and are designed to determine changes in flavour release as opposed to retention. More recently, spectroscopic techniques have been developed to describe the nature of interactions in terms of their specific mechanism and physical location, however examples of this approach remain limited.

Flavour release is influenced by both thermodynamic and kinetic mechanisms, and consequently, methods for quantifying the impact of protein-aroma interactions are based on these two phenomena. Thermodynamic factors determine the volatile partitioning between food and air phases while kinetic factors influence the rate at which equilibrium is achieved.<sup>33</sup> Voilley and co-workers<sup>57</sup> explained these factors as 1) the driving force to move materials and 2) the resistance to their flow. They are typically measured using either static conditions or dynamic headspace sampling (Figure 1.4), coupled with chromatographic methods.

The measurement of thermodynamic factors dominates protein research and is most commonly conducted using static headspace analysis (SHA) partnered with gas chromatography-mass spectrometry (GCMS) techniques.



Source: (Juteau, 2004)<sup>19</sup>

**Figure 1.4 Techniques used for (a) static and (b) dynamic headspace analysis**

It is based on the principle that volatiles will distribute themselves within a food system between the product and headspace, depending on interactions with individual matrix components until a state of thermodynamic equilibrium is reached.<sup>17</sup> That is, until there is no effective net transfer at the product-headspace interface.<sup>33</sup> The resulting compound volatility is described using the gas-matrix partition coefficient  $K_{g-m}$  which is also referred to as the distribution coefficient or Henry's constant. It is expressed as the ratio between the concentration of a volatile organic compound in the gas phase and in the product phase under equilibrium conditions.<sup>58</sup> For example the volatility of compound  $i$  at a given temperature would be calculated according to Eq. 1, where  $K_{g-m}$  is the gas-matrix partition coefficient,  $C_g^i$  is the gas phase concentration and  $C_m^i$  is the concentration in the matrix or product.

$$K_{g-m} = \frac{C_g^i}{C_m^i} \quad [1]$$

Two important factors must be considered in relation to calculated  $K_{g-m}$  values: (1) partition coefficients are temperature dependant, and (2) Henry's law, which states that at equilibrium the air concentration is proportional to the concentration in the product phase,<sup>59</sup> only holds under a restricted range of conditions; i.e. compounds must be at infinite dilution behaving as an ideal solution and remain unimolecular, showing no tendency to dissociate or associate in solution.<sup>17</sup>

In static headspace analysis, a sample is placed in a closed vessel and thermostated (i.e. held at a constant temperature) until equilibrium is achieved, before an aliquot of the vessel's headspace is sampled for analysis.<sup>60</sup> Traditionally, static methods utilise a direct approach to calculating  $K_{g-m}$  values, where the measurement of aroma compound concentration in each phase is performed once equilibrium conditions are reached, using an external standard which is both time consuming and incorporates potential sources of error.<sup>61</sup>

Consequently, the emergence of indirect SHA methods which require neither the external calibration of the detector or exact knowledge of the initial concentration of the volatile in the solution have become increasingly popular. The absence of a preparatory volatile extraction step and cleanliness of the headspace sample injection (which limits the frequency that cleaning and maintenance is required)<sup>62</sup> makes SHA methodology rapid and highly efficient, compared to traditional approaches.

One such method is the phase ratio variation (PRV) method, which was first described by Ettre and colleagues,<sup>63</sup> and has since been used extensively to investigate flavour interactions, in addition to being adopted for volatile research in non-food applications.<sup>64-67</sup> The method is based on the influence of sample volume on the equilibrium gas phase concentration and so relies on the relationship between  $K$  and the phase ratio  $\beta$ , which is defined as the ratio of headspace volume to sample matrix volume in a system.<sup>68</sup>

Performance of this method has been compared to other static headspace methods of vapour phase calibration and liquid calibration static headspace and found to be the most accurate in addition to the simplest to perform.<sup>69</sup> Moreover, PRV can be applied to mixtures of compounds in complex matrices and the precision is related to the volume of sample in the vial.<sup>68,70</sup> Typically, in PRV analyses an automated headspace sampler is coupled to a gas chromatograph equipped with a suitable detector. Strict control of vial conditions (e.g. sample composition, phase ratios and temperature), headspace sampling methodology and of course chromatography are considered essential for the successful application of PRV theory.

The volatility of aromas in water is a popular reference in quantifying the extent to which proteins modify partitioning. Percentage retention (% retention), is defined as the relative difference in the gas-matrix coefficient of an aroma compound in the presence of a solute with that measured in water. Retention is calculated using Eq. 2, where  $K_{g-m}$  and  $K_{g-w}$  are the gas-product and gas-water coefficients respectively.<sup>71</sup>

$$\% \text{ Retention} = \left( 1 - \left( \frac{K_{g-m}}{K_{g-w}} \right) \right) \times 100 \quad [2]$$

It is important to note however that instrumental results are not always reliable indicators of flavour perception in protein systems. Although methyl ketones were shown to be significantly retained by milk proteins by GCMS based headspace analysis, investigations using direct sampling following real-time aroma release indicated no retention effect. It is therefore hypothesised that reversibly bound compounds are able to be released in the mouth during consumption with flavour perception only affected by strong or irreversible covalent bonding.<sup>45</sup>

### 1.5.2 Direct sampling

Although conventional headspace techniques are well suited for studying aroma-solute interactions *in-vitro*, they do not take into account the numerous changes in the mouth that can affect volatile delivery to the olfactory epithelium and therefore, their subsequent perception.<sup>72</sup> To address this, researchers at the University of Nottingham devised specialised equipment and instrumental methods to sample volatiles directly from the nose or mouth space of consumers during consumption.<sup>8</sup> These methods are collectively known as direct sampling techniques and provide information on real time aroma release. More importantly, they enable the influence of human physiology on aroma release from different matrices to be determined.<sup>73</sup>

Direct sampling introduces analytes directly into a mass spectrometer without prior separation. For this reason, atmospheric pressure chemical ionisation (APCI) and proton transfer reaction (PTR) instrumentation (which is capable of ionising compounds in the presence of water vapour at atmospheric pressure) are used.<sup>74</sup> APCI and PTR also exhibit the high degree of sensitivity (as low as 10 µg/kg for most compounds) and rapid response times that are essential for breath-by-breath detection.<sup>73</sup> A significant limitation of this technique is quantitative identification, as samples are resolved entirely by mass, representing a major issue for compounds like terpenes, which share common ion masses, but impart distinctly different aromas.<sup>74</sup>

Although somewhat limited in protein studies, the technique has been used successfully to measure the release of 2-nonanone from milk protein solutions<sup>56</sup> and to confirm a correlation between time-release and time-intensity curves generated for gelatine gels by instrumental and sensory analysis, respectively.<sup>42</sup> To date there is no record of direct sampling being used to investigate volatile release from muscle derived proteins.

### 1.5.3 Descriptive sensory analysis techniques

Headspace analysis of volatile release during consumption does not truly represent the impact of matrix binding on flavour perception; the ultimate objective of interaction research from a consumer and commercial point of view. Hence sensory techniques that measure flavour perception after signals from flavour sensors have been processed by the brain are used to provide complimentary information to that acquired from instrumental analysis.

Descriptive sensory techniques and trained panels are used for this purpose. Panels are composed of individuals trained to detect qualitative and quantitative changes in foods and provide an objective assessment of product aroma characteristics.<sup>4</sup> Depending on the project aims and chosen methodology, this may involve rating the intensity of individual aromas in protein containing mixtures, against a series of reference solutions<sup>46</sup> or quantifying the deviation of multiple flavour attributes in a single sample from a control. This latter approach indicates how the characteristic flavour profile is altered and so is used for complex model food systems like milk or yoghurt that are flavoured with a number of aroma compounds.<sup>23, 75</sup> In this method, key sensory attributes are first selected by preliminary gas chromatography-olfactometry analysis and/or discussion with the sensory panel. The intensity of each attribute in a treated sample (i.e. a matrix with altered ingredients or structure) is then rated on a line scale anchored with 'slight', 'moderate' and 'intense' at 0%, 50% and 100% of the scale respectively, with a control reference identified as 'moderate' on the line scale. Deviation is then quantified as the distance marked from the 'moderate' midpoint.<sup>55</sup>

Because flavour perception is a dynamic process, time-intensity (TI) methods are also used to track how sensory characteristics change over a period of time. Results are graphically represented as a curve showing how overall flavour intensity rises and falls during consumption.<sup>76</sup> Using these curves, Guinard and Marty compared the flavour released from gelatin to starch and carrageenan gels at three different gel strengths.<sup>77</sup> By calculating the maximum perceived intensity ( $I_{\max}$ ) and total duration of flavour, they concluded that at comparable gel strengths, release from the gelatin matrix was similar to starch and greater than carrageenan. A decrease in  $I_{\max}$  with increasing firmness of gelatin gels indicated that in addition to the gelling agent, flavour release was affected by gel texture.

## 1.6 Summary and thesis objectives

The desire to understand how food matrices impact flavour has driven interaction studies since the 1970s, with the majority of published research concentrating on how carbohydrate, lipid and protein derivatives influence aroma release individually. Increasing industry interest in formulating foods that optimise both nutritional quality and flavour, has seen growth in more applied research using manufacturing grade ingredients and commercially representative, complete model food systems.

Although proteins perform many important functional roles in processed foods, applied research into their influence on flavour is limited. Furthermore, published information on the more fundamental aspects of protein-aroma interactions are largely focused on milk and soy proteins. Only a relatively small amount of elemental data concerning other proteins, particularly those present in skeletal muscle tissue, which represent compositionally significant components in processed meat products, is available.

To address this shortage of information, the following research project was designed to gain insight into the role of myofibrillar proteins, as the most abundant class and functionally important group, in flavour release from model systems. The study aims to generate fundamental information on the interaction between this important muscle fraction and a range of volatile aroma compounds with varying physicochemical properties. This included a number of novel compounds with demonstrated levels of bioactivity that identifies them as potential functional food ingredients with the capacity to extend shelf life, in addition to improving flavour.

The project consisted of two main phases. It began with a method development phase, involving laboratory methods being identified, optimised for available equipment and validated for both the extraction of myofibrillar proteins from pork muscle tissue and the subsequent SHA-GCMS analysis of matrices containing this material. Once finalised, techniques were then applied in an experimental phase to generate appropriate volumes of representative material for the preparation of carefully formulated model solutions for headspace analysis. Calculating partition coefficients using the indirect PRV method enabled the confirmation and quantitation of flavour interactions at a molecular level by tracking changes in compound volatility in the presence of added protein.

Currently the role of skeletal muscle proteins in flavour release from processed meat products is poorly understood. Such meat products are highly valued by consumers and retailers alike and are defined as any post-mortem muscle that has gone through major physical or chemical

alteration.<sup>78</sup> Along with functional ingredients such as phosphates, salts (sodium chloride, citrate, lactate) and hydrocolloids, which are added during manufacturing to restore or modify textural qualities of the muscle fibres,<sup>79</sup> flavouring agents are commonly introduced to improve the sensory experience for consumers and to create profitable value added product formats. Often in the case of sausages and meat patties, this is done by adding seasoning blends containing a number of herbs, spices or extracts thereof.

The research outcomes reported in this thesis provide fundamental insight into the role of skeletal muscle proteins on the functionality of volatile ingredients, and are of interest to both the scientific community and the food manufacturing industry, globally. In addition, the methods developed and experimental approach represent a solid basis on which to plan subsequent studies, involving more complex model solutions, alternative flavour compounds or multiphasic systems that would be considered more representative of real foods.

Confirming changes in volatile partitioning resulting from protein binding would also support the design of complimentary sensory studies that would determine the impact of any identified interactions on flavour perception or quality during consumption; this being the ultimate objective of any research contributing to the understanding of flavour interactions in foods.

## Chapter 2 Development of methodology to quantify interactions between flavour volatiles and meat proteins

Flavour is a critical part of the consumer enjoyment of processed and formulated foods. To date, considerable research has been conducted to understand how lipids and carbohydrate interact with flavour components in a food matrix. Comparatively, there is little scientific knowledge available on how protein, another major food component, affects the binding and release of flavour in food systems. The objective of the present research study was to explore, at a molecular level, how meat protein in a model food matrix interacts and binds with a selection of commercially important volatile flavour compounds. To achieve this goal it was necessary to first develop and validate a robust experimental methodology that could accurately measure the concentration of free and bound flavour components in a sample.

A number of different experimental methodologies were required in order to undertake the evaluation of flavour binding by meat proteins. First, a protein extraction and quantitation process was needed to obtain appropriate material for use in model solutions. Secondly, an optimised method for analysis and measurement of the chosen flavour compounds was required. For this, a method utilising static headspace gas analysis (SHA) techniques and gas chromatography mass spectrometry (GCMS) was developed. Finally, a method for data analysis and a calculation of bound versus free volatile components in a given sample was needed. The phase ratio variation method (PRV) approach was selected for this purpose, whereby partition coefficients of volatiles under defined conditions could be calculated and used to establish concentrations of bound versus free compound.

The following chapter aims to summarise the steps taken to develop the required methods as well as outline the key considerations that were addressed during the process. In addition, each section will document any major challenges that were encountered during this method development phase and detail the troubleshooting activities that were undertaken to resolve such issues.

### 2.1 Protein extraction and quantitation

Whilst a large proportion of dairy protein binding studies purchase their matrix solutes as manufacturing quality ingredients<sup>21, 29, 55, 56</sup> or analytical grade reagents of high purity,<sup>46, 80, 81</sup> the majority of meat protein studies obtain their solutes from the extraction of targeted components using muscle tissue from various animal species.

This separation of muscle constituents in food related studies is usually carried out to isolate the myofibrillar protein actomyosin, or its individual components, due to the important nutritional and functional roles they play in processed meat products.<sup>82</sup> Extraction is typically achieved using variations on a salt buffer method, the fundamentals of which have been described in detail by Perez-Juan et al.<sup>83</sup>

For the purpose of this study the entire class of myofibrillar proteins were selected for evaluation. Myofibrillar proteins are compositionally the most abundant group of proteins and are composed primarily of the complexed actomyosin.<sup>48</sup> Porcine muscle was selected as the starting material for extraction because of the volume of published research available using this particular species, and the potential industry significance of results due to the suitability of pork ingredients for the manufacture of structured meat products such as patties, burgers and sausages. These formats are usually composed of between 60 – 100% meat<sup>84</sup> making any functional qualities of muscle components of interest to manufacturers.

### 2.1.1 Phosphate buffer preparation

The first step in the extraction process was the preparation of two separate buffers. By definition buffers are aqueous systems that resist changes in pH when small amounts of acid or base are added, and are composed of a weak acid (proton donor) and its conjugate base (proton acceptor). Phosphate buffers and bicarbonate systems are the most extensively used mediums in biochemical research such as protein studies, and ultimately serve to provide conformational stability that in turn is related to structure dependant functionality.<sup>85</sup>

In this case, phosphate buffers were chosen for use in the initial protein extraction sequence and following myofibrillar homogenate preparations. Two litres of 50 mM solution was required for each extraction and was made using a combination of sodium phosphate dibasic heptahydrate (DSP) ( $\text{Na}_2\text{HPO}_4 \cdot 7\text{H}_2\text{O}$ , MW: 268.07) and sodium phosphate monobasic monohydrate (MSP) ( $\text{NaH}_2\text{PO}_4 \cdot \text{H}_2\text{O}$ , MW: 137.99), both of which were obtained from Sigma Aldrich (Australia). An initial quantity of 21.71 g DSP was added to approximately 1.8 L of ambient distilled water with agitation and allowed to dissolve completely before 2.62 g MSP was introduced. Once solubilised, 0.39 g of sodium azide ( $\text{NaN}_3$ , MW: 65.00) was added as a preservative. This particular compound is highly water soluble with bacteriostatic properties and so is commonly utilised in preparation of laboratory reagents, especially those containing proteins, to prevent bacterial contamination.<sup>86</sup> Care was taken to limit the dose rate to 0.03 M

(equivalent to 0.195%), i.e. a level at which it is considered not to interfere with protein binding.<sup>87</sup>

Throughout the buffer preparation process, an electrode was used to track changes in solution pH and to identify when stability was achieved and final pH adjustment was possible. The adjustment was carried out using a 4 M sodium hydroxide (NaOH, MW: 39.99) solution which was added drop-wise, allowing for equilibration to occur between each addition until a stable reading of pH 7.5 was attained. At this stage the solution was adjusted to the final volume of 2 L with distilled water before pH was again verified prior to storage at 4°C.

A variation of this buffer with added salt was also prepared for use during the final protein extraction phase. The process outlined above was repeated but with the addition of 58.44 g sodium chloride (NaCl, MW: 58.44) once the NaN<sub>3</sub> had dissolved completely, to give a final concentration of 0.5 M. 500 mL of the prepared salt buffer was sufficient for each extraction.

Both buffers were stored under refrigerated ( $\leq 5^{\circ}\text{C}$ ) conditions overnight to ensure solutions were sufficiently chilled in preparation for the protein extraction process, during which it is essential that temperatures remain low to prevent protein degradation. Temperature control is an important consideration for minimising thermal damage to proteins during the separation process, which would otherwise have implications for structure, and consequently, functionality during subsequent interaction trials. Although it is important to note that any rise in temperature will increase the rate of protein denaturation, it is the maintenance of conditions less than 32 °C which is critical, as this is the point at which myofibrillar proteins start to unfold. Further increases are followed by protein-protein associations in the region of 36–40 °C and gelation can occur at 45–50°C, when concentrations exceed 0.5%.<sup>88</sup>

### 2.1.2 Preparation of pork muscle homogenate

Retail quality post-rigor pork loin fillet (*Longissimus dorsi*) was purchased from a supermarket in Brisbane, Australia, and stored chilled (4°C) for no longer than 24 hours prior to use. This preliminary activity served to generate an appropriate input for the following extraction step and took place immediately prior to commencing extraction of myofibrillar protein.

Preparation began with mincing of the muscle tissue which was undertaken in a refrigerated laboratory. The fillet was first trimmed of any visible connective tissue or fat before it was cut into portions and fed through a pre-cooled mechanical grinder fitted with a 3 mm plate.

The ground pork was collected and weighed (30 g) into a 300 mL tall-form beaker with 200 g of cold 50 mM phosphate buffer at pH 7.5. To keep the solution cool throughout the blending process, the overhead mixer was placed over a tub of ice in which the beaker was secured. An Ika Ultra Turrax T25 homogeniser (Germany) fitted with a 12 mm shaft attachment was used for homogenisation, with 35 seconds at speed mark 5 determined adequate treatment for obtaining a sufficiently blended product. To avoid aeration, which can be particularly problematic when working with proteins, the shaft was placed far enough below the surface to ensure that no vortex effect resulted that would pull air into the solution. The duration of blending was deliberately kept to a minimum to prevent an increase in temperature.

The resulting muscle homogenate was weighed and divided equally into eight 50 mL falcon tubes in preparation for centrifugation.

### 2.1.3 Extraction of myofibrillar protein

The methodology of myofibrillar protein extraction using phosphate buffers and centrifugation is based on the different solubility characteristics that are found between the three major protein groups in muscle tissue. Sarcoplasmic proteins are soluble in water or dilute salt solutions, whereas the target myofibrillar proteins are soluble only in concentrated salt solutions; connective tissue proteins, including collagen and elastin, are largely insoluble in aqueous solutions.<sup>49</sup> As a result of these varying qualities, the extraction or purification process comprises two parts, each with different objectives. The initial step consists of a series of “washes” that remove the sarcoplasmic proteins from the homogenate, whilst the second step recovers the myofibrillar proteins from the remaining muscle components, and converts them into a soluble form suitable for quantitation, and the subsequent binding studies.

To begin the extraction process, the prepared muscle homogenate samples (described in section 1.1.2) were centrifuged at 4500 g and 4°C for 15 min (Eppendorf 5810R). This resulted in the formation of two distinct fractions (Figure 2.1) with the sarcoplasmic proteins located in the supernatant, whilst the pellet contained the myofibrillar and connective tissue proteins.

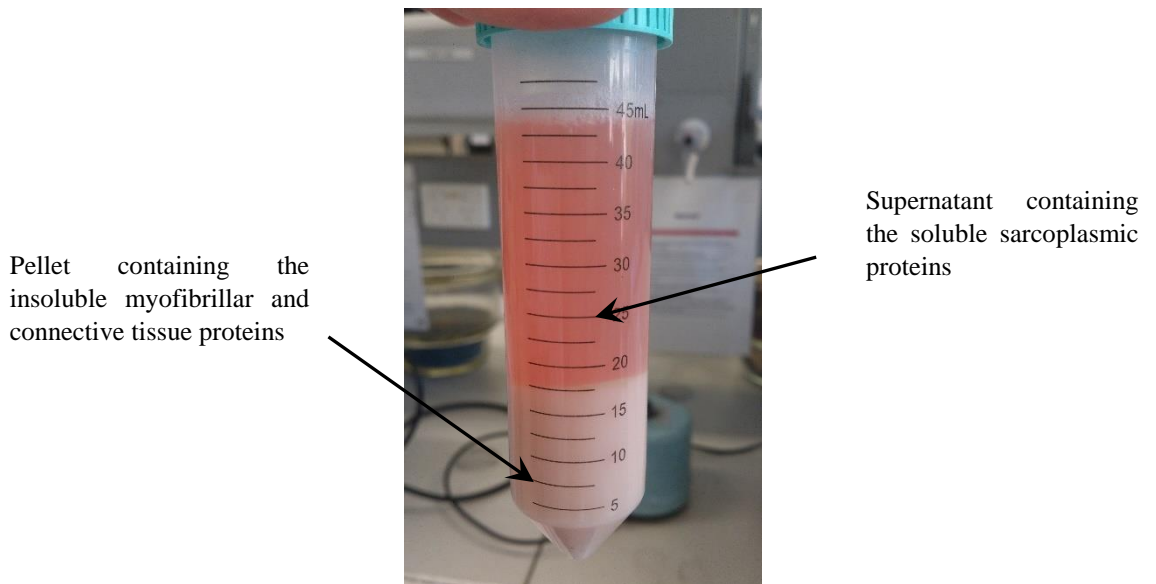


**Figure 2.1 Separation of muscle homogenate using a phosphate buffer**

The supernatant was discarded and each tube refilled with fresh, cold 50 mM phosphate buffer (4°C) to a total weight of 45 g, before being vortexed to redistribute the pellet. Centrifugation was then repeated at 4500 g and 4°C for 15 min. Again, the supernatant was discarded and the pellet redistributed, however following this the homogenate was passed through a screen to remove the coarser connective tissue components (Figure 2.2). After being redistributed equally into new tubes and centrifuged to repeat the prior cycles, the process was carried out one final time to achieve a total of 4 preliminary washing steps.



**Figure 2.2 Removal of insoluble connective tissue by screening**

The second phase of the extraction utilised the salt phosphate buffer at 0.5 M NaCl to recover the myofibrillar fraction from the pellet. The tubes were refilled with this solution once the supernatant was discarded in the previous step, vortexed and subjected to a slightly lengthier centrifugation, i.e. 4500 g at 4°C for 20 min. The supernatant was collected, as the myofibrillar protein component of the pork loin fillet.

To finish the process, yield was recorded to allow for adjustment of protein concentrate in the homogenate for consistency in the flavour interaction trials. The extraction process steps (Figure 2.3) were a modification of the method reported by Sun and coworkers<sup>89</sup> and took approximately 4 hours to complete, which enabled protein quantitation to be carried out on the same day.

From 30 g of mince an average yield of 250 g myofibrillar extract was achieved, that could be characterised as a translucent, white viscous solution with a high tendency to foam when agitated.

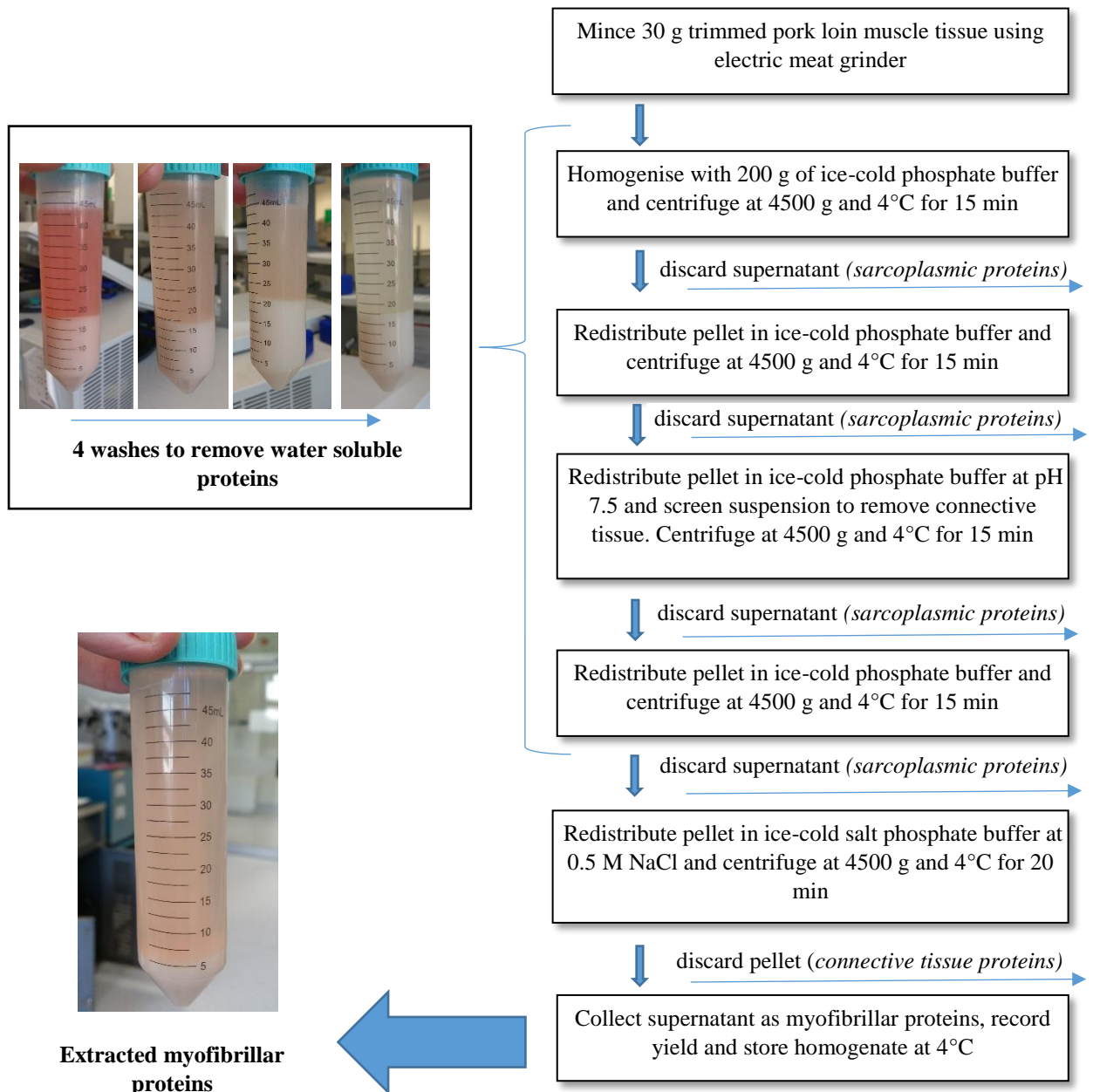


**Figure 2.3 Overview of process for the extraction of myofibrillar proteins**

#### 2.1.4 Quantitation of homogenate using BCA assay

Available colorimetric methods for protein quantitation can be divided into two groups based on their different approaches with regard to the underlying chemistry involved. They can be classified as ‘protein-dye binding’ methods (e.g. Coomassie/Bradford) or as methods that involve protein-copper chelating chemistry, such as the Lowrie and Bicinchoninic Acid (BCA) assays. The BCA method was selected as the most appropriate analytical technique for determining the myofibrillar concentration of the collected supernatant using bovine serum

albumin (BSA) as the protein standard; a common choice in general protein assay work due to its purity and availability.

Protein quantitation by way of the BCA method was first developed by Smith and colleagues<sup>90</sup> in 1985 and has since been widely adopted due to its simplicity and robustness in comparison to the other methods.<sup>91</sup> More specifically, the BCA or Smith assay has the unique advantage over other colorimetric methods because of its compatibility with samples that contain concentrations of up to 5% detergents (or surfactants) and relatively low variation in the amount of colour produced for different proteins (termed protein:protein variation).<sup>92</sup>

The chemistry underlying the selected BCA assay is a two-step process (Figure 2.4) which begins with the well-known reduction of  $\text{Cu}^{2+}$  to  $\text{Cu}^{1+}$  by protein in alkaline medium (the biuret reaction) followed by the highly sensitive and selective detection of the cuprous cation ( $\text{Cu}^{1+}$ ) by bicinchoninic acid. The chelation of copper with the protein (step 1) initially forms a blue coloured complex, before further colour development is achieved via the subsequent reaction of two molecules of BCA with each formed  $\text{Cu}^{1+}$  ion. This results in a deep purple coloured product of an intensity proportional to the number of peptide bonds present, that exhibits a strong absorbance at 562 nm with an almost linear response for increasing protein concentrations.<sup>90</sup>

Step 1.



Step 2.

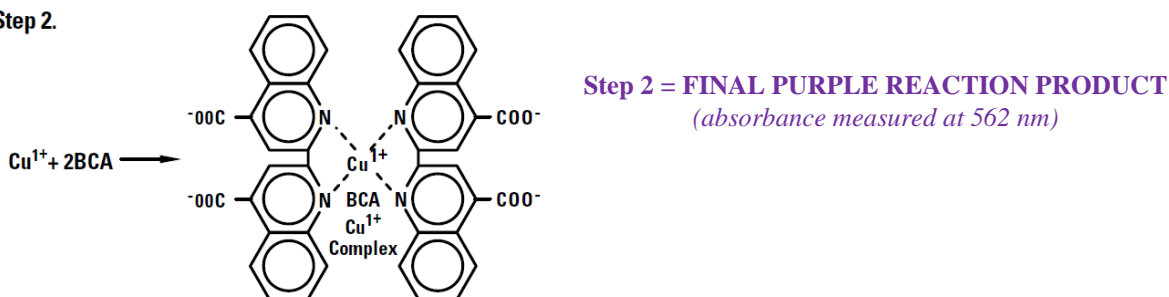


Figure 2.4 Overview of the two-step bicinchoninic acid assay

The concentration of the myofibrillar extract was determined by comparing assay results for prepared 'unknown' homogenate samples with that of a calibration curve constructed using a serial dilution of BSA standards, ranging from 20 to 20,000 µg/mL. To ensure assay results for the protein extract fell within this required working range, dilutions of 5, 10, 20, 30 and 50% were analysed. Both standards and samples were prepared simultaneously in a 96 well microplate using the necessary working reagents in the required ratios.<sup>93</sup>

Once completed, the solutions were mixed thoroughly on a plate shaker for 30 seconds before the plate was covered and incubated at 37 °C for 30 minutes, during which colour development occurred. The plate was allowed to cool to room temperature before absorbance of each well was measured at 562 nm using a spectrophotometer. A total of six replicates for each preparation was made to ensure the accuracy and precision of the assay, measures which are not only important because the test results are used to build the standard curve, but the degree of repetition also allowed the calculation of the standard deviation (STDEV) and coefficient of variation (CV) during data analysis (Table 2.1) which provided a degree of confidence in the preparatory laboratory techniques.

Where protein was present, the initial light green colour of the solution gradually changed towards a deep purple shade with increasing protein concentration. This is clearly demonstrated in Figure 2.5 by observing the variation in colour development of the dilution standards that run in descending protein concentration, and replicates of 6, down the left hand side of the plate. The row of "blank" replicates in the top row on the right shows the initial colour of the assay solutions prior to the occurrence of the previously detailed colorimetric reactions.

A visual check of the colour intensity in the series of sample dilutions in rows 2-6 below the blank wells confirms that a number of the prepared samples would fall within the range of the calibration curve generated from the assay results (Figure 2.6). Technical application notes for the BSA method emphasise both the necessity and value of constructing a standard curve each time samples are analysed, as the colour reaction has no true end point and is susceptible to variation based on incubation temperature, the types of protein present in the sample and the relative types of amino acids contained in the included proteins

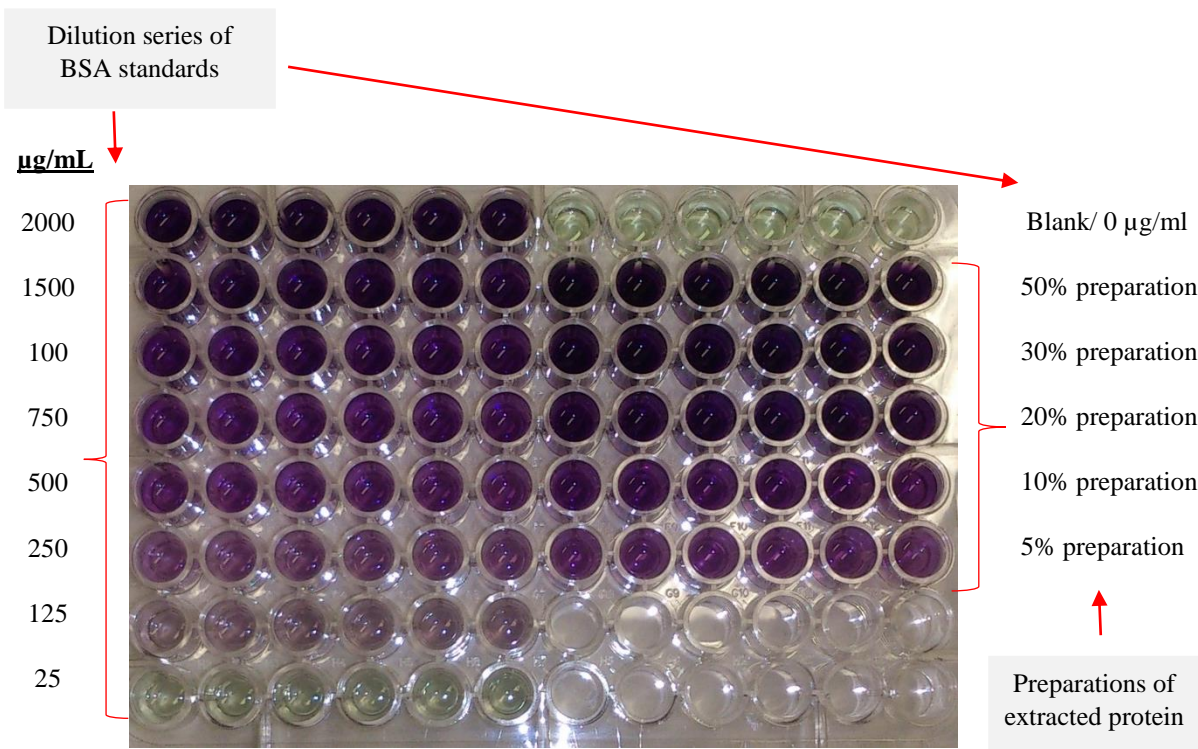


**Figure 2.5** Colour development of BSA standards and samples, indicative of protein concentration (6 replicates for each preparation)

**Table 2.1 Experimental data used to construct a standard curve and generate a regression equation for the calculation of sample protein concentration**

	Protein Concentration	Absorption at 562 nm												Mean	STDEV	CV
		Rep 1		Rep 2		Rep 3		Rep 4		Rep 5		Rep 6				
		reading	blank corrected	reading	blank corrected	reading	blank corrected	reading	blank corrected	reading	blank corrected	reading	blank corrected			
<b>Standards</b>	0	0.0943	-	0.0935	-	0.0965	-	0.0906	-	0.0871	-	0.0897	-	-	-	-
	25	0.1434	0.0491	0.1407	0.0472	0.1383	0.0418	0.1411	0.0505	0.141	0.0539	0.1343	0.0446	0.0479	0.0043	9.00%
	125	0.3161	0.2218	0.2976	0.2041	0.3042	0.2077	0.3064	0.2158	0.2908	0.2037	0.3029	0.2132	0.2111	0.0072	3.39%
	250	0.5325	0.4382	0.5123	0.4188	0.5216	0.4251	0.4877	0.3971	0.4935	0.4064	0.4933	0.4036	0.4149	0.0154	3.70%
	500	0.8708	0.7765	0.8571	0.7636	0.7808	0.6843	0.8005	0.7099	0.7778	0.6907	0.7869	0.6972	0.7204	0.0396	5.50%
	750	1.1567	1.0624	1.1624	1.0689	1.1914	1.0949	1.17	1.0794	1.1804	1.0933	1.1344	1.0447	1.0739	0.0193	1.79%
	1000	1.5562	1.4619	1.4406	1.3471	1.4997	1.4032	1.3285	1.2379	1.4737	1.3866	1.4789	1.3892	1.3710	0.0750	5.47%
	1500	2.1431	2.0488	2.018	1.9245	2.1085	2.012	2.0618	1.9712	1.9262	1.8391	2.0348	1.9451	1.9568	0.0731	3.74%
	2000	2.6156	2.5213	2.7065	2.613	2.4704	2.3739	2.6563	2.5657	2.5465	2.4594	2.6645	2.5748	2.5180	0.0880	3.50%
<b>Sample preparations</b>	<b>Concentration factor</b>	<b>reading</b>	<b>blank corrected</b>	<b>reading</b>	<b>blank corrected</b>	<b>reading</b>	<b>blank corrected</b>	<b>reading</b>	<b>blank corrected</b>	<b>reading</b>	<b>blank corrected</b>	<b>reading</b>	<b>blank corrected</b>	<b>Mean</b>	<b>STDEV</b>	<b>CV</b>
	5%	0.6582	0.5639	0.6495	0.556	0.6657	0.5692	0.6895	0.5989	0.6966	0.6095	0.6743	0.5846	0.5804	0.0210	3.61%
	10%	0.9921	0.8978	1.1007	1.0072	1.1027	1.0062	0.9835	0.8929	1.1025	1.0154	1.1082	1.0185	0.9730	0.0604	6.20%
	20%	1.8403	1.746	2.0725	1.979	1.9349	1.8384	1.9722	1.8816	1.9659	1.8788	1.8613	1.7716	1.8492	0.0843	4.56%
	30%	2.5559	2.4616	2.5997	2.5062	2.7498	2.6533	2.7827	2.6921	2.5191	2.432	2.8136	2.7239	2.5782	0.1265	4.91%
	50%	**	**	**	**	**	**	**	**	**	**	**	**	**	**	**

\*\* Colour too intense for spectrophotometric measurement

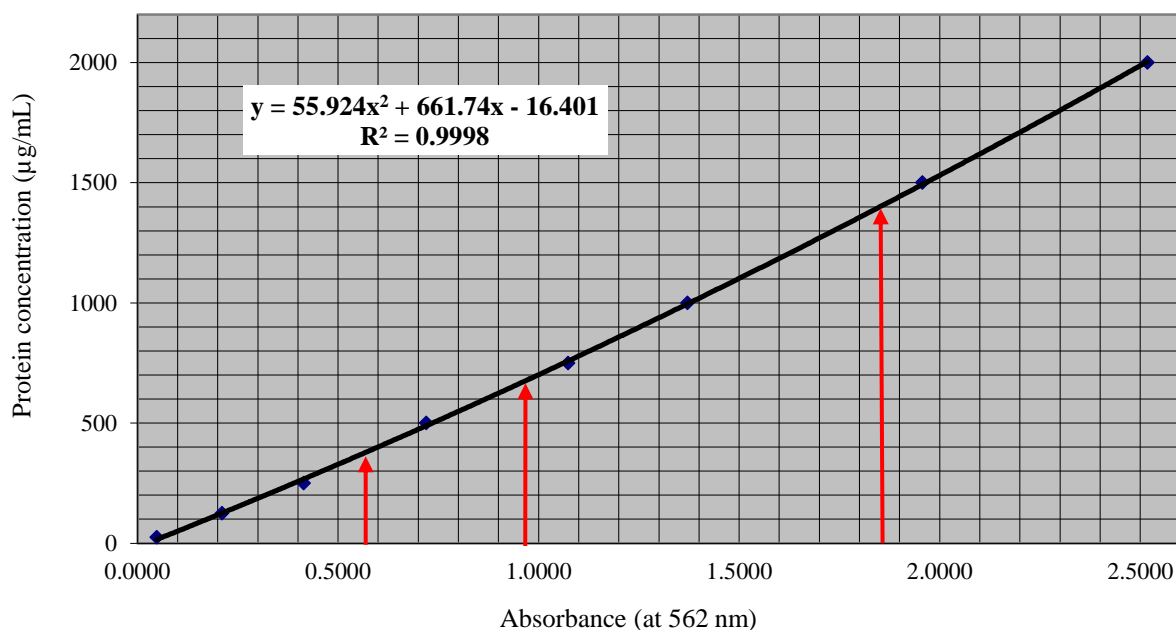


**Figure 2.6 Standard curve for bovine serum albumin (20 – 20 000 µL/mL) showing absorbance of 5%, 10% and 20% (left to right) sample preparations used to interpolate protein concentration (n=6 replicates)**

To begin calculations, the average absorbance measurement of the blank replicate was subtracted from the measurements of all other individual standard and unknown samples, before a standard curve was constructed by plotting the corrected absorbance at 562 nm for each BSA standard against its concentration in µg/mL. The absorbance values of the myofibrillar protein extract were then interpolated using the regression equation determined for the standard curve to calculate their concentrations. Although almost linear, the best fit regression line was found to be a curvilinear, second order or two-parameter polynomial that is expressed as a quadratic equation in the form  $ax^2 + bx + c = 0$ .

Care was taken at this step to select the most appropriate curve-fitting algorithm as the equation for this line that is used to calculate the protein sample concentrations based on their absorbance under identical conditions. The high correlation coefficient ( $R^2$ ) of 0.9998 in Figure 2.6 provides statistical confidence that the regression equation of  $y = 55.924x^2 + 661.74x - 16.401$  is an accurate expression of the relationship between the known protein concentration of the BSA dilution standards and their recorded absorbance.

After evaluating the absorbance figures of the prepared samples it was found that only three of the five included in the assay fell within the working range of the standards, with the 30% preparation exceeding the limit of the standard curve and 50% concentration too dark to obtain

an initial reading from the spectrophotometer. As a result, the final figure for total protein in the pork extract was reached by first determining the protein concentration (in  $\mu\text{g/mL}$ ) for each of the 5%, 10% and 20% preparations using the regression equation and substituting their absorbance reading for  $x$  to solve for  $y$ . The mean of these three readings was then calculated for a final value. The myofibrillar extract was found to contain a total protein content of  $7100 \mu\text{g/mL}$  (STDEV =  $427.22 \mu\text{g/mL}$ , CV = 6.02 %).

This concentration yield is comparable to a 2007 extraction study that aimed to optimise similar methodology for separating the main muscle proteins from pork and to subsequently characterise the recovered fractions.<sup>83</sup>

By applying the processes outlined in section 1.1 a final yield of 248 g of homogenate at  $7100 \mu\text{g/mL}$  was obtained equating to a total quantity of 1.76 g myofibrillar protein for the subsequent flavour binding studies. Based on available data regarding the total protein and relative proportion of the myofibrillar components in post-mortem muscle tissue,<sup>88</sup> this represented a recovery rate of approximately 60 % or 58.6 mg/g of meat.

Although not done in this current study, many authors who undertake preliminary myofibrillar protein extractions for further study follow quantitation with additional characterisation by measuring homogenate purity using sodium dodecyl polyacrylamide gel electrophoresis (SDS-PAGE) techniques.<sup>89, 94, 95</sup> The method separates proteins into their individual fractions and provides information about the profile of the extract. Most often authors are looking to confirm the absence of water soluble sarcoplasmic proteins and to confirm the presence of actomyosin as the most compositionally important and extensively studied muscle protein. This confirmation is achieved through the identification of high intensity bands at 200 kDa, 25 kDa, and 45 kDa mark on 7-12% resolving gels stained with silver, that correspond to the myosin heavy chain, myosin light chain and actin that make up the complexed protein post-mortem.<sup>83</sup>

## 2.2 Instrumental analysis of flavour-protein interactions

The development of an analytical approach to measure volatile binding by the extracted meat proteins, and subsequently express the magnitude of any interactions, required the optimisation of two separate but dependant methods. A static headspace analysis-gas chromatography (SHA-GC) procedure was chosen to measure the release of selected flavour compounds from model matrices whilst compound volatility and the extent of flavour binding was expressed using the gas-matrix partition coefficient ( $K_{g-m}$ ). This figure was calculated using data collected from samples prepared and analysed according to phase ratio variation techniques.

Because of the complexity involved in developing the following instrumental methods, only an overview of the process will be presented in each section in an attempt to demonstrate the logic behind each approach whilst discussing any issues within context. A detailed summary of the optimised methods applied in the final study can be found in Part 2.3.

### 2.2.1 Volatile selection

Prior to the development of any laboratory techniques a review was conducted to identify the most appropriate flavour compounds to include in the myofibrillar protein binding study. The outcome resulted in eleven different volatiles being selected, which initially can be divided into two discrete groups; those which had been studied extensively in flavour interaction studies previously and those which had not (Table 2.2). All members in this latter group were plant derived and chosen due to their significant levels of reported bioactivity in food studies,<sup>96-100</sup> which included antimicrobial and antioxidant capacity. This identified them as potential functional ingredients for processed meat products that could maximise quality and extend shelf life in addition to improve flavour.

Together the groups represented a wide range of physicochemical attributes. This is highly desirable throughout binding studies to enable the correlation of known volatile properties with protein interaction behaviour which can provide information about potential mechanisms or even locations of attraction with the molecules. Obtaining a wide range is particularly important when considering molecule hydrophobicity, or Log P, because reversible hydrophobic interactions are reported to be the most common mechanism involved in flavour retention by proteins.<sup>101</sup> The range of Log P values included for investigation extended from diacetyl (-1.34) which is hydrophilic as indicated by its negative value, to the highly hydrophobic *D*-limonene (4.83). It is expected that the higher the extent of shared hydrophobicity, the stronger the protein retention effect and reduction of headspace concentration

In addition to maximising this Log P range, inclusion of previously studied volatiles supported method development by enabling comparative or validation studies to be conducted, whilst also generating new information for these compounds to add to the field of protein binding with specific reference to those obtained from skeletal muscle tissue.

**Table 2.2 Physicochemical properties and grouping of volatile flavour compounds selected for protein interaction studies**

	Flavour Compound	CAS	Molecular Formula	Molecular Weight (g/mol)	Log P	Solubility in water (mol/L) at 20 °C*	
<b>Previously well studied flavour compounds</b>	1	Diacetyl	431-03-08	C <sub>4</sub> H <sub>6</sub> O <sub>2</sub>	86.09	-1.34 <sup>102</sup>	0.263
	2	Hexanal	66-25-1	C <sub>6</sub> H <sub>12</sub> O	100.16	1.80 <sup>102</sup>	0.022
	3	Ethyl hexanoate	123-66-0	C <sub>8</sub> H <sub>16</sub> O <sub>2</sub>	144.21	2.83 <sup>32</sup>	0.009840
	4	<i>D</i> -Limonene	5989-27-5	C <sub>10</sub> H <sub>16</sub>	136.23	4.83 <sup>102</sup>	0.00317
<b>Novel flavour compounds with bioactivity</b>	5	Eucalyptol	470-82-6	C <sub>10</sub> H <sub>18</sub> O	154.25	2.84 <sup>103</sup>	0.00215
	6	Neral	106-26-3	C <sub>10</sub> H <sub>16</sub> O	152.24	3.24 <sup>104</sup>	0.00173
	7	Geranial	141-27-5	C <sub>10</sub> H <sub>16</sub> O	152.24	3.26 <sup>104</sup>	0.00173
	8	Anethole	104-46-1	C <sub>10</sub> H <sub>12</sub> O	148.20	3.39 <sup>102</sup>	0.00117
	9	Thymol	-9-83-8	C <sub>10</sub> H <sub>14</sub> O	150.22	3.30 <sup>105</sup>	0.00261
	10	Carvacrol	499-75-2	C <sub>10</sub> H <sub>14</sub> O	150.22	3.52 <sup>106</sup>	0.00255
	11	Eugenol	95-53-0	C <sub>10</sub> H <sub>12</sub> O <sub>2</sub>	164.20	2.73 <sup>106</sup>	0.00443

\* Figures obtained from Discovery Studio Accelrys-Biovia Software

A 5000 µg/mL ethanolic standard of each compound was prepared as well as a composite solution containing all eleven volatiles at that same concentration. When combined, each volatile was considered to be at infinite dilution, which is a level at which the concentration is so low that Henry's law holds.<sup>7</sup> This is where there is a direct linear relationship between the amount of compound contained in a liquid phase or sample, and the corresponding atmosphere above. This dependant relationship is a fundamental assumption of SHA and therefore essential to satisfy during the proceeding study. Generally concentrations below 0.1 – 1% (1000 – 10,000 µg/mL) are considered adequate.<sup>60</sup>

### 2.2.2 Development of SHA-GCMS methodology for volatile analyses

Several different instrumental methods have been developed to measure partition coefficients,<sup>5</sup> however, the most frequently used approach is static headspace-gas chromatography analysis. The technique is relatively simple and so has become popular in other applications including the analysis of alcohol in blood and residual solvents in pharmaceutical products. It is also used extensively to measure monomers and polymers in plastics and fragrances in perfumes and cosmetics. In all these applications, the method overcomes the issue of complex matrices that contain non-volatile materials that can remain in GC systems and result in poor analytical performance.<sup>107</sup> SHA-GC avoids the time and cost associated with sample extraction and preparation techniques by directly sampling the volatile headspace from the container in which the sample is placed.

Although SHA-GC is known to have limitations related to quantitation and sensitivity in more traditional flavour research where targeted compounds are being measured in foods or complete profiles determined,<sup>12</sup> neither of these are of concern when determining  $K_{g-m}$  values. This is because the compound concentrations are able to be controlled as needed by the analyst and the actual amount that is present in the headspace above a sample is not necessarily quantified using standard calibration methods.

In classical SHA, the gas phase above a sample in a sealed vessel is analysed using a gas chromatograph fitted with autosampler after the system has reached thermodynamic equilibrium. In flavour binding studies, the presence of volatiles in the headspace is considered an expression of their phase partitioning and therefore affinity for the sample matrix.<sup>8</sup> Hence any modification of volatility (or partitioning) during the subsequent analysis of model matrices containing additional non-volatile components such as protein, can be attributed to a solute effect or flavour interaction. The magnitude of which is expressed by comparing the measured partition coefficients in otherwise identical conditions. Coefficients are calculated by dividing

the concentration of the compound detected in the gas phase ( $C_g^i$ ) by that measured in the sample matrix or product ( $C_p^i$ ) (Eq. 3).

$$K_{(g-m)} = \frac{C_g^i}{C_p^i} \quad [3]$$

The main objective in SHA-GC method development is to maximise the obtained peak area which is directly related to the concentration of the analyte in the headspace. In order to achieve the best performance, careful consideration is needed during both sample preparation and instrument setup. In terms of sample preparation, it is specifically the volatility of the compound being evaluated and the volume of sample in the vial that needs to be optimised. An understanding of how the partition coefficient (compound volatility) and the vial phase ratio (sample volume) relates to sample design is critical to success with this application (Figure 2.7).

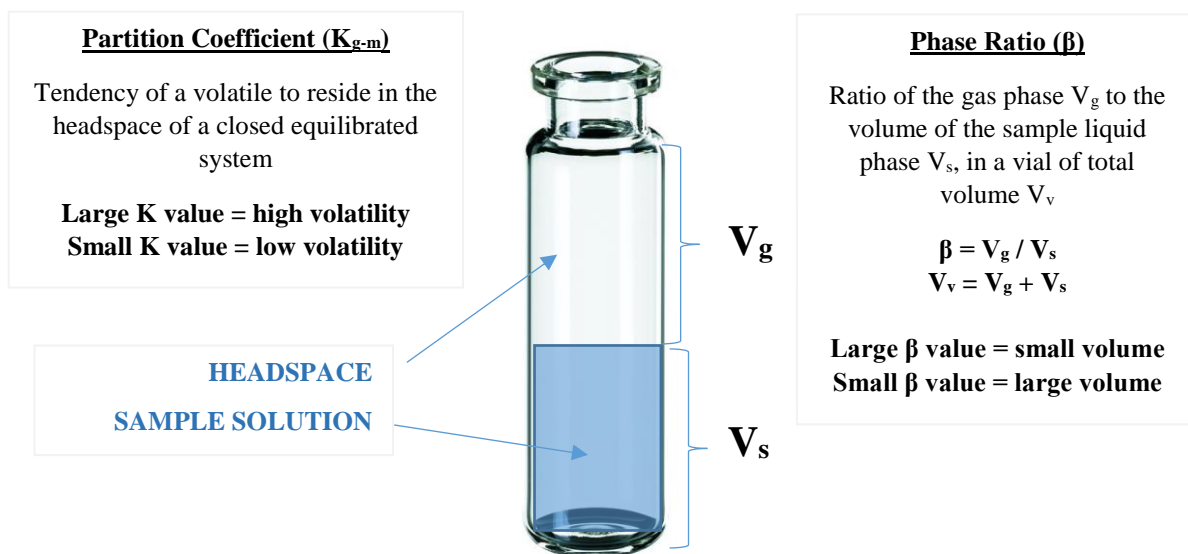


**Figure 2.7 Headspace vial configuration for static headspace gas chromatography**

This is because these two parameters work together to determine the final concentration of the volatile compound in the vial headspace; the relationship being expressed by the equation:

$$A \propto C_g = \frac{C_o}{\left(\frac{1}{K_{g-m}} + \beta\right)} \quad [4]$$

where  $A$  is the chromatographic peak area,  $C_g$  is the concentration of the volatile analyte in the gas phase,  $C_o$  is the original concentration in the sample,  $K_{g-m}$  is the gas-matrix partition coefficient and  $\beta$  is the vial phase ratio.<sup>60</sup> As such, achieving the lowest possible values for both  $K_{g-m}$  and  $\beta$  will result in higher concentrations of the volatile analytes in the gas phase and therefore better sensitivity.

Because determining the partition coefficient at a defined temperature and under otherwise controlled conditions was the aim of the current investigation, common SHA techniques such as increasing temperature, “salting out” using sodium or potassium chloride and adjusting pH<sup>108</sup> could not be used to improve headspace concentrations and therefore sensitivity. Sample related method development efforts to drive analytes into the vapour phase were instead predominantly focused on the volume of sample solution analysed; the volatile concentration of which, as previously mentioned, was restricted to the low ranges of infinite dilution where Henry’s law applies.

Because of the relationship that exists between  $\beta$  and  $K_{g-m}$  in determining headspace concentration (Eq. 4), success with improving sensitivity through increasing sample volume (or decreasing  $\beta$  value) was reliant on the magnitude of the corresponding  $K_{g-m}$ . For volatile compounds with large  $K_{g-m}$  values, an increase in sensitivity was seen while for those with lower  $K_{g-m}$  magnitudes, additional sample volume in the vial had little effect.

The optimal level of filling was found to be between 20 and 80% of the total vial volume to ensure sufficient gas phase for extraction and analysis. Regardless of the actual volume however, once chosen, accurately reproducing the selected sample volume/s and using vials of identical volume was critical to effective quantitation of partition constants due to the application of the PRV method.

All headspace vials utilised in the study were new and pre-cleaned to prevent any potential contaminants producing unknown chromatographic peaks or ghost peaks during analysis. Caps containing a septa with a PTFE face were also specifically sourced to prevent any possible bleeding of rubber contaminants into the headspace vials during vial equilibration at elevated temperatures or when pierced for sampling. Once used these were discarded along with vials.

Instrumentation required for SHA-GC can be related to the basic operations carried out during analysis. Simply a representative aliquot of headspace is transferred from the equilibrated and thermostated sample vessel onto the GC column where it is then separated and subsequently detected. The greatest challenge is ensuring that the sample composition that reaches the GC is representative of the headspace vapour, and that the headspace vapour is representative of the composition of the original sample matrix in the vial.

Chromatographic performance is greatly influenced by how the sample is introduced into the analytic column with one of three popular methods typically chosen. Transfer lines or pressure loop systems are sometimes used however a gas-tight syringe auto sampling system was utilised for this study. This design is universally favoured as the most simple, convenient and inexpensive option available.

Using a gas-tight headspace syringe for sampling, three main issues had to be considered and managed appropriately. Because the sample is being extracted from a heated vial, the syringe was also heated to prevent any condensation of volatiles prior to injection. A minimum syringe set point of 5°C hotter than the equilibration temperature is recommended however larger margins are often used to ensure the analytes remain in the gas phase during sampling. The potential for pressure differences between the sample vial and the syringe resulting in sample losses was also of concern and so an assembly fitted with gas lock systems to prevent leakage following extraction was sourced. Finally, the potential for residual analytes to remain in the syringe post injection causing contamination of the next GC run were addressed by purging the injection system with nitrogen between each analysis.

At the point of headspace sampling, the compounds within the vial must be at a state of thermodynamic equilibrium where there is no net transfer between phases. Using an incubator or heated tray/agitator to control the vial temperature during this time is critical as partition coefficients are temperature dependant, with log transformed  $K_{g-m}$  values relating linearly to temperature.<sup>24</sup> It is for this reason that comparisons have been made possible between values calculated for the same compound at different temperatures, and why temperature is always reported alongside a calculated partition coefficient. Great care must be taken at this equilibration step as even a small difference in temperature can have a large impact on a compound's partition coefficient.

Initial method development activities for vial configuration and instrument settings were based on parameters provided in a number of papers using direct injection static headspace methods,<sup>3, 41, 46, 71, 109</sup> with consideration also given to the theoretical approach to improving sensitivity, as previously discussed.

Preliminary trials using individual flavour compound standards diluted to 80 µg/mL in salt buffer were first undertaken to develop an SHA-GC method that was able to generate chromatographic peaks of adequate area and shape (i.e. narrow and symmetrical). This initial testing revealed the relative volatility of the chosen compounds at 35°C, and enabled their classification into 3 discrete groups, being high, medium and low volatility. As such, the resulting method would need careful optimisation to ensure the more volatile compounds were not overloaded, and the less volatile compounds were still detected reliably. Compounds *D*-limonene and ethyl hexanoate were most abundant in the headspace, while diacetyl and eugenol were the least abundant with only very small peak areas recorded.

Whilst optimising the relationship between partition coefficient and vial phase ratio is important for increasing sensitivity during sample design, determining the ideal headspace sample size and rate of injection are key during instrumental method development. The greatest sensitivity during this phase was achieved by maximising the size of the headspace sample transferred to the GC, and offsetting the larger volume by boosting the rate of sample introduction into the injection port along with carrier gas flow rate. Introducing a 1000 µL splitless headspace injection at 200 µL/s was found to give the ideal compromise between sensitivity and peak shape with only limited broadening noted for some early eluters when using a carrier gas velocity of 40 cm/s. If required, a larger sample size could have been considered, with the longer transfer times mitigated by the use of cryogenic cooling and sample refocusing at the head of the column.

This method was then validated using the composite flavour standard containing all compounds simultaneously diluted to a reduced concentration of 40 µg/mL in salt buffer. This confirmed adequate peak areas were recorded at this lower preferred working concentration and illustrated that baseline separation was still achieved. It also established individual retention times and target ions (Table 2.3) for each volatile as required for the mass spectrometer (MS) detector. Once recorded, target ions were used to improve the sensitivity of the MS detection method by adjusting the instrument acquisition from full scan to selected ion monitoring (SIM) mode, and for building a quantitation method for each compound to be applied during subsequent PRV trials. Sufficiently different retention times with clear baseline separation enabled thymol and carvacrol to share the same quantitation ion to overcome the difficulties of small peak areas partnered with a limited mass spectrum. In this case the resulting peaks were manually integrated for accuracy.

A system must be at thermodynamic equilibrium before SHA can be applied. Flavour volatiles will immediately begin moving into the atmosphere following sample transfer into a sealed

headspace vial until the distribution between the sample phase and gas phase above equals its partition coefficient. At this stage there is no net transfer between phases and the headspace can be analysed. The time point is determined experimentally by preparing a series of identical vials, placing them into the chosen thermostating device and undertaking headspace analyses at regular time intervals beginning immediately after preparation and incubation begins. By graphing the results, the point at which peak area stops increasing with time and plateaus can be determined, as the required equilibration period. The higher the equilibration temperature above ambient conditions, the longer it will take to achieve equilibration.

**Table 2.3 SHA-GC retention times and selected MS ions for SIM acquisition and quantitation**

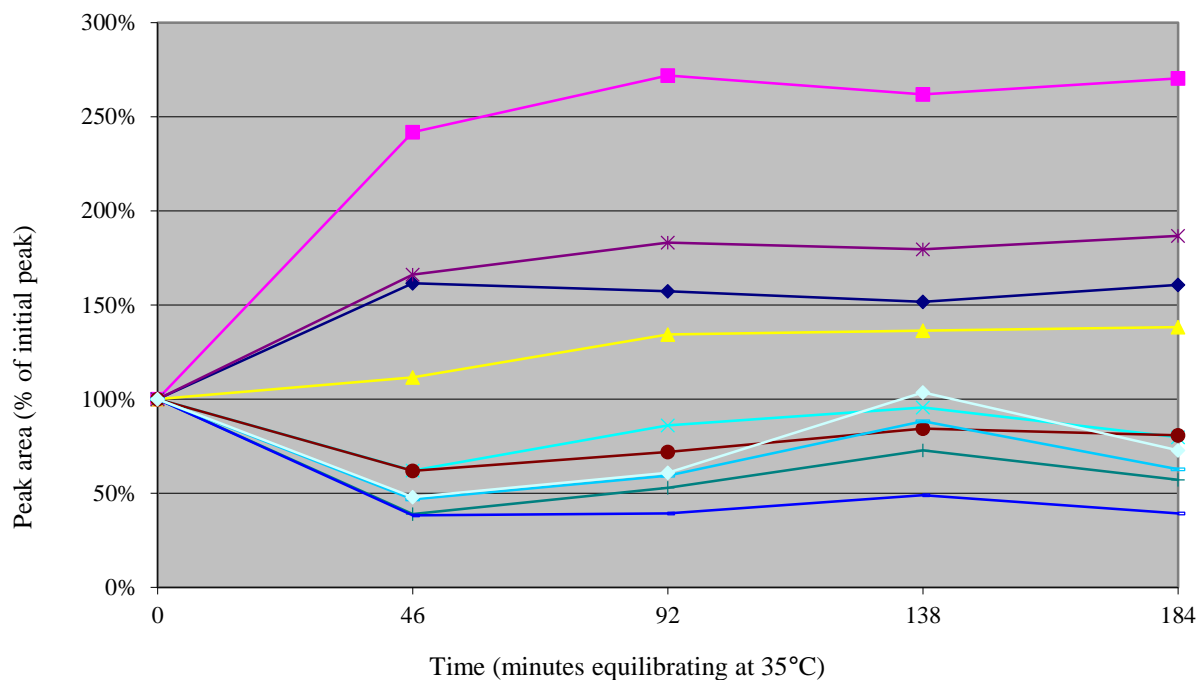
Compound	Relative Retention Time (min)	Selected Ions ( $m/z$ ) <sup>^</sup>
Diacetyl	2.333	42.20, <b><u>43.20</u></b> , 86.10
Hexanal	4.883	41.10, <b><u>44.10</u></b> , 56.10, 57.10
Ethyl hexanoate	10.132	43.10, <b><u>88.10</u></b> , 99.10, 101.10
<i>D</i> -Limonene	11.047	67.20, <b><u>68.20</u></b> , 79.20, 93.20
Eucalyptol	11.183	<b><u>43.10</u></b> , 73.10, 81.10, 108.10
Neral	17.210	<b><u>41.10</u></b> , 69.10, 91.10, 119.10
Geranial	18.034	41.10, <b><u>69.10</u></b> , 84.10, 91.10
Anethole	18.521	77.10, 117.10, 147.10, <b><u>148.10</u></b>
Thymol*	18.655	91.10, 115.10, <b><u>135.10</u></b> , 150.10
Carvacrol*	18.885	91.10, <b><u>135.10</u></b> , 136.10, 150.10
Eugenol	20.31	77.10, 103.10, 149.10, <b><u>164.10</u></b>

<sup>^</sup> Quantitative ions are in bold and underlined

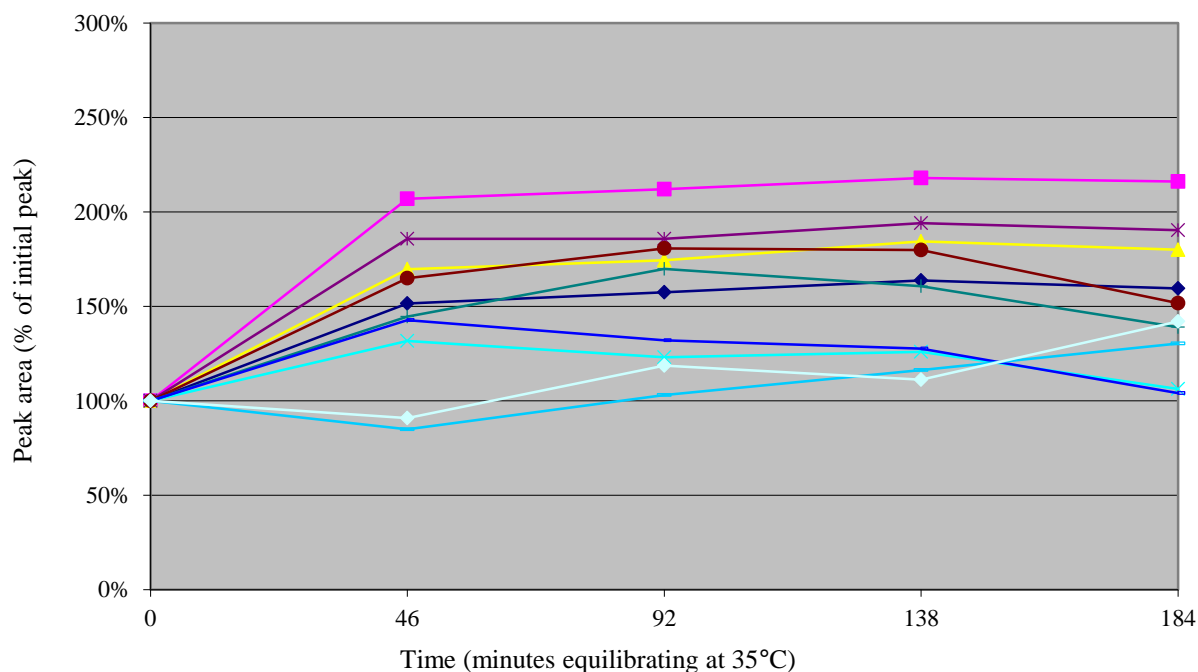
\* Compound for which chromatograms were manually integrated

Evolution of headspace trials were carried out using the previously validated GC method and 5 g of salt buffer spiked with 40 µg/mL of each volatile for simultaneous analyses in a 20 mL headspace vial. Unfortunately, instead of indicating steadily increasing peak areas before a plateau effect, the resulting graph showed fluctuating and sometimes decreasing concentrations over time. After reviewing preparatory methods, an improvement was seen by controlling the temperature of the sample matrix, capping it immediately following volatile transfer, minimising the headspace volume above pre-prepared sample prior to transfer and working quickly to pipette the required volumes into the prepared headspace vials (Figure 2.8). Setting a forced GC oven cool down time was also added to the method to prevent premature sampling of the headspace vial before the instrument was ready for injection and the multipurpose sampler prep-ahead function was introduced to ensure synchronisation between the headspace sampling and GC to reduce overall cycle time. The improved data set indicated that an

incubation time of 92 min at 35°C was sufficient for all volatiles to reach a state of thermodynamic equilibrium.



(a)



(b)

**Figure 2.8 Evolution of headspace graphs at 35°C showing improved results when comparing peak areas from (a) the initial trial with (b) those obtained following modified sample preparation techniques to limit volatile loss during vial filling**

While the graphs showed general improvement overall and clearly demonstrated expected behaviour for some compounds, there was still unexplained fluctuations in peak areas for others. Values for *D*-limonene and anethole varied, however it was the identical trends shown by the two isomer pairs, neral and geranial as well as thymol and carvacrol that were of most interest. This ‘mirrored’ behaviour was interpreted as a potential indicator of sample preparation or GCMS method issues that were affecting compounds of comparable physiochemical properties in the same way. To evaluate the method reproducibility, a series of troubleshooting equilibrium headspace trials were completed and peak area coefficients of variation calculated for review.

Upon completion a number of potential causes were discounted. These included possible interactions between compounds in composite samples with individual volatiles run independently, failure to satisfy the requirements of infinite dilution which was tested by decreasing the VOC concentrations to 4 µg/mL from 40 µg/mL and discrimination during GC sampling that was evaluated by removing standard pre-pressurisation of the vial prior to headspace extraction. With no significant improvement seen, the injection port was cleaned following confirmation that overdue instrument maintenance can also present as peak area reproducibility issues. The GC inlet was inspected for leaks during this time and all column connections were checked and tightened to eliminate these as potential causes.

Modifications to headspace sampling were also made at this time with a new syringe fitted to guarantee there were no leaks occurring through the Teflon plunger seal (which can occur with age and when a syringe has been previously used at a higher temperature). Fill volume was reduced from the full capacity of 2500 µL to 1000 µL so the full amount extracted from the sample vial was being injected into the GC avoiding any chance for discrimination. Because the problematic compounds were high boilers of lower volatility, instrument temperatures were adjusted slightly to prevent any condensation or loss of momentum through the system. The inlet was reduced from 210°C to 200°C, final oven temperature increased by 20°C to 220°C and the GC transfer line to the MS detector increased from 150°C to 250°C.

With the issue persisting, expertise was sought from the instrument manufacturer on possible GCMS configuration causes. Their main recommendations included –

1. using the enclosed incubator/agitator for thermostating rather than heated sample tray for enhanced sample temperature control and faster equilibration preventing any decomposition of volatiles
2. further increasing the headspace syringe temperature to 60°C (25°C above vial temperature) for preservation of headspace volatility

- introducing an inlet purge step to clear any residual vapours post column transfer following the splitless injection
- splitting the injection to deliver a final volume of 125  $\mu\text{L}$  – 250  $\mu\text{L}$  onto the head of the column
- using a larger volume (4 mm inner diameter) deactivated glass inlet liner to better accommodate the 1000  $\mu\text{L}$  of vapour injected, with deactivation preventing sample components absorbing onto active sites on the liner surface which can lead to tailing peaks and reported loss of response for selected analytes

Injection volumes and split combinations delivering 75  $\mu\text{L}$ - 250  $\mu\text{L}$  to the column were trialled following implementation of the other listed method revisions to produce significantly better results than had been seen previously (Figure 2.9). Calculated coefficients showed variation of less than 6% with a steady peak area recorded for each volatile across a series of 5 identical samples. At this point the method was considered sufficiently reproducible for use in measuring volatile partitioning investigations. Full details of the optimised SHA-GCMS method can be found in section 2.3.2 with instrument configuration provided in Appendix 1.

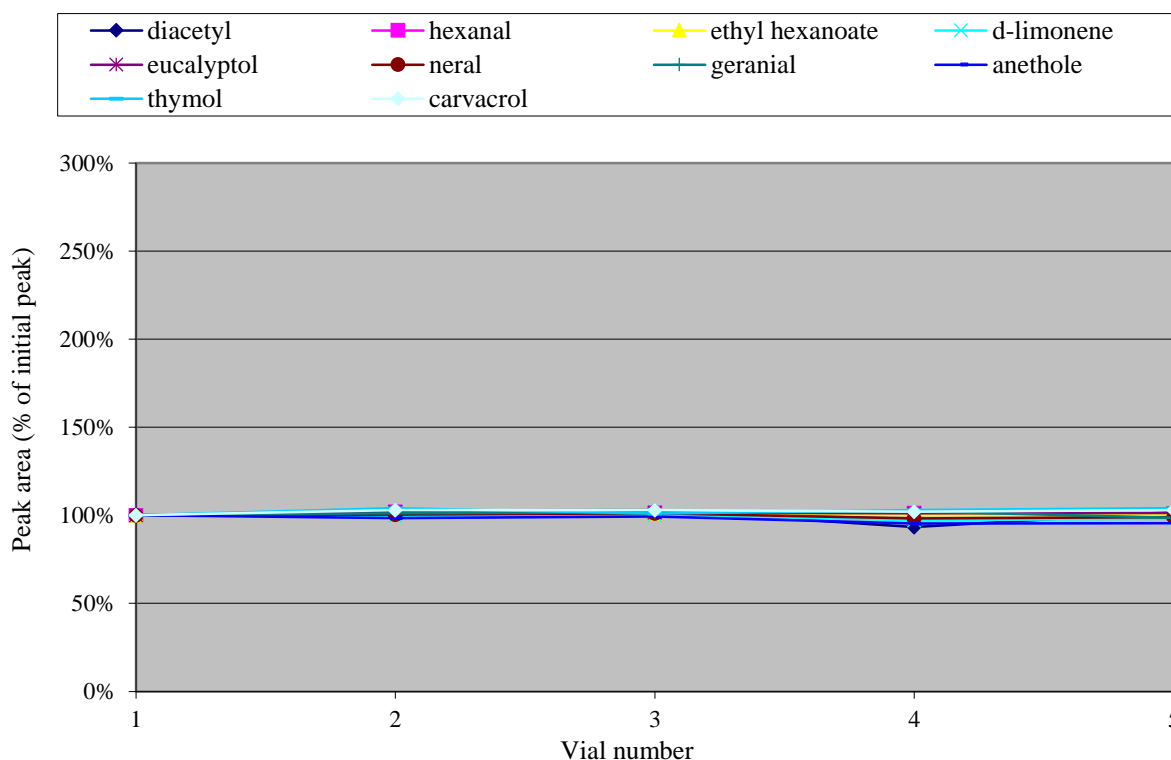


**Figure 2.9 Reproducibility of optimised SHA-GCMS method for use in partitioning trials for measuring  $K_{g-m}$**

### 2.2.3 Application of PRV techniques to measure flavour interactions

Partition coefficients can be measured using direct or indirect methods following SHA. Direct methods require aroma concentration to be quantitatively determined in both gas and matrix phases at equilibrium using traditional external calibration techniques. This approach is time consuming because of the requirement to generate substance-response factors for detector calibration and can also introduce possible sources of error.<sup>61</sup>

It is for this reason that indirect methods that do not require calibration steps for detection nor knowledge of exact matrix concentrations are gaining popularity. Instead the indirect approaches of phase ratio variation and phase ratio calibration are based on the influence of matrix volume on equilibrium headspace concentration. A comparison reported PRV to be the favoured approach<sup>69</sup> due to its simplicity and accuracy. Furthermore results generated for a number of flavour compounds using this approach have confirmed that the method produces results in close agreement to those obtained using direct methods.<sup>110</sup>

More specifically, PRV analysis is based on the relationship that exists between reciprocal peak area and the phase ratio in the vial containing the matrix sample. The coefficient is calculated by regression analysis of SHA-GC measurements of a series of headspace vials containing an identical matrix in a wide range of volumes or  $\beta$  phase ratios.

The method was first introduced by Ettre and colleagues in 1993<sup>63</sup> and is described by Eq. 5:

$$\frac{1}{A} = \frac{1}{f_i C_s} K + \frac{\beta}{f_i C_s} \quad [5]$$

where  $A$  is the chromatographic peak area at equilibrium,  $f_i$  is the proportional factor,  $C_s$  is the initial volatile concentration in the matrix, and  $\beta$  is the vial phase ratio. Containing only the two variables  $\beta$  and  $A$ , the relationship can be simplified as the following linear expression.

$$\frac{1}{A} = a\beta + b \quad [6]$$

By plotting  $1/A$  against  $\beta$ , the values of  $a$  and  $b$  can be determined respectively as the slope and y-intercept of the corresponding linear regression. The partition coefficient is calculated by Eq. 7, following verification of relationship linearity with  $R^2$  values greater than 0.8.<sup>26</sup> For accuracy

it is recommended that a minimum of four vials of different volume be analysed<sup>58</sup> to generate sufficient data points.

$$K = \frac{a}{b} \quad [7]$$

In this case the partition coefficient is expressed as the  $K_{g-m}$ , or gas-matrix distribution constant which describes compound volatility. Many authors invert Eq. 7 to report the alternative, being the retention effect of the matrix. As such, care is needed when considering published K values as results expressed in directional terms (increased or decreased) or as magnitudes (large or small values) can have opposite meanings.

To further evaluate SHA-GCMS methodology and assist in development of a practical understanding of how PRV is applied, a literature review was conducted to find a suitable study to replicate. A research paper published by Jouquand and colleagues<sup>110</sup> investigating the partitioning of hexanal using PRV was selected and repeated with only minor variations made to sample and instrumental conditions to accommodate differences in equipment. Analysing a series of vials of increasing volume containing hexanal in water generated a calculated  $K_{g-m}$  value of 0.0086 at 25°C. This was in good agreement with the findings of the original investigation which reported a  $K_{g-m}$  of 0.0110. Tabulating the chromatographic data, graphing the inverse peak area against  $\beta$  value and undertaking linear regression provided confirmation of the underlying data quality. Acceptable coefficients of variation were recorded for replicate vials and a correlation coefficient of 0.97 reported for the regression equation. Data analysis from this preliminary study is summarised in Appendix 2.

The  $\beta$  ratios used in the study provided a valuable starting point from which to base development activities for a composite method that would satisfy the requirements of all volatile compounds and to accommodate their anticipated variations in volatility and partitioning behaviour. It is well documented that a major challenge in PRV studies is obtaining adequate peak area differences between adjacent  $\beta$  values for compounds of low volatility.<sup>58, 63, 70</sup> A minimum overall ratio of 1.12 between the largest peak area in the series and the smallest is considered to be the minimum reasonable value, however it is accepted that accuracy is greatly improved as this figure increases.<sup>60</sup> Therefore evaluating and maximising peak area differences where possible is a key objective during method development.

Since increasing vial sample volume (within the acceptable range) has little effect on changing headspace concentration, using low volumes equating to higher  $\beta$  values for less volatile compounds is recommended.<sup>63</sup> This achieves the necessary magnitude of peak area differences due to the relationship that exists between vial volume and peak areas in closed systems.<sup>70</sup> Whilst the highest possible  $\beta$  values are sought after for analysing such volatiles, verifying the selected  $\beta$  values for all compounds fall within the range where a dependant relationship exists between headspace concentration and liquid volume is also critical (Figure 2.10).

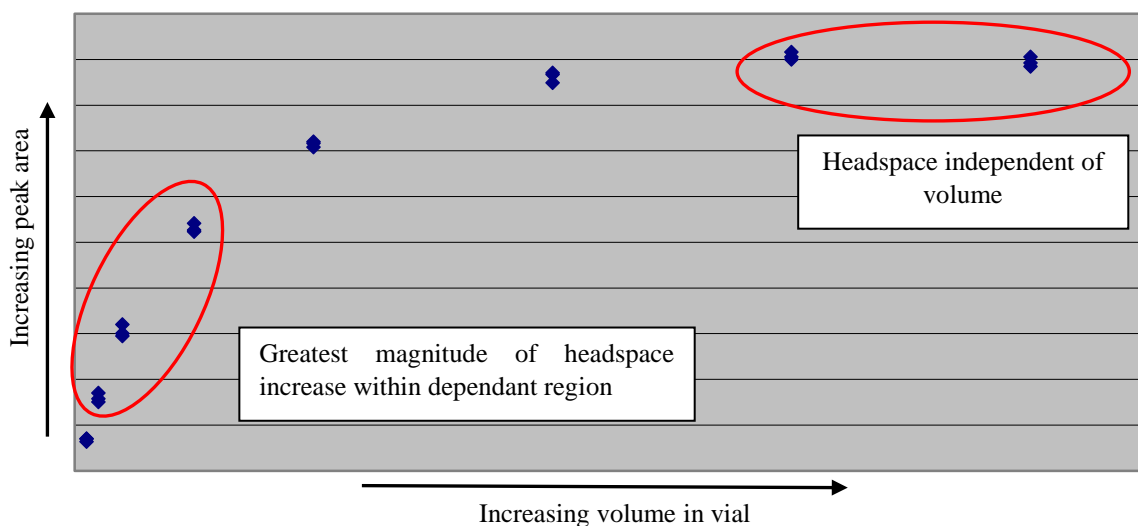


**Figure 2.10 Influence of sample volume in vial on headspace concentration depicting saturation at higher levels of filling**

Because a number of compounds recorded smaller peak areas than hexanal during previous SHA method development activities, the series of  $\beta$  values were extended to include larger values. The influence of vial sample volume was tested using matrix quantities of 50, 100, 200, 500, 1000, 2000, 3000 and 4000  $\mu\text{L}$  in 20 mL headspace vials equating to  $\beta$  values of 399, 199, 99, 39, 19, 9, 5.7 and 4 respectively. Graphing peak areas against vial sample volume confirmed the recorded peak areas to be in the dependant region.

The first PRV trials to calculate partitioning coefficients in water at 40  $\mu\text{g}/\text{mL}$  and 35°C were run over three consecutive days. A total of three independent replicates were completed with each of the eight different  $\beta$  ratios contained within a replicate analysed in triplicate for a total run time of approximately 22 hours. Results for each volatile were summarised in a method data table to evaluate variance and peak area ratios before the relationship between vial volume and recorded peak area was graphed. This step generated a visual representation of the data with the slope and overall shape providing an insight into compound volatility and likely magnitude of  $K_{g-m}$ . PRV calculations followed by plotting inverse peak areas against  $\beta$  to check

the condition of linearity had been satisfied, before values for the slope and y-intercept from the regression equation were used to calculate the partition coefficient (Eq. 7). Appendix 3 illustrates how this approach was used for calculating the partition coefficient of hexanal.

Whilst the approach was successful in producing partition coefficients for each replicate, a comparison of calculated figures for compounds showed considerable variations, with the more volatile analytes exhibiting the greatest differences. To view all the data simultaneously, chromatograms obtained for each vial volume (triplicate) were overlaid for visual inspection. For all  $\beta$  values, this revealed notable variations in peak magnitude between replicates, with an identical trend of area decrease for each successive replicate recorded for all volatiles.

To determine the extent of peak area loss for each compound over time and between replicates, vial volume against peak area was graphed (Figure 2.11).

In addition to showing the peak area reduction between PRV replicates, the graphs illustrate how each compound's volatility influences the shape of the graph and therefore the ability to increase sensitivity or headspace concentration using larger vial volumes. Limonene is easily seen as the most volatile compound with a continuing steep positive slope, while hexanal and ethyl hexanoate level out at higher volumes. Eucalyptol, in contrast, has the lowest volatility of those shown with a plateauing of the graph at 1 mL indicating no further increase in headspace concentration is available beyond this value through adjustment of  $\beta$  ratios.

As further investigation confirmed, chromatograms for compound triplicates overlaid well within each PRV trial (Figure 2.12), it was deduced that the problem was most likely not a GC method issue. Since each volatile was affected similarly, it was hypothesised that the cause was most likely instrumental and related to the MS detector.

Lower peak areas are the result of a reduced signal from the mass spectrometer detector which operates by performing three key operations in the following order:

- 1) creation of gas phase ions
- 2) separation of ions in space or time based on their mass-to-charge ratio
- 3) measurement of the quantities of ions of each mass-to-charge ratio

A variety of different methods and instrument configurations can be used to complete these tasks however the MS used in this study comprised an electron impact ionisation (EI) source, a quadrupole analyser and electron multiplier detector.

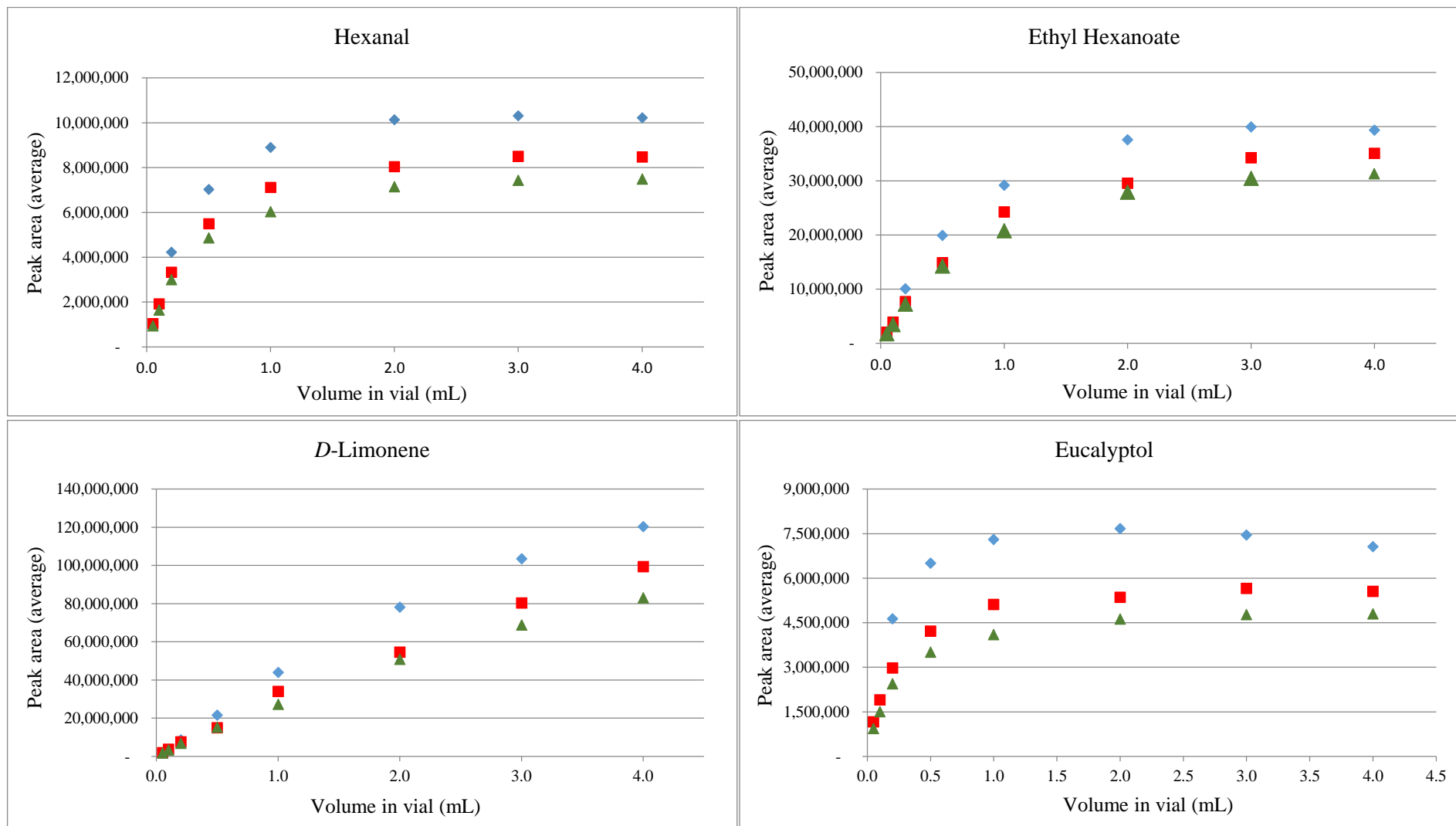


**Figure 2.11 Average peak areas of PRV replicates showing magnitude decreases with successive trials** ◆ Rep 1 ■ Rep 2 ▲ Rep 3

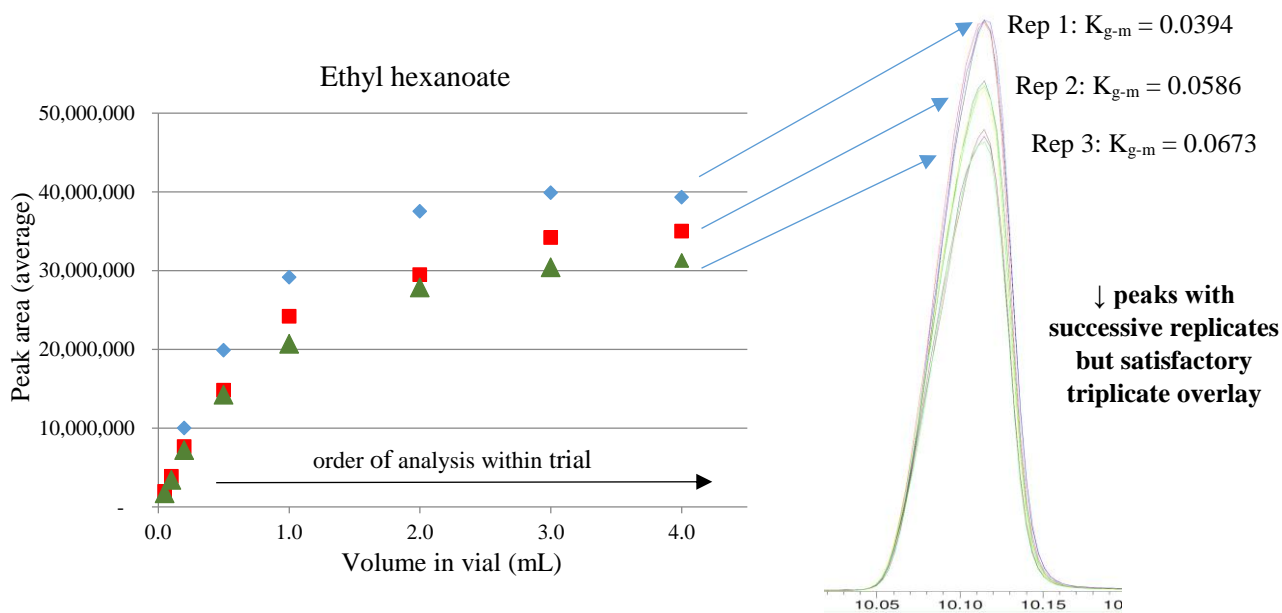
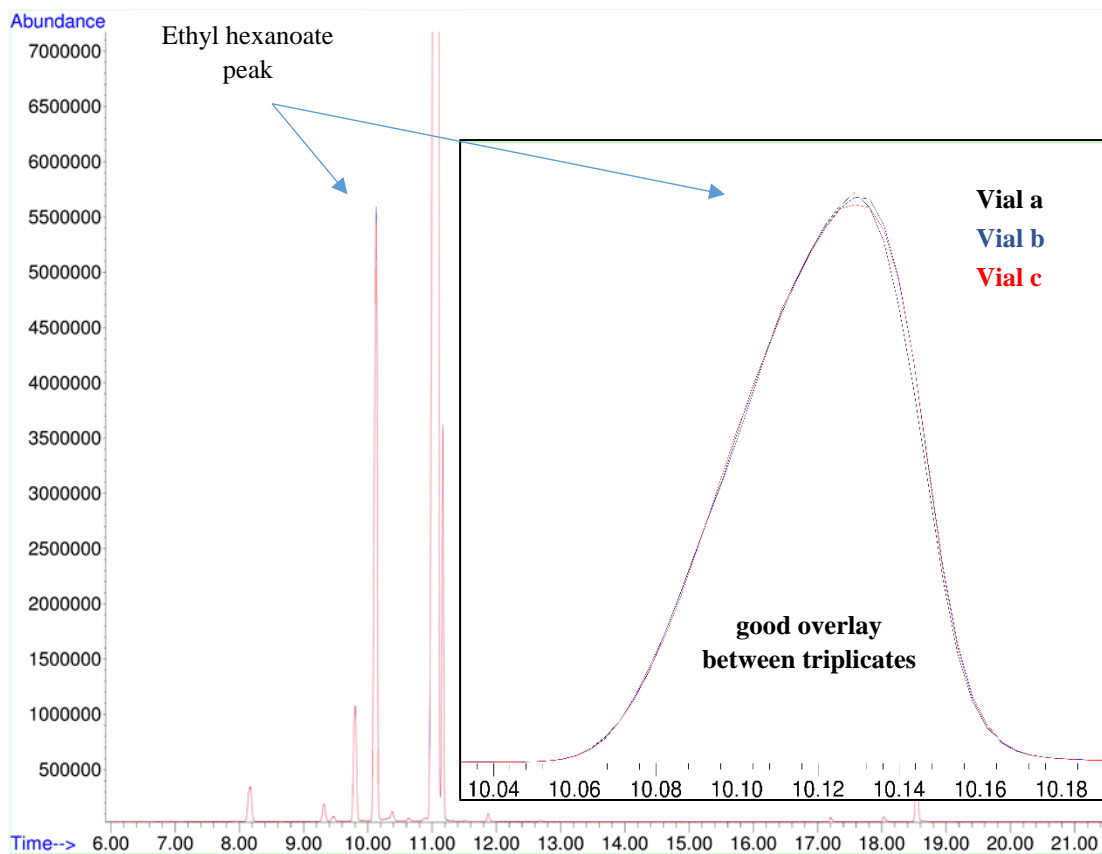


**Figure 2.12 Ethyl hexanoate peak from chromatogram showing strong agreement between triplicate samples but a continuous reduction in recorded areas for successive PRV replicates which equated to large variations in calculated partition coefficients**

In such a system, EI passes a beam of electrons through the gas phase sample which collide with neutral analyte molecules to produce a positively charged ion or fragment ion. It is only these charged products that are detected to produce a signal and resultant chromatogram. Failure to adequately ionise compounds entering the MS from the GC column would result in missed detection and consequently lower peak areas.

As a result of normal operation, all GCMS EI sources must be cleaned to maintain performance. The requirement is usually signalled by loss of analyte response which cannot be rectified with inlet and column servicing, method adjustments, tuning or escalating repeller or electron multiplier (EM) voltages. This seemingly described the situation being experienced.

Although performance is generally observed as a gradual loss over time, maintenance was carried out. The source was removed, dismantled and abrasively cleaned to remove the discolouration where electrons from the filament enter the source body. The opportunity to replace both filaments was also taken at this time, immediately prior to another three PRV trials being run. Results from PRV runs 4-6 confirmed an increase in initial signal strength however a continued reduction in peak area over time was again observed to a similar extent as previously (PRV 1-3; results for 6 volatile compounds are shown in Appendix 4).

A common issue in dynamic headspace analysis where volatiles are completely purged from a sample using a stream of inert gas and condensed in a trap prior to analysis is water vapour. When contained in a sample, the vapour can deteriorate the chromatographic process via condensation in transfer lines, creating absorptive areas in the injection port<sup>107</sup> and through interference particularly during MS analysis.<sup>60</sup> The water problem is not so pronounced in SHA due to the much smaller volumes of headspace sampled, and when raised, the issue is usually discussed in reference to avoiding coelution of water with the analyte of interest. For example during the analysis of ethanol as blood alcohol.<sup>70</sup> It is managed by a recommendation to thermostate samples below 80°C where water vapour pressure is still relatively low.

PRV trials 1-6 were thermostated and analysed at 35°C which is well below this temperature however the potential interference of water was investigated further. As an initial check, a comparison of tune reports immediately prior to and following 3 complete PRV runs (24 vials each) was conducted. The reduction in peak area was observed as expected but water values in tune reports actually showed a decrease from 0.80% to 0.59% following analyses.

After consulting several senior researchers with expertise in the field of equilibrium headspace analysis and speaking at length with a number of application specialists representing the instrument manufacturer, a potentially limiting factor for the use of MS detectors in PRV trials

was identified. When introduced into the detector, water as well as oxygen and solvents including methanol react with the charged filament to form rhenium oxide on its surface. The reaction modifies the physical properties of the filament and reduces its ability to generate electrons that are essential for ionising compounds entering the MS chamber.

To reduce the damage caused by compounds such as water, it is advised that methods should be configured so that the filament is charged only a few seconds prior to the elution of the first volatile. By this time the water and any other damaging low molecular weight compounds have passed through the system. This can minimise the damage but not eliminate the problem completely, as exposure even when the filament is not charged will still result in some degree of corrosion.

Subsequently, a review of instrumentation utilised in published PRV trials was conducted to conclude no other comparable study reported using GCMS instrumentation. While MS detectors had been successfully utilised to calculate partition coefficients in research using solid phase microextraction of headspace or SHA with external calibration for quantitation, all available SHA-GC combined with indirect PRV determination of  $K_{g-m}$  utilised a flame ionisation detector (FID). Nowhere in these papers, however, was the selection of detectors addressed or emphasised as being critical to the method.

FID is used extensively in volatile analyses predominantly because of its wide linear operating range, however it is also highly valued for its unit carbon response, low cost, ease of use, speed of response and ruggedness. It is not sensitive to oxygen and water like the MS and so is more suitable for repeated headspace sampling above aqueous matrices, such as in SHA-PRV, where both components are naturally present. The detector operates by passing sample and carrier gas from the column through a hydrogen-air flame connected to electrodes. When an organic compound is burned, there is an increase in ions produced. This is recorded as a current proportional to the mass of sample being burnt, and following amplification is used to create the chromatogram.<sup>111</sup>

Given the apparent limitations of MS detection and volume of evidence supporting the use of FID, access to a suitable instrument was organised and the method reviewed to accommodate the change in equipment. A column change to a less polar phase improved baseline separation between limonene and eucalyptol and other minor adjustments were made to headspace sampling and GC conditions to optimise chromatographic quality. The resulting GC-FID method (detailed in section 2.3.3) was used in PRV trials 7-9 to confirm peak area stability as shown in Figure 2.13, which translated into comparable calculated partition coefficients.

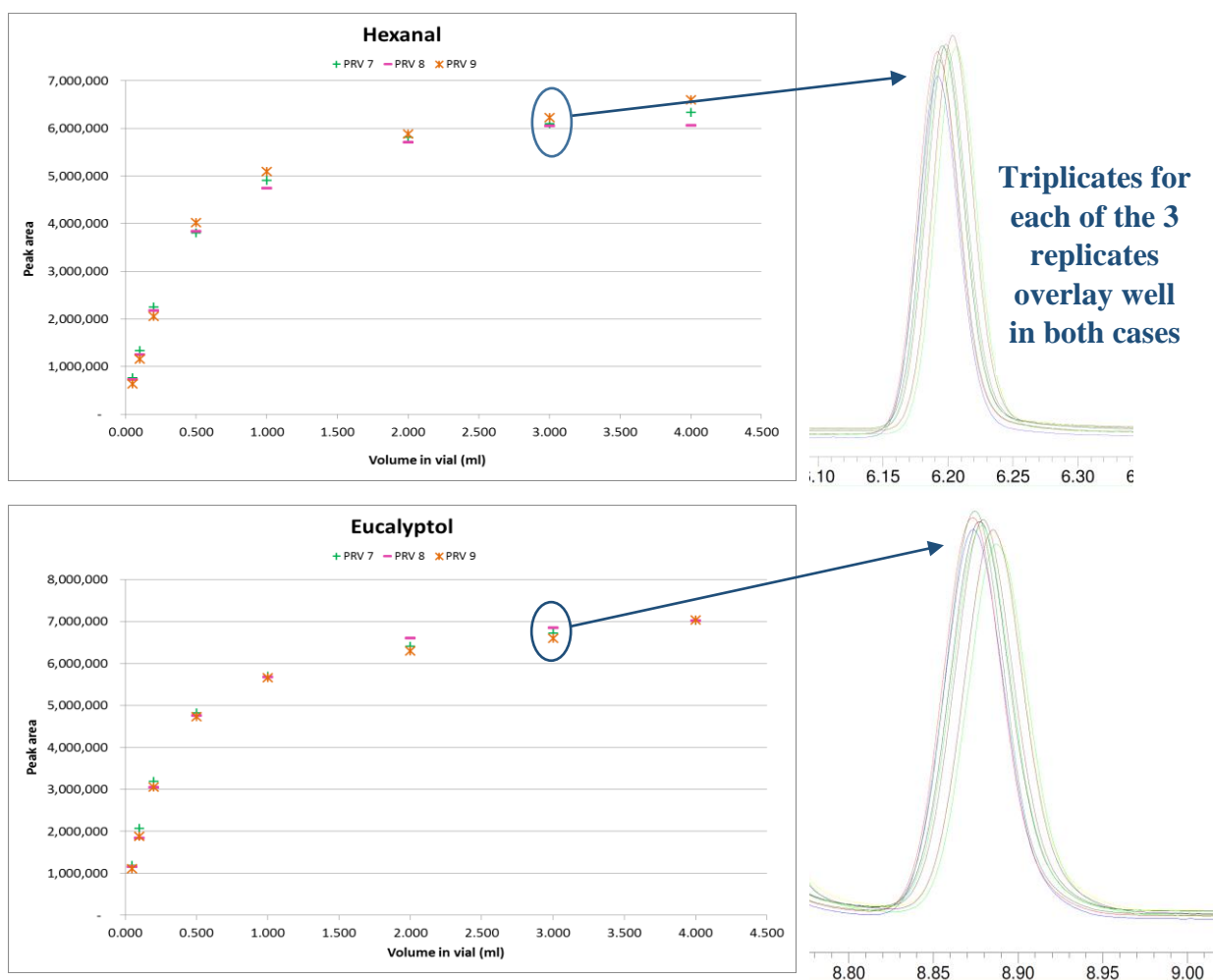


**Figure 2.13 Chromatographic overlay and graphical representation of PRV data confirmed that stable peak areas were obtained using GC-FID instrumentation**

The decision was made at this point to remove *D*-limonene from the study due to difficulties encountered with applying PRV methodology to this particular compound because of its high degree of volatility. This is a documented limitation with the PRV method<sup>61, 63</sup> and one that is more difficult to overcome than the issue of low volatility which can be addressed using higher  $\beta$  ratios. The problem presents due to non-linearity at higher  $\beta$  values (smaller vial volumes) that results from deviations between the ideal PRV calculations and the values obtained from experimental data.<sup>112</sup> The deviation remains small for low to medium volatility analytes but significantly increases with headspace concentration. Unfortunately the recommendation to use  $\beta$  values of  $\leq 20$  to overcome this phenomenon was unsuccessful. Although improved (Figure 2.14), the resulting partition coefficients still displayed large negative values due to the steep slope and corresponding negative y-intercept of the regression equation obtained from the PRV graph.

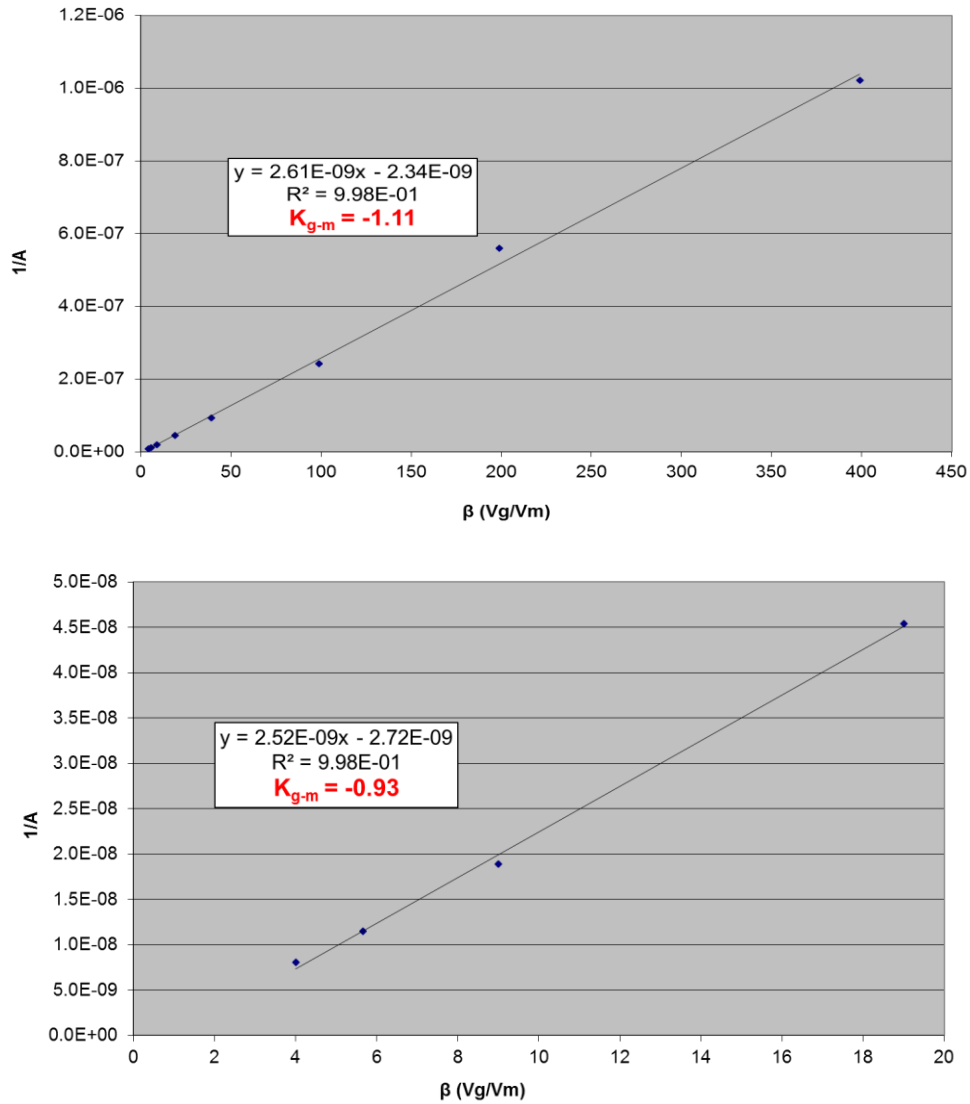


**Figure 2.14 Effect of reducing limonene  $\beta$  values to address the known limitations of applying PRV methodology to highly volatile compounds**

The following chapter details how the resulting SHA GC-FID method was applied to calculate partition coefficients for each of the remaining 11 volatiles. Firstly in water, for method validation via comparison with other published data, and then to measure individual flavour interactions within a protein containing food matrix.

## 2.3 Optimised methods summary

### 2.3.1 Myofibrillar protein extraction and quantitation from pork muscle

Chilled pork loin muscle was trimmed of all connective tissue and visible fat before being passed through a mechanical grinder with a 3 mm plate. Prepared mince was homogenised with ten times the volume of ice-cold 50 mM phosphate buffer at pH 7.5 containing 0.02 % sodium azide ( $\text{NaN}_3$ ) using an Ultra-Turrax T25 homogeniser (Ika, Germany) fitted with a 12 mm diameter shaft attachment at speed mark 5 for 35 sec. The homogenate was prepared over ice and immediately centrifuged at 4500 g and 4°C for 15 min (Eppendorf 5810R). Separated supernatant was discarded and the remaining pellet resuspended in 2 times the volume of cold 50 mM phosphate buffer. This process was repeated a further 3 times with the final suspension passed through a fine mesh screen to remove residual connective tissue. The washed pellet was then resuspending in four times the volume of 50 mM phosphate buffer at pH 7.5 containing 0.02%  $\text{NaN}_3$  and 0.5 M NaCl before being centrifuged at 4500 g and 4°C for 20 min. The supernatant was collected as a solubilised myofibrillar protein suspension and chilled immediately. Total protein concentration was determined using the bicinchoninic acid method with bovine serum albumin (BSA) as a standard (Pierce BCA Protein Assay Kit, Thermo Scientific, USA).

### 2.3.2 Static headspace analysis of flavour compounds using GCMS

Analyses were conducted using a 6890N gas chromatograph coupled to a 5975 mass spectrometer (Agilent Technologies, Palo Alto, CA, USA) with a low polarity Zebron ZB-5 ms capillary column installed (Phenomenex, 30 m x 250  $\mu\text{m}$  i.d x 0.25  $\mu\text{m}$  film thickness). The instrument was fitted with an automated Multipurpose Sampler (MPS2)(Gerstel) equipped with a temperature controlled incubator/agitator at 35°C and 2.5 mL gastight headspace syringe heated to 60°C. Helium (BOC gases ultrahigh purity) was used as the carrier gas with a linear velocity of 40 cm/s and a flow rate of 1.2 mL/min. The GC oven temperature program began at 40°C for 1 min before increasing at a rate of 5 °C/min to 220°C for a total time run time of 37 min. A 14 min oven cooldown immediately followed.

Samples were prepared using 20 mL glass headspace vials and contained 5 g of 50 mM phosphate buffer with 0.5 M NaCl spiked with 40  $\mu\text{g}/\text{mL}$  of each volatile for simultaneous analysis. Vials were thermostated for 60 min under 500 rpm agitation before 2500  $\mu\text{L}$  of headspace was extracted in a single stroke at 200  $\mu\text{L}/\text{sec}$ . Sample was immediately transferred

to the PTV inlet held at 200°C where a 2500 µL 20:1 split injection was made at 125 µL/sec. Following each transfer the headspace syringe was flushed with nitrogen for 180 s.

The MS ion source was set to 250°C with positive ion impact spectra recorded in SIM mode using the ions detailed in Table 2.3. Data analysis was conducted using MSD ChemStation Data Analysis software (Agilent Technologies) with identification achieved by GC retention times and library reference spectra (NIST Spectral Library 2005). Quantitation was carried out using the selected ion for each compound and is reported as total peak area.

### 2.3.3 Calculation of partition coefficients using GCFID with the PRV method

Increasing volumes (50, 100, 200, 500, 1000, 2000, 3000 and 4000 µL) of sample containing 40 µg/mL of each volatile were prepared in 20 mL headspace vials and equilibrated at 35°C under agitation for 60 min. Headspace samples from prepared vials were injected using a 2.5 mL gas-tight headspace syringe preheated to 80°C and fitted to an automated Multi Purpose Sampler (MPS2) (Gerstel, Germany). An injection volume of 1000 µL was made in splitless mode at 200°C and a rate of 400 µL/sec following a 1000 µL vial headspace extraction at 200 µL/sec. After each injection, the headspace syringe was flushed for 180 s with nitrogen.

Headspace analysis was conducted using a 6890N gas chromatograph (GC) equipped with a flame ionisation detector (FID) (Agilent Technologies, Palo Alto, CA, USA). The aroma compounds were separated on a CARBOWAX capillary column (Alltech 2374, i.d. = 320 µm, length = 30 m, film thickness = 0.25 µm). Helium (BOC gases ultrahigh purity) was used as the carrier gas with a linear velocity of 26 cm/s and a flow rate of 1.3 mL/min. The GC oven temperature program began at 40°C for 1 min before increasing at a rate of 5 °C/min to 200°C. A ramp of 30°C/min followed to a maximum 240°C and finished with a hold period of 5 min giving a total time run time of 39.33 min. The detector temperature was set at 300°C with air and H<sub>2</sub> flow rates at 400 and 30 mL/min respectively. N<sub>2</sub> was used as the makeup gas with a flow rate of 25 mL/min.

Data analysis was conducted using MSD ChemStation Data Analysis software (Agilent Technologies) with identification achieved using GC retention times and results reported as total peak area. For each analyte, reciprocal peak areas were plotted against vial phase ratio ( $\beta$ ) before a linear regression was fit. The partition coefficient was determined by dividing the slope of the equation by the y-intercept to express the magnitude of compound volatility in the system.

## Chapter 3 Measuring the impact of myofibrillar proteins on volatile partitioning using the PRV method

### 3.1 Preface

This following chapter is presented as a manuscript in preparation for submission to Journal of Agricultural and Food Chemistry and has been written according to the journal's author guidelines. As required, the manuscript presents original research in the application of chemistry and will be submitted as a research article under the category of food and beverage chemistry/biochemistry.

The manuscript aims to summarise the content of the preceding introduction and method chapters before reporting details of the protein binding study undertaken. Results are presented and discussed with reference to related research in the field of flavour interactions before recommendations for future research are made. Once published, this manuscript will contribute new information to the wider scientific community regarding both volatile binding by meat proteins and the flavouring potential of selected novel volatile compounds that are becoming increasingly recognised as bioactive food ingredients.

# Statement of Authorship

Title of Paper	Impact of myofibrillar proteins on volatile partitioning using PRV methodology
Publication Status	<input type="checkbox"/> Published <input type="checkbox"/> Accepted for Publication <input type="checkbox"/> Submitted for Publication <input checked="" type="checkbox"/> Unpublished and Unsubmitted work written in manuscript style
Publication Details	

## Principal Author

Name of Principal Author (Candidate)	Jessica Sanderson		
Contribution to the Paper	Designed study, undertook method development activities, performed all analyses, interpreted experimental data, wrote manuscript and acted as corresponding author.		
Overall percentage (%)	80		
Certification:	This paper reports on original research I conducted during the period of my Higher Degree by Research candidature and is not subject to any obligations or contractual agreements with a third party that would constrain its inclusion in this thesis. I am the primary author of this paper.		
Signature		Date	12/07/2016

## Co-Author Contributions

By signing the Statement of Authorship, each author certifies that:

- i. the candidate's stated contribution to the publication is accurate (as detailed above);
- ii. permission is granted for the candidate to include the publication in the thesis; and
- iii. the sum of all co-author contributions is equal to 100% less the candidate's stated contribution.

Name of Co-Author	Steve Fuller		
Contribution to the Paper	Provided technical input during method development and troubleshooting advice throughout analyses.		
Signature		Date	14/7/16

Name of Co-Author	Kerry Wilkinson		
Contribution to the Paper	Provided input into experimental design, assisted with technical elements of laboratory method development and provided structural/editing advice on manuscript.		
Signature		Date	<i>10/08/2016</i>

Name of Co-Author	Yasmina Sultanbawa		
Contribution to the Paper	Provided input into experimental design, assisted with technical elements of laboratory method development and proof read the manuscript.		
Signature		Date	<i>10/8/16</i>

Name of Co-Author	Heather Smyth		
Contribution to the Paper	Provided input into experimental design, assisted with technical elements of laboratory method development and provided structural/editing advice on manuscript.		
Signature		Date	<i>9/8/16</i>

1 **Impact of myofibrillar proteins on volatile partitioning using PRV methodology**

2

3 Jessica L Sanderson<sup>\*#^1</sup>, Steve C Fuller<sup>#</sup>, Kerry L Wilkinson <sup>^</sup>, Yasmina F Sultanbawa<sup>§</sup> and

4 Heather E Smyth<sup>§</sup>

5

6 <sup>#</sup> Innovative Food Technologies, Queensland Department of Agriculture and Fisheries, P.O

7 Box 156, Archerfield, Queensland 4108, Australia

8 <sup>^</sup> School of Agriculture, Food and Wine, The University of Adelaide, Waite Campus, PMB 1,

9 Glen Osmond, South Australia 5064, Australia

10 <sup>§</sup> Centre for Nutrition and Food Science, Queensland Alliance for Agriculture and Food

11 Innovation, University of Queensland, P.O. Box 156, Archerfield, Queensland 4108, Australia

12 <sup>1</sup> Current address –Mitchell’s Quality Foods, 18 Buchanan Road, Banyo, Queensland 4014,

13 Australia

14 \*Corresponding Author – Telephone: +617 3646 4347, email: [sandersonjess8@gmail.com](mailto:sandersonjess8@gmail.com)

15

16

17 **KEYWORDS:** flavor interactions, volatile binding, myofibrillar protein, partition coefficient,

18 phase ratio variation (PRV)

19 **ABSTRACT:** Myofibrillar proteins in skeletal muscle tissue play a significant role in defining  
20 the textural properties of processed meat products and can affect flavor quality by modifying  
21 aroma volatile release via selective flavor interactions. The influence of extracted pork protein  
22 on the volatility of 11 different compounds were studied using phase ratio variation (PRV)  
23 methodology. Initial determinations of gas-matrix partition coefficients ( $K_{g-m}$ ) in water at 35°C  
24 demonstrated varying degrees of volatility with the behaviour largely attributable to compound  
25 hydrophobicity. Subsequent calculations of retention percentages (R%) in matrices containing  
26 2 mg/mL protein homogenate returned positive values in all cases, confirming myofibrillar  
27 muscle components were binding volatiles to different extents, thereby reducing each  
28 compound's availability for sensory perception within the food matrix.

## 29 INTRODUCTION

30 Flavor perception is well established as a key determinant in consumer acceptability of foods  
31 and is largely determined by volatile organic compounds (VOC) contained within the product  
32 matrix. When food is eaten, these flavor molecules are released from the substrate into the  
33 mouth, where they can travel via the retronasal passage to the olfactory epithelium and  
34 detection by olfactory receptors elicits a sensory response. Non-volatile food matrix  
35 components such as proteins, carbohydrates and lipids are capable of binding volatile  
36 compounds, thereby limiting their availability for delivery, detection and perception.<sup>1</sup> This not  
37 only reduces the overall intensity but can result in significant changes to characteristic profiles  
38 due to the highly selective nature of interactions.<sup>2</sup>

39 Proteins are a group of structurally diverse macromolecules that impart important nutritional  
40 and functional qualities to foods. They can derive from either plant or animal origins and are  
41 extensively used in processed foods for their functional properties including gelation,  
42 thickening, emulsification and foaming.<sup>3</sup> Proteins have little flavor of their own, but influence  
43 flavour perception through selective molecular interactions that can either enhance or diminish  
44 volatile release.<sup>4</sup>

45 Protein interactions with volatile components are far more complicated than those involving  
46 carbohydrates and lipids, due to the diversity in protein functionality available for interaction;  
47 for example, amino acid side chains, terminal ends of proteins and hydrophobic pockets.<sup>3</sup>  
48 Binding can take place via weak reversible hydrophobic interactions, in addition to stronger  
49 ionic effects and irreversible covalent bonding,<sup>2</sup> depending on the availability of active sites.  
50 Historically, the majority of flavor interaction involving proteins have focused on the dairy  
51 protein  $\beta$ -lactoglobulin. This is primarily due to its presence in a wide variety of processed  
52 milk based products, such as yoghurts and custards, but also because its structure is well  
53 defined, facilitating identification of the mechanisms involved in volatile binding.

54

55 Myofibrillar proteins are the most abundant class of meat proteins and represent approximately  
56 63% of total protein muscle content. The class comprises mainly actin and myosin, which form  
57 the contractile units in skeletal tissue and complex to form actomyosin in post rigor muscle.<sup>5</sup>  
58 Complexed actomyosin is composed of 22 different amino acids, of which 10 are essential and  
59 therefore nutritionally significant.<sup>6</sup> In addition to their biological roles, the myofibrillar  
60 component of animal muscle tissue also performs a significant structural role in the formation  
61 and final texture of processed meat products.<sup>3</sup>

62 Early flavor interaction studies involved vegetable proteins and were aimed at management of  
63 endogenous off flavours, while dairy proteins have been the focus of research in recent years.  
64 However research involving meat derived proteins remains comparatively scarce. Literature  
65 concerning fish<sup>7</sup> and pork extracts<sup>8-12</sup> provide only limited, highly specific information and  
66 utilise analytical methods that generate results which are not always relevant or directly  
67 comparable to one another.

68 Flavor volatiles tend to be distributed between a food system and its headspace, the extent to  
69 which depends on interactions with individual matrix components, until a state of  
70 thermodynamic equilibrium is reached.<sup>1</sup> Consequently flavor interactions are described by  
71 measuring changes in compound volatility using the gas-liquid partition coefficient  $K_{g-m}$ . This  
72 is expressed as the ratio between the concentration of a given volatile organic compound in the  
73 gas phase and in the product phase at equilibrium.<sup>13</sup>

74 Partition coefficients have traditionally been measured using direct static headspace analysis  
75 (SHA) methods which are time consuming and incorporate potential sources of error due to  
76 their use of external standards.<sup>14</sup> However the emergence of indirect approaches, including the  
77 phase ratio variation (PRV) method, which do not require external calibration of the detector  
78 nor exact knowledge of the initial volatile concentration in solution, are becoming increasingly  
79 popular. PRV methodology is considered clean, rapid and highly efficient and furthermore has  
80 been validated against direct approaches in comparative studies. It is also considered the most  
81 accurate and simple to perform of the indirect methods available.<sup>15</sup>

82 The PRV method is based on the influence of sample volume on the equilibrium gas phase  
83 concentration and so relies on the relationship between  $K_{g-m}$  and the phase ratio  $\beta$ , which is  
84 defined as the ratio of headspace volume to sample matrix volume in a given system.<sup>16</sup> As a  
85 result, PRV can be applied to mixtures of compounds in complex matrices and precision is  
86 simply related to the solubility of a compound in solution and control of the volume of sample  
87 in the vial.<sup>16, 17</sup>

88 Proteins do not contribute to the perception of flavor directly,<sup>18</sup> however the existence of  
89 protein-flavor interactions can indirectly impact the availability of volatile aroma compounds  
90 through selective binding that changes the intensity and characteristic profiles of food flavor.  
91 Understanding the nature of such interactions is therefore of great interest to the manufacturing  
92 industry in particular during the formulation of protein based foods that contain flavor active  
93 components. This study aims to provide fundamental insight into the partitioning behaviour of  
94 several key volatile compounds derived from botanical sources. Several of the compounds  
95 show levels of bioactivity that make them potential functional ingredients, and these have not  
96 been previously considered in flavor interaction studies. Furthermore it aims to define the  
97 impact of myofibrillar proteins, as a major component of processed meat products, on volatile  
98 partitioning using model systems and the PRV method to calculate coefficient values.

99

## 100 **MATERIALS AND METHODS**

101 **Materials and Chemicals.** All analytical grade solvents and analytical grade chemicals  
102 (including diacetyl, hexanal, ethyl hexanoate, *D*-limonene, eucalyptol, citral, anethole, thymol,  
103 carvacrol and eugenol) were purchased from Sigma Aldrich (Castle Hill, Australia). Fresh post  
104 rigor portions of pork loin fillet (*Longissimus dorsi*) were purchased from a retail supermarket  
105 (Brisbane, Australia).

106 **Preparation of Standard Solutions.** A composite stock solution containing 10,000  $\mu\text{g/mL}$  of  
107 each volatile in ethanol was prepared and stored at  $-18^\circ\text{C}$ .

108 **Preparation of Myofibrillar Protein Extract.** Myofibrillar protein extraction commenced  
109 within 24 hours of purchase and was carried out in a refrigerated laboratory at 4°C. All visible  
110 fat and connective tissue was removed, before the fillet was passed through a pre-cooled  
111 mechanical grinder fitted with a 3mm plate. Only freshly prepared mince was used for  
112 extraction. A myofibrillar protein suspension was obtained using methodology adapted from  
113 Sun and colleagues.<sup>19</sup> Freshly prepared pork loin mince was homogenized with ten times the  
114 volume of ice-cold 50 mM phosphate buffer (pH 7.5) containing 0.02 % sodium azide (NaN<sub>3</sub>)  
115 using an Ultra-Turrax T25 homogeniser (Ika, Germany) fitted with a 12 mm diameter shaft  
116 attachment at speed mark 5 for 35 s. NaN<sub>3</sub> was employed as an antimicrobial agent and added  
117 at a concentration below which it would interfere with protein binding.<sup>20</sup> The homogenate was  
118 prepared over ice and immediately centrifuged at 4500 g and 4°C for 15 min (Eppendorf  
119 5810R). Separated supernatant was discarded and the remaining pellet resuspended in 2 times  
120 the volume of cold 50 mM phosphate buffer. This process was repeated a further 3 times, with  
121 the final suspension passed through a fine mesh screen to remove residual connective tissue.  
122 Finally, the washed pellet was resuspended in four times the volume of 50 mM phosphate  
123 buffer (pH 7.5) containing 0.02% NaN<sub>3</sub> and 0.5 M NaCl before being centrifuged at 4500 g  
124 and 4°C for 20 min. The supernatant was collected as a solubilized myofibrillar protein  
125 suspension and chilled immediately for use in volatile binding studies. Total protein  
126 concentration was determined on the day of extraction using the colorimetric bicinchoninic  
127 acid method with bovine serum albumin (BSA) as a standard (Pierce BCA Protein Assay Kit,  
128 Thermo Scientific, USA). The reported value is the mean of three measurements.

129 **Sample Preparation.** Partition coefficients for each compound were measured in three  
130 different matrices: deionized water, 50 mM phosphate buffer containing NaCl and an aqueous  
131 protein solution at a concentration of 2 mg/mL.

132 Working solutions of all sample matrices were prepared in a 200 mL stoppered Erlenmeyer  
133 flask with minimal headspace prior to transfer to headspace vials for analysis. To standardize  
134 protein concentration, the myofibrillar extract was brought to room temperature before being

135 diluted for binding studies. Sodium phosphate buffer (50 mM) containing 0.5 M NaCl was  
136 used to reduce the total protein concentration from an initial value of 7.1 mg/mL to a final  
137 working strength of 2 mg/mL. Composite volatile standard solutions were added to working  
138 solutions at a rate of 10 µg/mL. Each flavored working solution was allowed to equilibrate for  
139 a period of 2 hr at 23°C before being transferred into 20 mL headspace vials for analysis.

140 For each matrix, increasing volumes of 50, 100, 200, 500, 1000, 2000, 3000 and 4000 µL were  
141 prepared in 20 mL headspace vials equating to β phase ratios of 399, 199, 99, 39, 19, 9, 5, 7  
142 and 4 respectively (in triplicate).

143 **Static Headspace Analysis Gas Chromatography (SHA-GC).** The SHA-GC method was  
144 optimised to ensure conditions allowed all compounds to achieve thermodynamic equilibrium.  
145 Individual vials were sampled once, after being thermostated at 35°C (with agitation) for a  
146 period of 60 min.

147 Headspace samples from prepared vials were injected using a 2.5 mL gas-tight headspace  
148 syringe, preheated to 80°C and fitted to an automated Multi Purpose Sampler (MPS2) (Gerstel,  
149 Germany). An injection volume of 1000 µL was made in splitless mode at 200°C and a rate of  
150 400 µL/s following a 1000 µL vial headspace extraction at 200 µL/s. After each injection, the  
151 headspace syringe was flushed for 180 sec with nitrogen to eliminate any residual analytes.

152 Instrumental analysis was conducted using a 6890N gas chromatograph (GC) equipped with a  
153 flame ionisation detector (FID) (Agilent Technologies, Palo Alto, CA, USA). The aroma  
154 compounds were separated in a CARBOWAX capillary column (Alltech 2374, i.d. = 320 µm,  
155 length = 30 m, film thickness = 0.25 µm). Helium (BOC gases ultrahigh purity) was used as  
156 the carrier gas with a linear velocity of 26 cm/s and a flow rate of 1.3 mL/min. The GC oven  
157 temperature program began at 40°C for 1 min before increasing at a rate of 5 °C/min to 200°C.  
158 A ramp of 30°C/min followed to a maximum 240°C and finished with a hold period of 5 min  
159 giving a total time run time of 39.33 min. The detector temperature was set at 300°C.

160 To establish elution order and retention times for compound identification, pure volatiles were  
161 run individually using liquid injection followed by a headspace method to confirm peak  
162 identity. Finally the prepared composite ethanolic standard was analyzed at 40  $\mu\text{g/mL}$  in water,  
163 using the optimised SHA-GC method (described above). Results confirmed baseline separation  
164 of all compounds and revealed the relative volatility of each, indicating their potential for  
165 inclusion in PRV analyses. Method validation and analysis of sample solutions were performed  
166 in triplicate with chromatographic responses recorded as total peak area. Data analysis was  
167 carried out using ChemStation Data Analysis Software (Agilent Technologies).

168 **PRV Data Analysis.** Partition coefficients for each compound were determined by graphing  
169 reciprocal chromatographic peak areas against vial phase ratios and dividing the slope of the  
170 linear regression by the y-intercept. The correlation coefficient was used to determine how  
171 accurately the equation expressed the data and to confirm the concentrations used were within  
172 the required linear range.

173  $K_{g-m}$  values calculated from SHA-GC trials are reported as the mean of three independently  
174 run PRV analyses and K-value calculations plus their standard deviation. Protein retention  
175 effect (R%) is expressed as relative compound volatility in the prepared homogenate compared  
176 to a phosphate salt buffer control. The error bars displayed in Figures 3 and 6 represent a 95%  
177 confidence interval.

178 **Statistical Analyses.** Data analysis was performed using PSPP software (GNU version 0.9.0  
179 2015 for Windows). Partitioning data was subjected to a one-way analysis of variance  
180 (ANOVA) to determine significant differences in volatility, before a Fisher's Least  
181 Significance Difference (LSD) test was applied to identify the effect of individual matrix  
182 solutes on calculated coefficients for each compound ( $p < 0.05$ ).

183

184 **RESULTS AND DISCUSSION**

185 The flavor volatiles selected for PRV trails exhibited a wide range of physicochemical  
186 properties (Table 1). Compounds were chosen due to their purported bioactivity and/or because  
187 of their commercial importance and previous inclusion in binding studies; the latter allowing  
188 for validation of the results obtained for novel compounds in this study, as well as the range of  
189 physicochemical characteristics evaluated, to assist in identifying trends in protein binding  
190 behaviour.

191 Several flavor active botanical products have recently been found to possess significant levels  
192 of bioactivity and are therefore of interest as natural food preservatives, in addition to their  
193 primary flavorant capacity. These include native Australian plant ingredients which contain  
194 high levels of essential oils and aroma volatiles that are thought to be responsible for such  
195 efficacy.<sup>21</sup> Lemon myrtle for example contains high levels of the VOC citral, an isomeric  
196 mixture of two aldehydes neral and geranial, which have demonstrated antimicrobial activity  
197 against a range of gram positive and gram negative bacteria yeast and mould.<sup>22</sup> Anise myrtle  
198 in comparison contains appreciable amounts of anethole as the predominant flavor volatile  
199 however has shown a similar range of bioactivity.<sup>23</sup> Other VOC responsible for the distinctive  
200 flavor profiles of more traditional and perhaps widely utilised herbs have also been confirmed  
201 as possessing such antimicrobial effects in food systems. These include thymol,<sup>24</sup> carvacrol<sup>21</sup>  
202 and eugenol<sup>25</sup> which are the key volatile components in thyme, oregano and cloves  
203 respectively.

204 A composite ethanolic stock solution was utilized for investigations as initial efforts using  
205 propylene glycol, a common solvent found in commercial flavorings and many other  
206 interaction studies, was unsuccessful due to the relative insolubility of *D*-limonene.

207 Preparation of the pork loin fillet and subsequent myofibrillar extraction took place under  
208 refrigerated conditions, and over ice, to prevent temperature related protein degradation.  
209 Following extraction and prior to binding studies, the homogenate was diluted to standardize  
210 the protein concentration, enable comparisons with other literature and facilitate handling by  
211 decreasing the foaming potential.

212 **Application of PRV to determine gas-matrix partition coefficient K.** The volatility of  
213 compounds in selected matrices was established by applying the principles underpinning PRV  
214 analyses.<sup>26</sup> In this indirect analytical method the partition or distribution coefficient (K) is  
215 calculated based on the relationship between the reciprocal chromatographic peak area at  
216 equilibrium (A) and the phase ratio ( $\beta$ ) of the vial containing sample solution:

217

$$219 \quad \frac{1}{A} = \frac{1}{f_i C_s} K + \frac{\beta}{f_i C_s} \quad [1]$$

218

$$220 \quad \beta = \frac{V_g}{V_m} \quad [2]$$

221

222 where  $f_i$  is the proportional factor,  $C_s$  is the initial volatile concentration in the matrix,  $V_g$  is the  
223 vial headspace volume and  $V_m$  the sample matrix volume. Eq. 1 with two unknown variables  
224 of phase ratio ( $\beta$ ) and peak area (A) corresponds to a linear equation which can be simplified  
225 and expressed as:

226

$$227 \quad \frac{1}{A} = a\beta + b \quad [3]$$

228

229 with  $a = (K/f_i C_s)$  and  $b = (1/f_i C_s)$ . The partition coefficient (K) is therefore able to be  
230 calculated (Eq. 4) using values for  $a$  (slope) and  $b$  (y-intercept) which are obtained by plotting  
231  $1/A$  against  $\beta$  within the verified linear region:

232

$$233 \quad K = \frac{a}{b} \quad [4]$$

234

235 Table 2 illustrates how the partition coefficient was determined from measured peak areas  
236 using the above approach and provides a comparative overview of the data generated for  
237 thymol, hexanal and ethyl hexanoate during the PRV calculation process.

238 For the purpose of this study we have chosen to express the partitioning of each flavor  
239 compound as the gas-matrix ( $K_{g-m}$ ) coefficient, so in terms of its release from the matrix. Hence  
240 a larger the  $K_{g-m}$  value indicates a higher degree of volatility and resulting headspace  
241 concentration. A number of authors<sup>26-28</sup> report the alternate matrix-gas coefficient ( $K_{m-g}$ )  
242 instead as a measure of retention. To enable comparisons of partitioning data between studies  
243 applying different expression approaches, the coefficients can simply be converted using the  
244 following equation:

245

$$246 \quad K_{m-g} = \frac{1}{K_{g-m}} \quad [5]$$

247

248 Partition coefficients for each compound were measured in three different matrices; deionized  
249 water, 50 mM phosphate buffer containing NaCl and an aqueous protein solution at a  
250 concentration of 2 mg/mL. Evaluation in water alone enabled the calculation of a compound's  
251 volatility under experimental conditions commonly utilised by other researchers whilst the  
252 latter pair allowed the retention effect of myofibrillar protein on each volatile to be reported.  
253 Retention effect is routinely expressed as % retention (R%) in flavor interaction studies<sup>13, 29-31</sup>  
254 and defined as the relative difference in the partition coefficient of an aroma compound in the  
255 presence of a solute such as protein with that measured in water or an appropriate control (Eq.  
256 6). The control in this case being the salt phosphate buffer which is required to enable the  
257 extracted myofibrillar proteins to retain their native structure and remain soluble in an aqueous  
258 solution.

259

$$260 \quad \% \text{ Retention (R\%)} = \frac{K_c - K_p}{K_c} \times 100 \quad [6]$$

261

262 where  $K_c$  and  $K_p$  are the gas-matrix partition coefficients of the flavor volatile in a control and  
263 the protein solution respectively.

264 **SHA-GC and PRV Method Development.** A number of different parameters were trialed  
265 during the development of the final optimised SHA-GC method to maximise the quality of the  
266 chromatography for the 11 different compounds. Also to ensure the magnitudes and ranges of  
267 the obtained peaks were sufficient to enable the use of PRV data analyses. Of particular  
268 importance was maximising the peak area differences between vials to improve accuracy, and  
269 achieving a minimum 1.12 ratio between the largest ( $A_2$ ) and smallest ( $A_1$ ) peak area recorded  
270 in a series. This value is considered to be the lowest reasonable ratio of  $A_2/A_1$  for reliability<sup>32</sup>  
271 and so was monitored closely for the lower volatility compounds such as eugenol, thymol and  
272 carvacrol. As shown in Table 2 the ratio was easily achieved for ethyl hexanoate and hexanal  
273 which had values of 18.82 and 9.58 respectively whilst thymol recorded a much lower value  
274 of 2.01. In general terms, if  $K_{g-m}$  is large then a wide range of peak areas will be obtained.<sup>17</sup>  
275 Comparing the final reported partition coefficients for ethyl hexanoate and hexanal with  
276 thymol validates this fact with thymol returning a considerably lower coefficient than the other  
277 two analytes.

278 GC conditions evaluated during this stage included injection volume (1000, 2500  $\mu$ l), split ratio  
279 (50:1, 20:1, splitless), column flow rate (1.0, 1.5 mL/min), injection speed (200, 400, 600  $\mu$ L/s)  
280 and headspace syringe temperature (40, 80°C). An alternate column was also tested (Phenom  
281 Zebron ZB5, i.d. = 250  $\mu$ m, length = 35 m, film thickness = 0.25  $\mu$ m) however baseline  
282 separation between *D*-limonene and eucalyptol could not be achieved given the close proximity  
283 of their retention times using this particular phase and dimensions.

284 Although volatile matrix concentrations of 40  $\mu\text{g/mL}$  were utilised to determine retention times  
285 initially, this was decreased to 10  $\mu\text{g/mL}$  following an observation of working solution  
286 instability. The issue presented as solution turbidity initially and evolved into surface droplet  
287 formation over a number of hours in static storage. Subsequent calculations estimating the  
288 theoretical maximum solubility of each volatile in the composite solution confirmed that a  
289 number exceeded the concentration at which complete dissolution was possible.

290 During PRV analyses, it is critical that each compound is considered to be at infinite dilution  
291 without any interaction effects, and so behaves as an ideal solution. That is where the activity  
292 coefficient equals unity, or for very dilute solutions where Henry's law is obeyed.<sup>26</sup> The  
293 working solution that is decanted into a series of 24 headspace vials (i.e. 8 different volumes  
294 in triplicate) must be absolutely homogenous and identical in composition to ensure that any  
295 changes in obtained peak areas are attributed to the difference in the vial phase ratio  $\beta$ .  
296 Reducing the matrix VOC concentration to 10  $\mu\text{g/mL}$  for each compound satisfied the  
297 calculated theoretical requirements for complete dissolution whilst still enabling sufficient  
298 signal strength and adequate peak areas for calculations. The reduction also adjusted the  
299 concentrations to well below the general recommendation for SHA-GC of less than 0.1-1%  
300 (1000 – 10,000  $\mu\text{g/mL}$ ) where interaction are believed to be insignificant.<sup>32</sup>

301 A common practice to verify infinite dilution experimentally is to measure the partitioning of  
302 a single volatile alone and compare this with the value and underlying data when that same  
303 compound is analyzed in the company of others.<sup>15, 16</sup> Results shown in Figure 1a,b validate that  
304 conditions of infinite dilution were achieved with partition coefficient values of 0.0133 and  
305 0.0130 obtained when eucalyptol was analyzed individually and in a composite aqueous  
306 solution containing the other analytes. Importantly, the graphs also clearly illustrate that the  
307 condition of regression linearity were met with correlation coefficients ( $R^2$ ) for the generated  
308 equation approaching 1.0, and comparable to values published elsewhere<sup>15, 16, 26, 27</sup> which are  
309 generally greater than 0.96.

310 The selection of appropriate matrix volumes or more specifically the resulting vial  $\beta$  values is  
311 highly important in PRV analyses and based primarily on volatility.<sup>17</sup> As such, a wide range of  
312 phase ratios were evaluated due to the large variation in expected partitioning behaviour  
313 between included compounds.

314 When determining  $\beta$  value range, the effect of sample volume on headspace concentration and  
315 the resulting peak area is considered. Although there is an objective to maximise the ratio of  
316 biggest to smallest peak areas, caution must be exercised when selecting the largest matrix  
317 volume, and consequently smallest  $\beta$  value for analysis. This is because the headspace  
318 concentration above a sample will rise steadily with increasing vial volume up until a point at  
319 which saturation occurs.<sup>17</sup> Because PRV trials are fundamentally based on the relationship  
320 between a series of different vial volumes and their resulting peak area, it is imperative that the  
321 chosen ratios satisfy this dependant relationship (Figure 2). Once headspace concentration  
322 reaches saturation, PRV analyses cannot be applied and alternate static headspace methods  
323 such vapour phase calibration (VPC) and liquid calibration static headspace (LC-SH) must be  
324 used.<sup>15</sup>

325 Although the relationship between temperature and volatile partitioning is well established,  
326 control of working solution temperature during the decanting of the bulk flavored matrix into  
327 the PRV series of headspace vials is not addressed in method literature. In addition,  
328 recommendations to minimise headspace above flavored working solutions are not made; a  
329 factor that would enable the early partitioning of volatiles prior to the preparation of headspace  
330 vials of controlled VOC concentration and phase ratios. As a consequence, details of such  
331 experimental conditions are not made available routinely for published PRV trials.

332 Due to relatively low levels of solubility, sonication was considered to assist the dissolution of  
333 some compounds into the aqueous matrix. Introducing this process inadvertently resulted in  
334 unexplained variations in series peak area magnitudes between replicates (Figure 3), an effect  
335 that was ultimately attributed to variations in the working solution temperature during  
336 decanting. Filling headspace vials immediately following a period of sonication (40 min) that

337 raised the working solution temperature (40°C), resulted in lower peak areas than a solution  
338 that had been allowed to cool to ambient (23°C). At the cooler temperature, a higher  
339 concentration of volatile remained in solution in accordance with Henry's Law for detection  
340 during headspace analysis. This observation holds great significance as maximising peak area  
341 or detector response is not only highly desirable, but essential in cases of lower volatility and  
342 a key focus during PRV method optimisation activities.<sup>13, 17</sup>

343 Interestingly the final calculated partition coefficient for the trial decanted at 40°C was 0.1615  
344 while the cooler fill at 23°C was 0.1490. So although the matrix concentration and resulting  
345 peak areas were reduced due to temperature induced loss of VOC into the headspace, the actual  
346 partition coefficients were comparable. The result further verifies that the condition of infinite  
347 dilution was satisfactorily met and demonstrates the underlying principle of PRV methodology.  
348 That is that K values can be reliably calculated by establishing the relationship between vial  
349 phase ratio and the inverse of recorded peak area provided the matrix composition is kept  
350 constant within a series. The amount of VOC in the solution is irrelevant.

351 Although SHA-GC conditions were optimised to include all of the nominated volatiles, d-  
352 limonene was removed before matrix effects were established due to difficulties in obtaining  
353 satisfactory data for PRV analysis. Greater peak area magnitudes during SHA-GC method  
354 development and published partition coefficients of 0.2510 at 30°C<sup>16</sup> and 1.5 at 35°C<sup>33</sup> in a  
355 water and saline solution respectively confirm the compound to be highly volatile and therefore  
356 subject to a common PRV method limitation.<sup>34</sup>

357 The method incompatibility issues are bought about by a deviation between the ideal  
358 assumptions underlying PRV calculations and the more realistic experimental conditions. As  
359 such, the issue is always present but magnified by situations of high volatility. Choosing large  
360  $\beta$  values as recommended<sup>26, 34</sup> was unsuccessful in alleviating the problem, with regression  
361 analysis returning negative values for the y-intercept and so consequently  $K_{g-m}$  constant.

362 **Impact of matrix solutes on volatile partitioning.** Partition coefficients of the ten volatiles  
363 was established at 35°C using the optimised combined SHA-GC and PRV methodology that  
364 had been experimentally validated for suitability and precision. Collected data was subjected  
365 to linear regression analysis as described in Eq. 1-3 and the gas-matrix partition coefficient  
366 calculated using Eq. 4. Regression models fit well to the experimental data in all cases with  
367 correlation coefficients higher than 0.968 for each of the included compounds. The measured  
368  $K_{g-m}$  values are summarised in Table 3 and represent the volatility of each flavor compound in  
369 water or the corresponding matrix. Reported figures from similar comparable studies using  
370 water matrices have also been included where possible alongside calculated experimental  
371 figures for further validation of the method, with the expectation that a higher temperature of  
372 determination will return larger values and those utilising conditions less than 35°C will be  
373 lower. All comparison partition coefficients were obtained using the PRV method as previous  
374 studies have shown appreciable differences between figures obtained using alternate indirect  
375 headspace methods.<sup>15</sup>

376 Gas-matrix partition coefficients in water varied between compounds with the ester ethyl  
377 hexanoate demonstrating the greatest volatility ( $K_{g-m} = 0.0562$ ) and eugenol, a member of the  
378 phenylpropanoid family the lowest ( $K_{g-m} = 0.00097$ ). The behaviour of flavor volatiles in water  
379 can be attributed to their physicochemical attributes, namely their saturated vapour pressure,  
380 solubility in water and molecular weight.<sup>35</sup> This theory has been best demonstrated in cases  
381 where a homologous series of compounds, such as ketones have been analyzed where the  
382 differences between each individual volatile are distinct, measureable and well understood. For  
383 example authors have been able to establish a strong linear relationship between increasing  
384 carbon chain length, the related decrease in polar characteristic and reduction in measured  $K_{g-}$   
385  $m$  values.<sup>16, 27</sup> Unfortunately the effect of the listed compound attributes is not as easily defined  
386 here, with the selected volatiles representing a number of different chemical families, their  
387 functional groups and combined other individual physicochemical characteristics.  
388 Nevertheless, the data agrees with published values and general findings from other PRV

389 studies, such as the hydrophilic diacetyl having a low degree of volatility when compared to  
390 that of ethyl hexanoate which is considered to have mid-range hydrophobicity.<sup>28</sup> Further, the  
391 results for the two sets of included stereo or spacial isomers: neral and geranial plus thymol  
392 and carvacrol, are comparable. Between them these pairs share identical chemical formulae  
393 and bond structure, however, possess different geometrical positions of atoms in space. As  
394 such similar  $K_{g-m}$  values would be expected based on their shared physiochemical properties,  
395 which is indeed confirmed.

396 Perhaps the most valuable outcome of establishing volatility in water was enabling the effect  
397 of the non-volatile solutes used in the phosphate buffer to be identified; a vital first step in  
398 determining any binding or retention effects of the extracted myofibrillar protein. During the  
399 protein extraction process, a chilled 50 mM sodium phosphate buffer solution adjusted to a  
400 final pH of 7.5 was used. The composition of which prevented any denaturation or  
401 conformation changes from the proteins' native structure. The buffer therefore preserving the  
402 structure dependant functionality which would otherwise be modified in response to  
403 environmental conditions.

404 Skeletal muscle proteins can be broadly categorised into the three main classes: sarcoplasmic,  
405 myofibrillar and connective tissue, with each group differing in their solubility in aqueous salt  
406 solutions.<sup>5</sup> A fact that is exploited during the extraction process to facilitate the collection of  
407 the desired fraction. In this case the target being the most abundant portion, the myofibrillar  
408 proteins. The sarcoplasmic proteins which are soluble in water or dilute salt solutions are  
409 washed out of the minced muscle during the initial phases of rinsing before 0.5 M NaCl is  
410 added to the phosphate buffer. The ionic strength is adjusted at this point because myofibrillar  
411 proteins demonstrate solubility only in concentrated salt solutions. Hence, during the final  
412 washing steps the myofibrillar proteins are solubilised from the formally collected pellet into  
413 the aqueous buffer and isolated from any remaining and insoluble connective tissue.

414 This salt sodium phosphate buffer at pH 7.5 therefore represented the control or blank matrix  
415 for the subsequent protein interaction study. When compared to water, all but one of the

416 volatiles returned a higher partition coefficient indicating that the matrix solutes increased the  
417 headspace concentration by generating a repulsion effect. The magnitude and direction of the  
418 partitioning change is best illustrated using the calculated retention percentage (Figure 4)  
419 obtained using Eq. 6. Excluding eugenol which had only a small positive retention effect,  
420 negative values were recorded for all volatiles ranging from -13.89% to -66.80%.

421 The increased partition or distribution coefficient is attributed to the inclusion of sodium  
422 chloride in the buffer solution which in this case operates primarily as a functional additive to  
423 solubilise the myofibrillar proteins in an aqueous environment. Salts however are extensively  
424 used elsewhere in headspace gas chromatography for another reason, and that is to improve  
425 headspace sensitivity. Along with pH adjustments and derivatization, the addition of  
426 compounds like NaCl are used to adjust the composition of the matrix and increase volatile  
427 concentration in the headspace or gas phase.<sup>32</sup> In an effect referred to as salting out in analytical  
428 chemistry, salts in aqueous solutions decrease the solubility of polar organic volatiles in the  
429 sample matrix and promote their transfer into the headspace.<sup>36</sup> It is for these reasons that salt  
430 levels must be carefully maintained in flavor-protein binding studies and their impact on  
431 volatile partitioning addressed during reporting. Comparing  $K_{g-m}$  values measured in water  
432 against those in buffer shows this modification of compound volatility is significant for seven  
433 out of the 10 included compounds. Although carvacrol returned a larger retention percentage  
434 than some other analytes, greater variations in the underlying data that is symptomatic of low  
435 volatility in PRV analyses prevented this value from rating significance.

436 The effect of protein on partitioning is remarkably different to that of sodium chloride. In fact  
437 a decrease in volatility when compared to the buffer values is seen for all compounds when the  
438 myofibrillar homogenate was introduced into the matrix at a final concentration of 2 mg/mL.  
439 Unlike salt which exhibits an indirect effect by changing the characteristic of the matrix,  
440 compound retention by proteins are understood to result from direct interactions with the flavor  
441 molecule itself, the strength of which is dependent on the chemical properties of both parties  
442 and the environmental conditions.<sup>13</sup> The positive retention values (Figure 5) confirmed that the

443 pork muscle extract was in fact capable of modifying partitioning by imparting a binding effect  
444 as was hypothesised based on available literature.

445 The measured reduction in gas phase concentration is again variable between compounds with  
446 the citral isomers neral and geranial demonstrating the greatest retention effect with figures of  
447 55.88% and 59.09% recorded. Ethyl hexanoate followed with a decreased headspace presence  
448 of just over one third of the original value before the monoterpene phenol isomers of carvacrol  
449 and thymol placed with reductions of 33.68% and 28.57% respectively. The lowering of  $K_{g-m}$   
450 values adjusts the partition coefficient to that comparable with water for many compounds,  
451 with the extracted protein mitigating the effects of the added salt in the buffer. This overall  
452 trend is clearly evident when a direct comparison of the partition coefficients is made by  
453 graphing the data for all of the included matrices and grouping results by individual flavor  
454 compound (Figure 6). Presenting the data in this fashion also facilitates an appreciation of the  
455 magnitude of partitioning differences between the included analytes. Ethyl hexanoate leads as  
456 the most volatile followed by a mid-range group which includes anethole, eucalyptol and  
457 hexanal. The remaining compounds eugenol, carvacrol, thymol, geranial, neral and diacetyl  
458 show a far smaller headspace presence.

459 Under certain situations flavor compounds are able to form strong irreversible covalent bonds  
460 with proteins via amide and ester formation and the condensation of aldehydes such as the  
461 included hexanal with amino ( $\text{NH}_2$ ) and sulfhydryl groups.<sup>18</sup> However as with most proteins,  
462 the remainder of the binding is likely the results of weak and reversible interactions that involve  
463 hydrophobic associations, ionic attraction and hydrogen bonds.<sup>3, 37</sup> Therefore it is expected that  
464 in general the amount of flavor absorbed to the protein surface increases with greater levels of  
465 shared hydrophobicity.<sup>38</sup> This is evident in the data when comparing results for the hydrophilic  
466 molecule diacetyl with the hydrophobic geranial and carvacrol.

467 Protein-flavor interactions are site specific meaning that binding only occurs when compatible  
468 regions are available on both molecules. As a consequence they are negatively affected by any  
469 structural protein-protein bonds such as those which are responsible for maintaining the

470 molecules three dimensional structure. Adversely they are assisted by thermal, physical and  
471 chemical denaturation of the protein that corresponds to a loss of order that opens up access to  
472 the internal surface.<sup>2</sup> Examples of which in relation to food and meat products could include  
473 the addition of salts, adjustment of acidity, mincing, freezing and cooking.

474 Although a limited number of similar flavor binding studies using extracted skeletal muscle  
475 proteins have been undertaken, very few direct comparisons of specific data can be made due  
476 to significant differences in the experimental methodology applied. For example the protein  
477 fraction studied,<sup>11</sup> the processing history of the muscle from which the extract was obtained<sup>12</sup>  
478 and the selected range of volatile compounds studied. Matrix conditions such as composition  
479 (e.g. ionic strength, pH) and post-extraction protein processing (e.g. freezing) also varied  
480 greatly in deliberate strategies to investigate relevant food formulation and processing  
481 conditions that are known to induce changes in protein conformation. The result being a  
482 modification in three dimensional structure that changes the characteristics of the exposed and  
483 therefore available binding sites for volatile interactions.<sup>39</sup> Perhaps the only appropriate direct  
484 comparison from this study would be the retention value of 24.59% recorded for the aldehyde  
485 hexanal which had been previously reported under similar experimental conditions as  
486 approximately 20% in the presence of pork myofibrillar proteins.<sup>12</sup>

487 Nevertheless, the same general finding was common amongst all studies. Skeletal muscle  
488 proteins interact with volatile compounds to change their partitioning behaviour and ultimately  
489 their presence in the headspace. The direction and magnitude of the change varies considerably  
490 depending on the exact circumstances, however it can be concluded that meat derived proteins  
491 as food matrix components will affect the availability of volatile flavor compounds for  
492 perception by consumers.

493 The current study demonstrates the successful application of SHA-GC partnered with PRV  
494 analyses to the investigation of binding of flavor compounds by protein. An indirect headspace  
495 methodology was applied to establish the partitioning behaviour of commonly utilised flavor  
496 volatiles along with selected novel, plant derived aroma compounds of increasing food industry

497 importance in the presence of meat proteins. The pork myofibrillar extract was found to bind  
498 all of the volatiles studied to an extent and impact their partitioning in model systems. The  
499 study also illustrated a known limitation of the PRV methodology in overcoming non-linearity  
500 for more volatile compounds, such as d-limonene in this case, at high  $\beta$  values.<sup>14</sup>

501 Understanding the relationship between non-volatile proteins and volatile flavor compounds,  
502 two important groups of food matrix components, is essential for maximising flavor delivery  
503 and controlling aroma perception by consumers. Future research to validate the mechanisms  
504 of volatile binding by muscle proteins along with studies to measure the impact of various food  
505 processing parameters would be of great value to both the scientific community and  
506 manufacturing industry alike.

507

#### 508 **ABBREVIATIONS USED**

509 ANOVA, analysis of variance; BSA, bovine serum albumin; FID, flame ionization detector;  
510 GC, gas chromatograph; LC-SH, liquid calibration static headspace; LSD, least significant  
511 difference; PRV, phase ratio variation; SHA, static headspace analysis; SHA-GC, static  
512 headspace analysis-gas chromatography; VOC, volatile organic compound; VPC, vapour  
513 phase calibration

514

#### 515 **ACKNOWLEDGEMENTS**

516 This research project was supported by the Queensland Government's Department of  
517 Agriculture and Fisheries, the University of Queensland and the University of Adelaide. The  
518 authors wish to acknowledge and thank Agilent Technologies and Dr Anne Tromelin for their  
519 invaluable technical advice during method optimisation.

## REFERENCES

1. Van Ruth, S. M.; Roozen, J. P. Delivery of flavours from food matrices. In *Food flavour technology*, Sheffield Academic Press: Sheffield, 2002; pp 167-184.
2. Reineccius, G. *Flavor chemistry and technology*. 2nd ed.; CRC Press: Boca Raton, 2006.
3. Tromelin, A.; Andriot, I.; Guichard, E. Protein-flavour interactions. In *Flavour in food*, Woodhead Publishing Limited: Cambridge, 2006; pp 172-207.
4. Guichard, E. Flavour retention and release from protein solutions. *Biotechnol. Adv.* **2005**, *24*, 226-229.
5. Lawrie, R. A.; Ledward, D. A. Chemical and biochemical constituents of muscle. In *Lawrie's meat science*, 7th ed.; Woodhead Publishing Limited: Cambridge, 2006; pp 75-127.
6. Kauffman, R. G. Meat composition. In *Meat science and applications*, CRC Press: Boca Raton, 2001; pp 1-18.
7. Damodaran, S.; Kinsella, J. E. Binding of carbonyls to fish actomyosin. *J. Agric. Food. Chem.* **1983**, *31*, 856-859.
8. Pérez-Juan, M.; Flores, M.; Toldrá, F. Binding of aroma compounds by isolated myofibrillar proteins: Effect of protein concentration and conformation. *Food Chem.* **2007**, *105*, 932-939.
9. Pérez-Juan, M.; Flores, M.; Toldrá, F. Effect of ionic strength of different salts on the binding of volatile compounds to porcine soluble protein extracts in model systems. *Food Res. Int.* **2007**, *40*, 687-693.
10. Pérez-Juan, M.; Flores, M.; Toldrá, F. Effect of pork meat proteins on the binding of volatile compounds. *Food Chem.* **2008**, *108*, 1226-1233.
11. Gianelli, M. P.; Flores, M.; Toldra, F. Interactions of soluble peptides and proteins from skeletal muscle on the release of volatile compounds. *J. Agric. Food. Chem.* **2003**, *51*, 6828-6834.
12. Perez-Juan, M.; Flores, M.; Toldra, F. Model studies on the efficacy of protein homogenates from raw pork muscle and dry-cured ham in binding selected flavor compounds. *J. Agric. Food. Chem.* **2006**, *54*, 4802-4808.

13. Benjamin, O.; Leus, M.; Everett, D. W. Static headspace analysis of volatile compounds released from  $\beta$ -lactoglobulin-stabilized emulsions determined by the phase ratio variation method. *Food Res. Int.* **2011**, *44*, 417-424.
14. Tromelin, A.; Ayed, C.; Lubbers, S.; Pagès-Hélary, S.; Andriot, I.; Guichard, E. Proposed alternative phase ratio variation method for the calculation of liquid–vapour partition coefficients of volatiles. *J. Chromatogr. A* **2012**, *1263*, 158-168.
15. Athès, V.; Peña y Lillo, M.; Bernard, C.; Pérez-Correa, R.; Souchon, I. Comparison of experimental methods for measuring infinite dilution volatilities of aroma compounds in water/ethanol mixtures. *J. Agric. Food. Chem.* **2004**, *52*, 2021-2027.
16. Savary, G.; Guichard, E.; Doublier, J.-L.; Cayot, N. Mixture of aroma compounds: determination of partition coefficients in complex semi-solid matrices. *Food Res. Int.* **2006**, *39*, 372-379.
17. Ettre, L. S.; Kolb, B. Headspace-gas chromatography: the influence of sample volume on analytical results. *Chromatographia* **1991**, *32*, 5-12.
18. Kühn, J.; Considine, T.; Singh, H. Interactions of milk proteins and volatile flavor compounds: implications in the development of protein foods. *J. Food Sci.* **2006**, *71*, 72-82.
19. Sun, L.-C.; Yoshida, A.; Cai, Q.-F.; Liu, G.-M.; Weng, L.; Tachibana, K.; Su, W.-J.; Cao, M.-J. Mung bean trypsin inhibitor is effective in suppressing the degradation of myofibrillar proteins in the skeletal muscle of blue scad (*decapterus maruadsi*). *J. Agric. Food. Chem.* **2010**, *58*, 12986-12992.
20. Fares, K.; Landy, P.; Guillard, R.; Voilley, A. Physicochemical interactions between aroma compounds and milk proteins: effect of water and protein modification. *J. Dairy Sci.* **1998**, *81*, 82-91.
21. Veldhuizen, E. J.; Tjeerdsma-van Bokhoven, J. L.; Zweijtzer, C.; Burt, S. A.; Haagsman, H. P. Structural requirements for the antimicrobial activity of carvacrol. *J. Agric. Food. Chem.* **2006**, *54*, 1874-1879.
22. Wilkinson, J. M.; Hipwell, M.; Ryan, T.; Cavanagh, H. M. A. Bioactivity of *backhousia citriodora*: antibacterial and antifungal activity. *J. Agric. Food. Chem.* **2003**, *51*, 76-81.
23. De, M.; De, A. K.; Sen, P.; Banerjee, A. B. Antimicrobial properties of star anise (*Illicium verum* Hook f). *Phytotherapy Research* **2002**, *16*, 94-95.
24. Sivropoulou, A.; Papanikolaou, E.; Nikolaou, C.; Kokkini, S.; Lanaras, T.; Arsenakis, M. Antimicrobial and cytotoxic activities of origanum essential oils. *J. Agric. Food. Chem.* **1996**, *44*, 1202-1205.

25. Sanla-Ead, N.; Jangchud, A.; Chonhenchob, V.; Suppakul, P. Antimicrobial activity of cinnamaldehyde and eugenol and their activity after incorporation into cellulose-based packaging Films. *Packag. Technol. Sci.* **2012**, *25*, 7-17.
26. Ettre, L. S.; Welter, C.; Kolb, B. Determination of gas-liquid partition coefficients by automatic equilibrium headspace-gas chromatography utilizing the phase ratio variation method. *Chromatographia* **1993**, *35*, 73-84.
27. Jouquand, C.; Ducruet, V.; Giampaoli, P. Partition coefficients of aroma compounds in polysaccharide solutions by the phase ratio variation method. *Food Chem.* **2004**, *85*, 467-474.
28. Heilig, A.; Çetin, S.; Erpenbach, K.; Höhn, J.; Hinrichs, J. Inherent and process-induced hydrophobicity influences aroma retention in fat-free dairy matrices. *Int. Dairy J.* **2011**, *21*, 696-702.
29. Nongonierma, A. B.; Colas, B.; Springett, M.; Quéré, J.-L. L.; Voilley, A. Influence of flavour transfer between different gel phases on perceived aroma. *Food Chem.* **2007**, *100*, 297-305.
30. Nongonierma, A. B.; Springett, M.; Le Quéré, J.-L.; Cayot, P.; Voilley, A. Flavour release at gas/matrix interfaces of stirred yoghurt models. *Int. Dairy J.* **2006**, *16*, 102-110.
31. Martuscelli, M.; Savary, G.; Pittia, P.; Cayot, N. Vapour partition of aroma compounds in strawberry flavoured custard cream and effect of fat content. *Food Chem.* **2008**, *108*, 1200-1207.
32. Kolb, B.; Ettre, L. S. *Static headspace-gas chromatography: theory and practice*. John Wiley & Sons: New Jersey, 2006.
33. Jouquand, C.; Malhiac, C.; Grisel, M. Determination of specific interactions between aroma compounds and xanthan/galactomannan mixtures. In *Dev. Food Sci.*, Elsevier: Amsterdam, 2006; Vol. 43, pp 421-424.
34. Tromelin, A.; Lubbers, S.; Andriot, I.; Guichard, E. Improvement of partition coefficients determination of aroma compounds in food matrices by the phase ratio variation method. In *Flavour Science*, Academic Press: San Diego, 2014; pp 401-406.
35. Amoore, J. E.; Buttery, R. G. Partition coefficient and comparative olfactometry. *Chem. Senses* **1978**, *3*, 57-71.
36. Yang, X.; Peppard, T. Solid-phase microextraction for flavor analysis. *J. Agric. Food. Chem.* **1994**, *42*, 1925-1930.

37. Guichard, E. Interactions between flavor compounds and food ingredients and their influence on flavor perception. *Food Rev. Int.* **2002**, *18*, 49.
38. Plug, H.; Haring, P. The role of ingredient-flavour interactions in the development of fat-free foods. *Trends Food Sci. Technol.* **1993**, *4*, 150-152.
39. Damodaran, S.; Kinsella, J. E. Flavor protein interactions. Binding of carbonyls to bovine serum albumin: thermodynamic and conformational effects. *J. Agric. Food. Chem.* **1980**, *28*, 567-571.
40. Royal Society of Chemistry. ChemSpider.(<http://www.chemspider.com/>) (19/12/2015).
41. National Center for Biotechnology Information. PubChem Compound Database.(<https://pubchem.ncbi.nlm.nih.gov>) (19/12/2015).
42. Bylaite, E.; Ilgūnaitė, Ž.; Meyer, A. S.; Adler-Nissen, J. Influence of  $\lambda$ -carrageenan on the release of systematic series of volatile flavor compounds from viscous food model systems. *J. Agric. Food. Chem.* **2004**, *52*, 3542-3549.
43. Savary, G.; Hucher, N.; Petibon, O.; Grisel, M. Study of interactions between aroma compounds and acacia gum using headspace measurements. *Food Hydrocolloids* **2014**, *37*, 1-6.
44. Lafarge, C.; Cayot, N.; Hory, C.; Goncalves, L.; Chassefont, C.; Le Bail, P. Effect of konjac glucomannan addition on aroma release in gels containing potato starch. *Food Res. Int.* **2014**, *64*, 412-419.

## FIGURE CAPTIONS

**Figure 1.** Graphical comparison of PRV calculations used to verify that eucalyptol displayed the properties of an ideal solution when evaluated individually (a) within a water matrix and (b) in a composite solution at 35°C, and that the conditions of linearity were met.

**Figure 2.** Relationship between increasing vial volume and resulting peak area for hexanal, with the chosen  $\beta$  values illustrating the plateau effect at higher volumes where the headspace concentration eventually becomes independent of matrix volume.

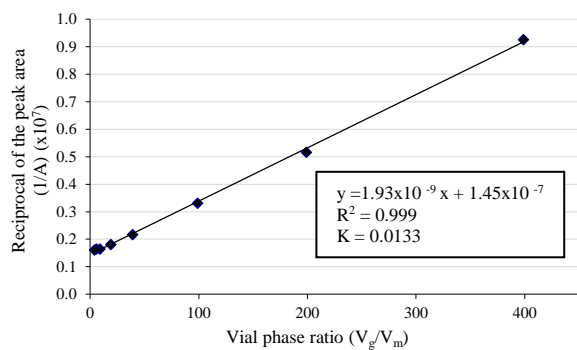
**Figure 3.** Effect of working solution temperature during the filling of headspace vials on the peak areas obtained for anethole in replicate PRV trials.

**Figure 4.** Retention of aroma compounds by a phosphate buffer containing 0.5 M NaCl salt as compared to water at 35°C.

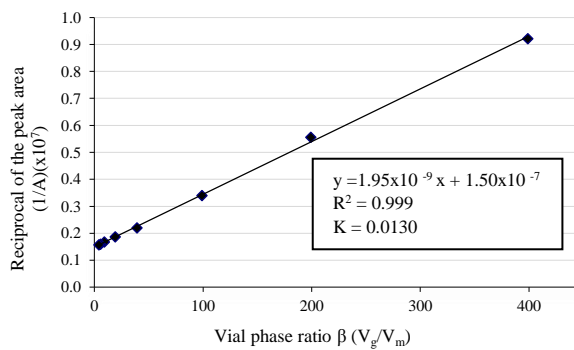
**Figure 5.** Retention of aroma compounds by myofibrillar protein at 2 mg/mL in solution as compared to a phosphate buffer control containing salt at 35°C. Values marked with an asterisk (\*) are significantly different.

**Figure 6.** Comparison of measured  $K_{g-m}$  values between all matrices.

**Figure 1.**



**(a)**



**(b)**

**Figure 2.**

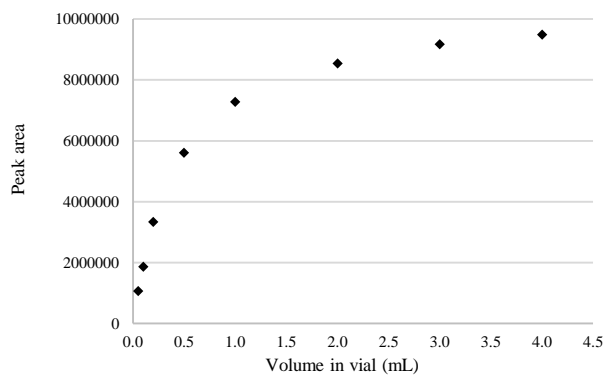


**Figure 3.**

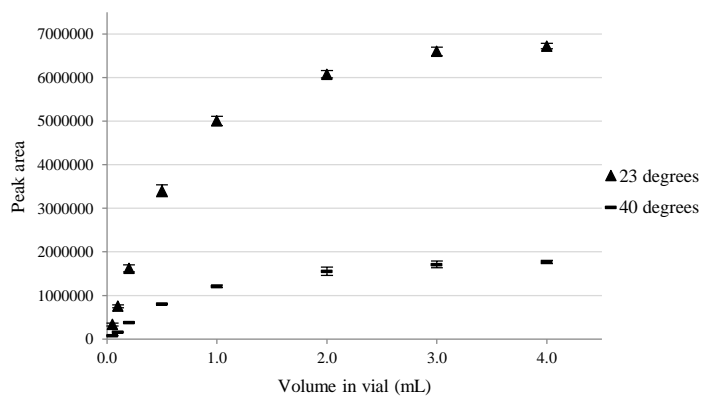


**Figure 4.**

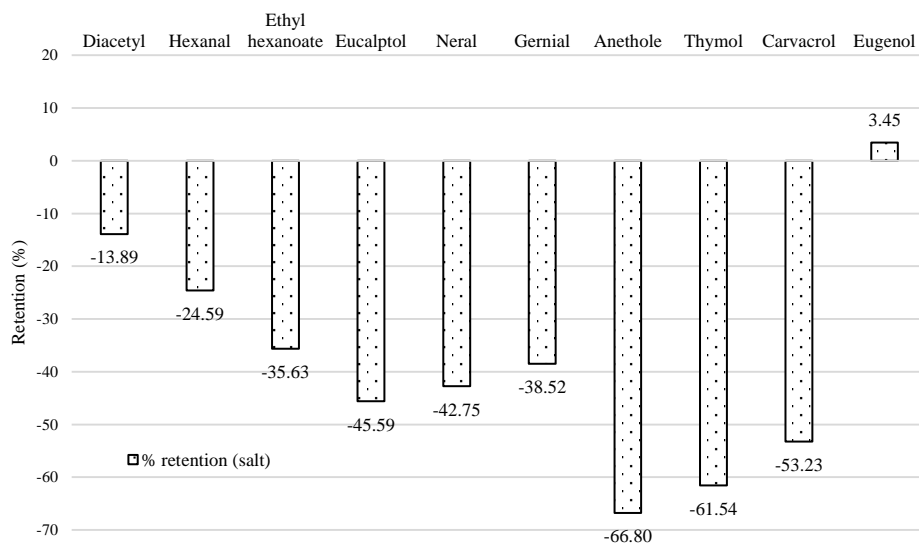


**Figure 5.**

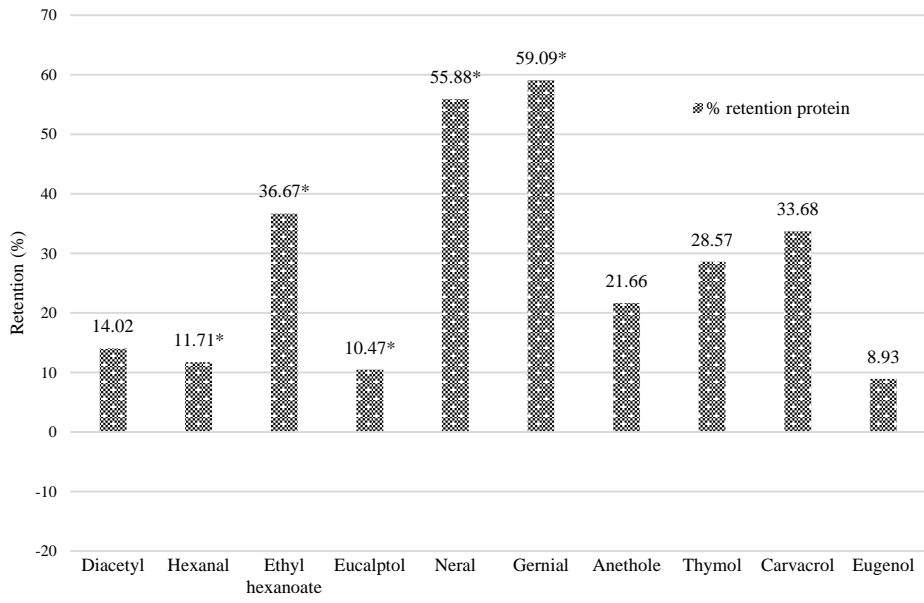


**Figure 6.**

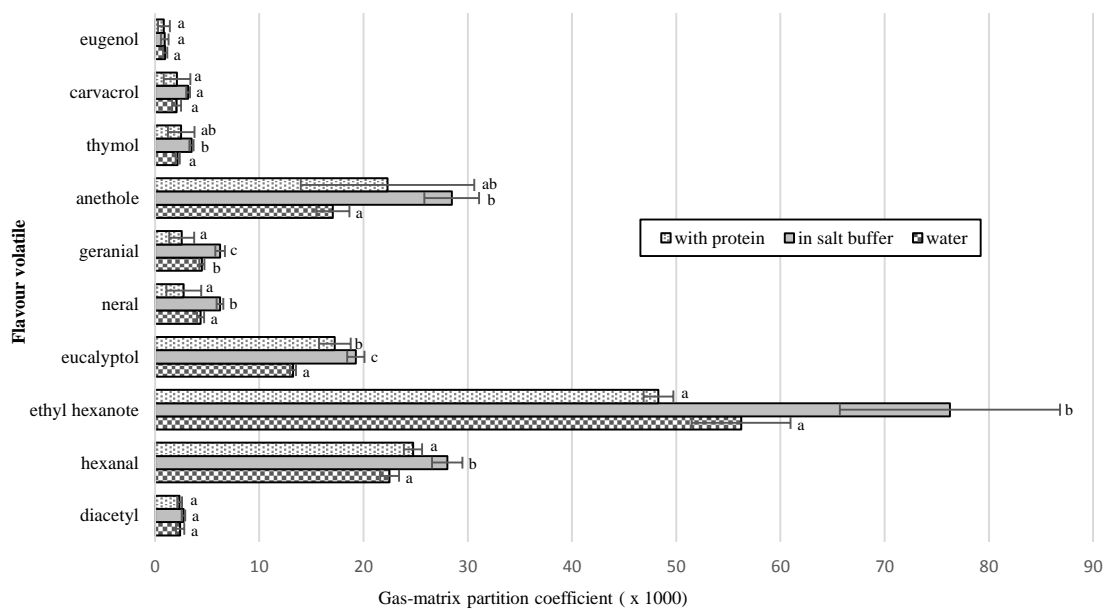


**Table 1. Physicochemical properties and attributes of flavour volatiles.**

flavour compound	CAS	molecular formula	molecular weight (g/mol)	chemical class	solubility in water (mol/L) at 20°C <sup>a</sup>	retention (min)	odor descriptor <sup>b</sup>
diacetyl	431-03-08	C <sub>4</sub> H <sub>6</sub> O <sub>2</sub>	86.09	ketone	0.263	4.414	buttery
hexanal	66-25-1	C <sub>6</sub> H <sub>12</sub> O	100.16	aldehyde	0.022	6.178	green grass, tallow
ethyl hexanoate	123-66-0	C <sub>8</sub> H <sub>16</sub> O <sub>2</sub>	144.21	ester	0.009840	9.623	fruity, pineapple
<i>D</i> -limonene	5989-27-5	C <sub>10</sub> H <sub>16</sub>	136.23	aromatic hydrocarbon	0.00317	8.658	citrus, oranges
eucalyptol	470-82-6	C <sub>10</sub> H <sub>18</sub> O	154.25	cyclic ether	0.00215	8.847	camphor, spicy
neral	106-26-3	C <sub>10</sub> H <sub>16</sub> O	152.24	aldehyde	0.00173	20.328	citrus, lemon
geranial	141-27-5	C <sub>10</sub> H <sub>16</sub> O	152.24	aldehyde	0.00173	21.442	citrus, lemon
anethole	104-46-1	C <sub>10</sub> H <sub>12</sub> O	148.20	phenol	0.00117	23.463	aniseed, liquorice
thymol	89-83-8	C <sub>10</sub> H <sub>14</sub> O	150.22	phenol	0.00261	30.528	herbal, thyme
carvacrol	499-75-2	C <sub>10</sub> H <sub>14</sub> O	150.22	phenol	0.00255	31.021	herbal, oregano
eugenol	95-53-0	C <sub>10</sub> H <sub>12</sub> O <sub>2</sub>	164.20	phenol	0.00443	30.117	herbal, clove

<sup>a</sup>Figures obtained from Discovery Studio Accelrys-Biovia Software

<sup>b</sup>Data obtained using ChemSpider <sup>40</sup> and Pubchem Compound Databases <sup>41</sup>

**Table 2. PRV calculations used to determine the partition coefficient (K) of thymol, hexanal and ethyl hexanoate in water at 35°C.**

compound	volume of solution in vial (μL)	phase ratio (β)	peak area (first replicate)	peak area difference (A <sub>2</sub> /A <sub>1</sub> )	linear regression analysis			partition coefficient (K <sub>g-m</sub> )
					slope (a)	intercept (b)	correlation coefficient (R <sup>2</sup> )	
thymol	50	399	86 065					
	100	199	115 527					
	200	99	137 898					
	400	39	146 179					
	1000	19	157 309	2.01	1.42x 10 <sup>-8</sup>	5.91 x 10 <sup>-6</sup>	0.9909	0.0024
	2000	9	167 088					
	3000	5.7	171 773					
	4000	4	173 047					
hexanal	50	399	1 058 583					
	100	199	1 997 229					
	200	99	3 337 134					
	400	39	5 766 335					
	1000	19	7 464 918	9.58	2.13 x 10 <sup>-9</sup>	9.02 x 10 <sup>-8</sup>	0.9996	0.0236
	2000	9	9 015 769					
	3000	5.7	9 581 347					
	4000	4	10 151 560					
ethyl hexanoate	50	399	917 048					
	100	199	1 723 988					
	200	99	3 233 021					
	400	39	6 685 721					
	1000	19	10 265 298	18.82	2.62 x 10 <sup>-9</sup>	4.85 x 10 <sup>-8</sup>	0.9999	0.0540
	2000	9	14 418 106					
	3000	5.7	15 805 054					
	4000	4	17 254 307					

**Table 3. Gas-matrix partition coefficients ( $K_{g-m} \times 10^3$ ) of volatiles in different matrices at 35°C compared to published values.**

volatile compound	water <sup>ab</sup>	phosphate buffer <sup>ab</sup>	protein suspension <sup>ab</sup>	PRV literature values in water <sup>c</sup>
diacetyl	2.40 ± 0.44 a	2.73 ± 0.15 a	2.35 ± 0.21 a	1.26 (30) <sup>16</sup>
hexanal	22.50 ± 0.98 a	28.03 ± 1.29 b	24.75 ± 0.78 a	11.6 (30) <sup>16</sup> 11.0 (25) <sup>27</sup> 25.7 (37) <sup>42</sup>
ethyl hexanoate	56.23 ± 5.13 a	76.27 ± 9.35 b	48.30 ± 1.27 a	30.2 (30) <sup>16</sup> 27.6 (25) <sup>15</sup> 58.0 (30) <sup>43</sup>
eucalyptol	13.23 ± 0.31 a	19.27 ± 0.72 c	17.25 ± 1.34 b	
neral	4.37 ± 0.35 a	6.23 ± 0.29 b	2.75 ± 1.48 a	
geranial	4.50 ± 0.26 b	6.23 ± 0.40 c	2.55 ± 1.06 a	
anethole	17.07 ± 1.71 a	28.47 ± 2.31 b	22.30 ± 7.35 ab	
thymol	2.17 ± 0.21 a	3.50 ± 0.17 b	2.50 ± 1.13 ab	
carvacrol	2.07 ± 0.47 a	3.17 ± 0.15 a	2.10 ± 1.13 a	1.1 (25) <sup>44</sup>
eugenol	0.97 ± 0.21 a	0.93 ± 0.32 a	0.85 ± 0.49 a	

<sup>a</sup>Results are shown as a mean for triplicate samples with the standard deviation ( $\times 10^3$ )

<sup>b</sup>Values with different superscript letters within a row differ significantly (LSD,  $p < 0.05$ )

<sup>c</sup>Temperature at which the partition coefficient was determined shown in brackets

## Chapter 4 Conclusions and future directions

### 4.1 Conclusion

Food flavour is a major determinant of consumer satisfaction and so consequently factors that influence the release of volatiles during consumption are of great interest to researchers and the greater food industry alike. Flavour interactions involve the selective binding of aroma compounds to non-volatile food matrix components and can be investigated using a number of different analytical methods as discussed. This thesis demonstrates how the technique of static headspace analysis (SHA) partnered with the indirect approach of phase ratio variation (PRV) can be used to successfully describe the impact of myofibrillar meat proteins on headspace concentrations of important flavour volatiles.

The method development activities documented in Chapter 2 present the theoretic basis of combined SHA-PRV, emphasise the elements which are considered critical to successfully applying the technique and provide a detailed account of the optimised methodologies developed for the subsequent study. The results of reported in Chapter 3 outline the nature of flavour interactions with protein containing food matrices. Here the relationship that formed between extracted myofibrillar components of post-rigor pork muscle and a range of selected flavour volatiles is illustrated before being quantified using partitioning, or system distribution coefficients  $K_{g-m}$ .

Results confirmed that at a concentration of 2 mg/kg and in an aqueous environment, porcine myofibrillar proteins (in their native state) are capable of binding flavour compounds to various extents, reducing their headspace concentration and therefore their availability for orthonasal detection and consumer perception. Analytical data indicated the volatility of isomers nerol and geranial was reduced by the greatest extent, with retention percentages of up to 59%, followed by ethyl hexanote, for which notable modifications were also observed. In comparison, eugenol was least affected, with less than a 10% difference being recorded when protein was introduced into the matrix. The extent of retention and volatility reduction was found to be compound specific, however, comparable behaviour between structural isomers was observed, a review of flavour physicochemical properties and consultation of previously published research indicates that binding is likely the result of shared hydrophobicity between the protein molecule and the volatiles studied.

Using a salt buffer as the control for retention studies illustrated the importance of considering multicomponent or more complete model food systems in such investigations. Adding sodium

chloride to the predominantly water based matrix, in order to solubilise the protein and retain structural integrity during analysis, significantly changed the partitioning behaviour with 'salting out' observed. This effectively cancelled any retention effect of the protein when compared to the water based control. It also highlights the significance of considering salt content or the resulting ionic strength of any minced or reformed meat products investigated in future analyses. Salts such as sodium and potassium chloride are core components of these processed food types, due to the dual role they perform in both flavour enhancement and protein functionality during forming and cooking.

Method limitations were encountered for both SHA and PRV techniques during the determination of compound partition coefficients using the selected approaches. The most significant being the inability to use GCMS instrumentation, or more specifically mass spectrometer detection, during SHA-PRV. A continuous decrease in MSD signal throughout analysis was found to be caused by the repeated introduction of water, as a component of sample headspace, into the detector chamber. This caused degradation of the filament which effectively reduced the capability of the instrument to ionise compounds eluting from the column which is an essential step for signal generation in such systems. The problem was overcome by utilising a flame ionisation detector instead, which employs an alternate and adequately sensitive method of compound detection that is not affected by water vapour.

Difficulties were also experienced initially with reproducibility during SHA trials which emphasised the importance of ensuring the composition of each vial in a PRV series was identical and that instrumental conditions were optimal for the system being tested.

The most well documented problems with using PRV equations to calculate  $K_{g-m}$  are the difficulties encountered when applying the technique to compounds of either very high or very low volatility. Due to the inclusion of a diverse range of volatiles which included compounds from these groups, both problems were experienced. Issues reported for eugenol which showed the lowest volatility were overcome by adjusting the vial phase ratio to obtain the required minimum recommended difference between the largest and smallest peak area which is considered an important factor for result accuracy.

Unfortunately the difficulties in analysing limonene were not able to be overcome using documented method adjustments. Even when applied, the extremely high level of volatility for this compound created large differences between the theoretical and experimental values that are graphed during the process of PRV analysis. Repeated failures to generate reliable data led to the decision to preclude limonene from the study.

## 4.2 Future directions

The information presented upon completion of this research project contributes new knowledge to the field of protein-flavour interactions, however further scientific investigations are required to more comprehensively understand the impact of skeletal myofibrillar proteins on flavour volatile behaviour.

As an initial step, future studies should continue examining the impact of extracted protein on the volatility of relevant flavour compounds using simple binary or tertiary model solutions containing functional ingredients that are necessary and relevant to processed meat products. These could incorporate different salts such as potassium or sodium chloride and phosphates including potassium pyrophosphate and sodium tripolyphosphate. When studied, they should be investigated at appropriate levels, as found in different product formats, and in combination with environmental conditions that are altered (e.g. pH, ionic strength) or applied during the manufacture or consumer preparation of such products (e.g. prolonged storage, freezing, cooking).

Given the difficulties reported with analysing high volatility compounds using the phase ratio variation method, researchers electing to utilise this rapid and increasingly popular technique would be advised to consider using the non-linear regression approaches published by Atlan and co-workers<sup>113</sup> and Tromelin and co-workers.<sup>61</sup> The alternate data processing methods overcome several drawbacks associated with traditional linear regression analysis that are likely to assist with enabling compounds such as limonene to be studied in this manner.

Once the extent of protein binding has been established, further instrumental analyses could be undertaken to reveal highly specific details regarding the molecular basis of the interaction. Spectroscopic methods have the ability to locate the physical location of binding within the protein molecule and to characterise the nature of the interactions.

The overarching objective of any flavour interaction study is to optimise the flavour quality of foods for consumers, through better understanding the factors affecting this phenomenon. As such, it is essential that the human element is addressed when investigating the significance of protein-flavour interactions. Sensory studies incorporating descriptive analysis techniques and panels of trained assessors would provide final confirmation of the net impact of volatile binding by myofibrillar proteins on perceived flavour intensity. In addition, the evaluation of flavoured protein-based model solutions containing additional non-volatile components of relevance could provide useful information on the ability of instrumental techniques to predict,

or accurately express, the potential for detected interactions to influence flavour quality in terms of magnitude or characteristic profile.

Together the results obtained from these suggested studies would help form a comprehensive understanding of the extent, nature and sensory impact of the myofibrillar protein component of processed meat products such as burgers, patties, restructured muscle cuts and sausages. Such knowledge would enable food industry stakeholders to design highly optimised, cost effective formulations for the manufacture of premium flavoured, value-added convenience products for the growing consumer market.

## Appendices



Method file static hs20 hot inlet 125ul split 20 160518

Coffee analysis

Max temperature: 320 'C  
Nominal length: 30.0 m  
Nominal diameter: 250.00 um  
Nominal film thickness: 0.25 um  
Mode: constant flow  
Initial flow: 1.0 mL/min  
Nominal init pressure: 48.7 kPa  
Average velocity: 36 cm/sec  
Inlet: Front Inlet  
Outlet: MSD  
Outlet pressure: vacuum

FRONT DETECTOR (NO DET)

BACK DETECTOR (NO DET)

SIGNAL 1

Data rate: 20 Hz  
Type: test plot  
Save Data: Off  
Zero: 0.0 (Off)  
Range: 0  
Fast Peaks: Off  
Attenuation: 0

SIGNAL 2

Data rate: 20 Hz  
Type: test plot  
Save Data: Off  
Zero: 0.0 (Off)  
Range: 0  
Fast Peaks: Off  
Attenuation: 0

COLUMN COMP 1

(No Detectors Installed)

COLUMN COMP 2

(No Detectors Installed)

THERMAL AUX 1

Use: Unspecified  
Description: ODP Transfer Line  
Initial temp: 50 'C (Off)  
Initial time: 0.00 min  
# Rate Final temp Final time  
1 0.0(Off)

THERMAL AUX 2

Use: MSD Transfer Line Heater  
Description: MSD Transfer Line  
Initial temp: 250 'C (On)  
Initial time: 0.00 min  
# Rate Final temp Final time  
1 0.0(Off)

POST RUN

Post Time: 0.00 min

TIME TABLE

Time	Specifier	Parameter & Setpoint
------	-----------	----------------------

GC Injector

Front Injector:

Injector not configured, use these parameters if it becomes configured

Sample Washes	2
Sample Pumps	6
Injection Volume	1.00 microliters
Syringe Size	10.0 microliters
PostInj Solvent A Washes	2

Method file static hs20 hot inlet 125ul split 20 160518  
PostInj Solvent B Washes 0  
Viscosity Delay 0 seconds  
Plunger Speed Slow

Back Injector:  
No parameters specified

Column 1 Inventory Number : AB005  
Column 2 Inventory Number :

#### GERSTEL MPS Headspace Injection

##### SYRINGE SETTINGS

Syringe : 2.5ml-HS  
ITEX : not used - use these parameters if it becomes  
'used'  
Syringe Temperature : 60 'C  
Flush Time : 180 s

##### SAMPLE PREPARATION

Headspace : from Agitator  
  
Incubator : Agitator  
Incubation Temperature : 35 'C  
Incubation Time : 60.00 min  
Agitator On Time : 10 s  
Agitator Off Time : 1 s  
Agitator Speed : 500 rpm

##### SAMPLE PARAMETERS

Inj. Volume : 2500.0 uL  
Inj. Speed : 125.00 uL/s  
Pullup Delay : 0 s  
Fill Volume : 2500.0  
Fill Strokes : 0  
Fill Speed : 200.00 uL/s  
Pre Inj. Delay : 0 s  
Post Inj. Delay : 0 s  
Inj. Penetration : 25.00 mm  
Sample Tray Type : VT32-20  
Vial Penetration : 20.00 mm

##### MULTIPLE HEADSPACE SAMPLE ENRICHMENT (MHSE) AND/OR PRESSURIZE

Pressurize : not used - use these parameters if it becomes  
'used'  
MHSE Inj. per Run : 1

##### MS ACQUISITION PARAMETERS

General Information

-----

Tune File : atune.u  
Acquisition Mode : Scan/SIM

MS Information

-- -----

Solvent Delay : 1.50 min

EM Absolute : False  
EM Offset : 0  
Resulting EM Voltage : 2129.4

[Raw Scan Parameters]

Low Mass : 30.0  
High Mass : 170.0  
Threshold : 150  
Sample # : 2 A/D Samples 4

[Sim Parameters]

GROUP 1

Group ID : Diacetyl  
Resolution : Low  
Plot 1 Ion : 43.20  
Ions/Dwell In Group ( Mass, Dwell) ( Mass, Dwell) ( Mass, Dwell)  
( 43.20, 25) ( 86.10, 25) ( 42.20, 25)

GROUP 2

Group ID : Hexanal  
Resolution : High  
Group Start Time : 4.00  
Plot 1 Ion : 44.10  
Ions/Dwell In Group ( Mass, Dwell) ( Mass, Dwell) ( Mass, Dwell)  
( 44.10, 25) ( 56.10, 25) ( 41.10, 25)  
( 57.10, 25)

GROUP 3

Group ID : Ethyl Hexanoate  
Resolution : High  
Group Start Time : 9.90  
Plot 1 Ion : 88.10  
Ions/Dwell In Group ( Mass, Dwell) ( Mass, Dwell) ( Mass, Dwell)  
( 88.10, 25) ( 99.10, 25) ( 43.20, 25)  
(101.10, 25)

GROUP 4

Group ID : Lim and Eucal

Method file static hs20 hot inlet 125ul split 20 160518

Resolution : High  
Group Start Time : 10.80  
Plot 1 Ion : 68.20  
Ions/Dwell In Group ( Mass, Dwell) ( Mass, Dwell) ( Mass, Dwell)  
( 68.20, 25) ( 93.20, 25) ( 67.20, 25)  
( 79.20, 25) ( 43.10, 25) ( 81.10, 25)  
( 71.10, 25) (108.10, 25)

GROUP 5  
Group ID : Neral and Geran  
Resolution : High  
Group Start Time : 12.00  
Plot 1 Ion : 69.10  
Ions/Dwell In Group ( Mass, Dwell) ( Mass, Dwell) ( Mass, Dwell)  
( 69.10, 25) ( 41.10, 25) ( 91.10, 25)  
(119.10, 25) ( 84.10, 25)

GROUP 6  
Group ID : Ane Thy Carva  
Resolution : High  
Group Start Time : 18.30  
Plot 1 Ion : 148.10  
Ions/Dwell In Group ( Mass, Dwell) ( Mass, Dwell) ( Mass, Dwell)  
(148.10, 25) (147.10, 25) (117.10, 25)  
( 77.10, 25) (135.10, 25) (150.10, 25)  
( 91.10, 25) (115.10, 25) (136.10, 25)

GROUP 7  
Group ID : Eugenol  
Resolution : High  
Group Start Time : 19.20  
Plot 1 Ion : 164.10  
Ions/Dwell In Group ( Mass, Dwell) ( Mass, Dwell) ( Mass, Dwell)  
(164.10, 25) (149.10, 25) (103.10, 25)  
( 77.10, 25)

[MSZones]

MS Quad : 150 C maximum 200 C  
MS Source : 250 C maximum 250 C

END OF MS ACQUISITION PARAMETERS

TUNE PARAMETERS for SN: GCMS-0

-----

EMISSION : 34.610  
ENERGY : 69.922  
REPELLER : 25.264  
IONFOCUS : 90.157

Method file static hs20 hot inlet 125ul split 20 160518

ENTRANCE\_LE : 22.000  
EMVOLTS : 2129.412  
AMUGAIN : 1539.000  
AMUOFFSET : 121.500  
FILAMENT : 1.000  
DCPOLARITY : 0.000  
ENTLENSOFFS : 20.078  
MASSGAIN : -917.000  
MASSOFFSET : -36.000

END OF TUNE PARAMETERS

-----

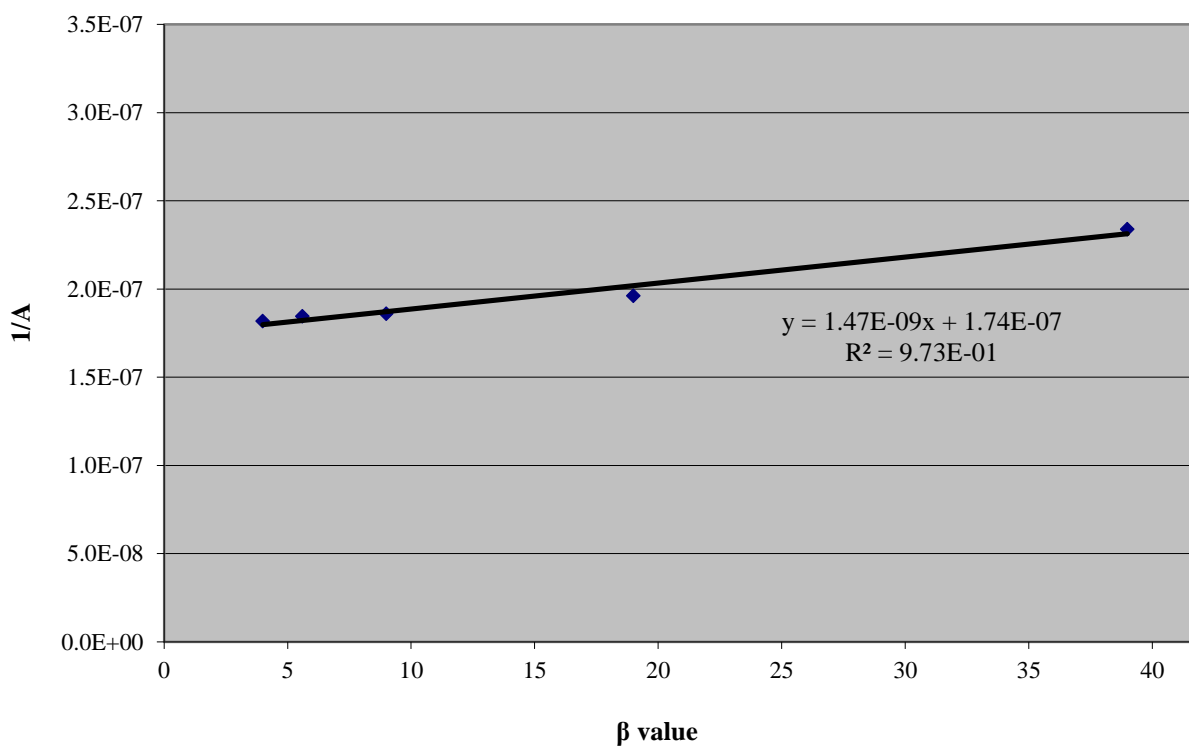
PostRun InstCntl macro(s) exist: msacq2.mac

END OF INSTRUMENT CONTROL PARAMETERS

-----

## Appendix 2 Preliminary PRV study using hexanal

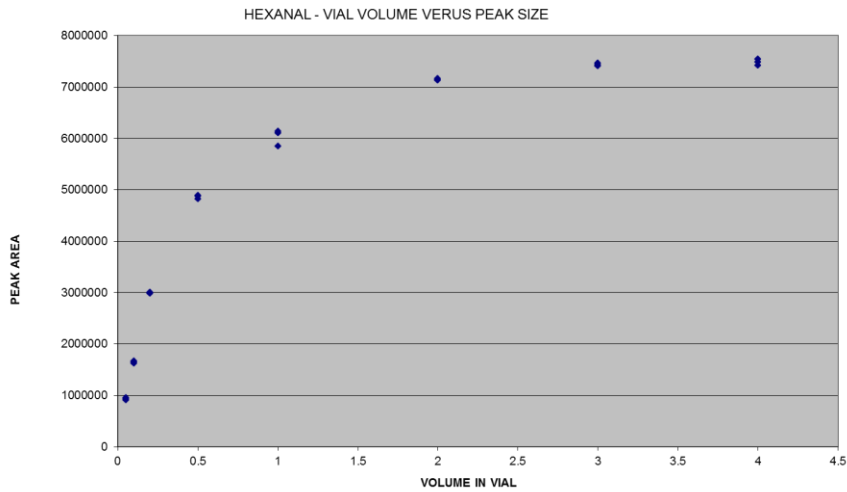
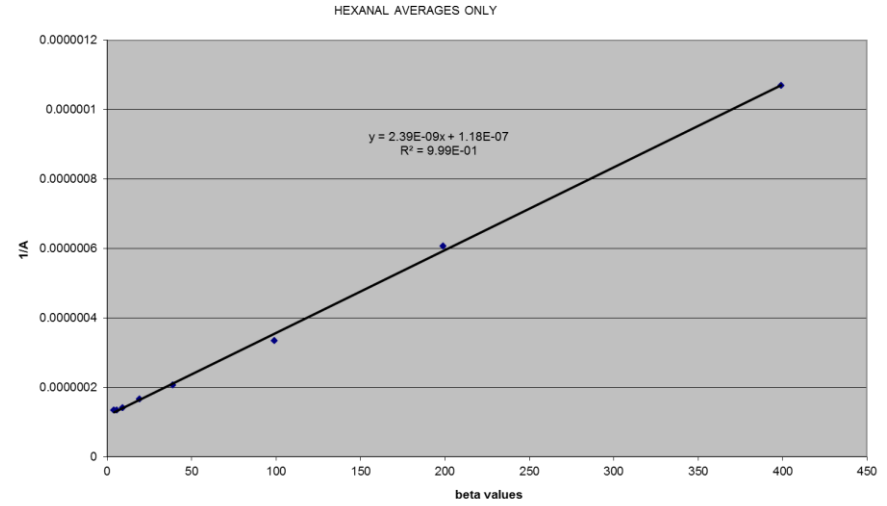
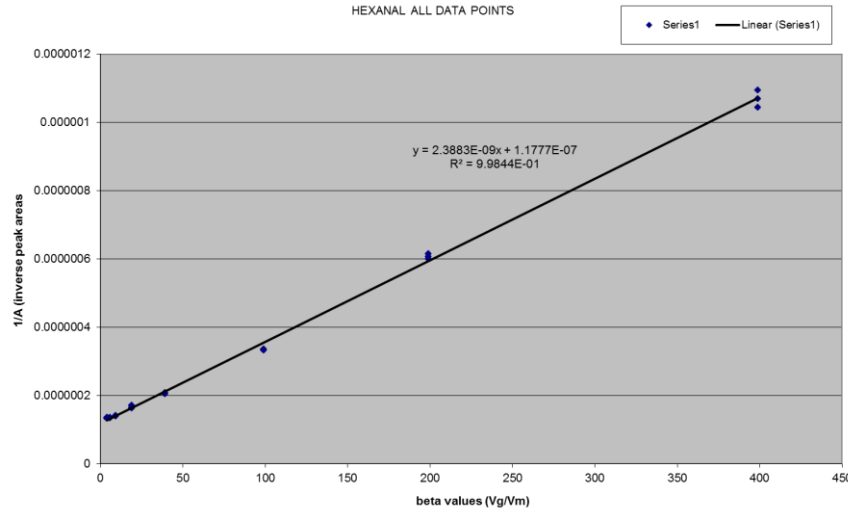
Sample volume	Data						Graph		
	Peak Area (A)	Mean A	Stdev	CV	$\beta$	1/A	$\beta$	1/A	
0.5mL	a	4,009,070	4,276,384	294,751	6.89	39	$2.494 \times 10^{-7}$	39	$2.338 \times 10^{-7}$
	b	4,592,485					$2.177 \times 10^{-7}$		
	c	4,227,599					$2.365 \times 10^{-7}$		
1mL	a	5,648,454	5,096,381	564,835	11.08	19	$1.770 \times 10^{-7}$	19	$1.962 \times 10^{-7}$
	b	5,121,094					$1.953 \times 10^{-7}$		
	c	4,519,595					$2.213 \times 10^{-7}$		
2mL	a	5,850,878	5,379,271	424,880	7.90	9	$1.709 \times 10^{-7}$	9	$1.859 \times 10^{-7}$
	b	5,260,569					$1.901 \times 10^{-7}$		
	c	5,026,366					$1.990 \times 10^{-7}$		
3mL	a	5,527,207	5,417,797	95,643	1.77	5.6	$1.809 \times 10^{-7}$	5.6	$1.846 \times 10^{-7}$
	b	5,350,069					$1.869 \times 10^{-7}$		
	c	5,376,115					$1.860 \times 10^{-7}$		
4mL	a	5,644,089	5,502,866	171,753	3.12	4	$1.772 \times 10^{-7}$	4	$1.817 \times 10^{-7}$
	b	5,311,668					$1.883 \times 10^{-7}$		
	c	5,552,841					$1.801 \times 10^{-7}$		



### PRV calculations

$$\begin{aligned}
 K_{g-m} &= \frac{\text{slope}}{\text{intercept}} \\
 &= \frac{1.47 \times 10^{-9}}{1.74 \times 10^{-7}} \\
 &= \mathbf{8.58 \times 10^{-3}}
 \end{aligned}$$

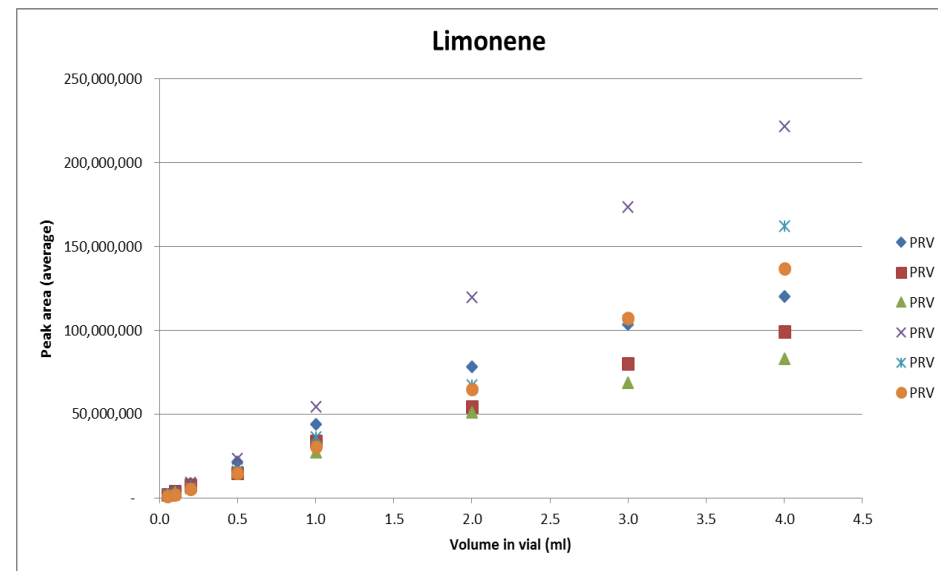
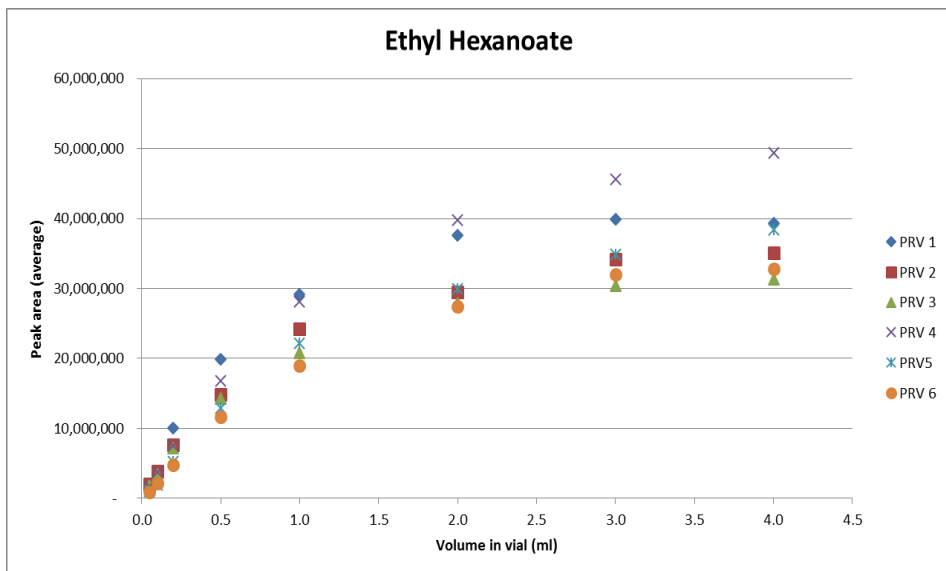
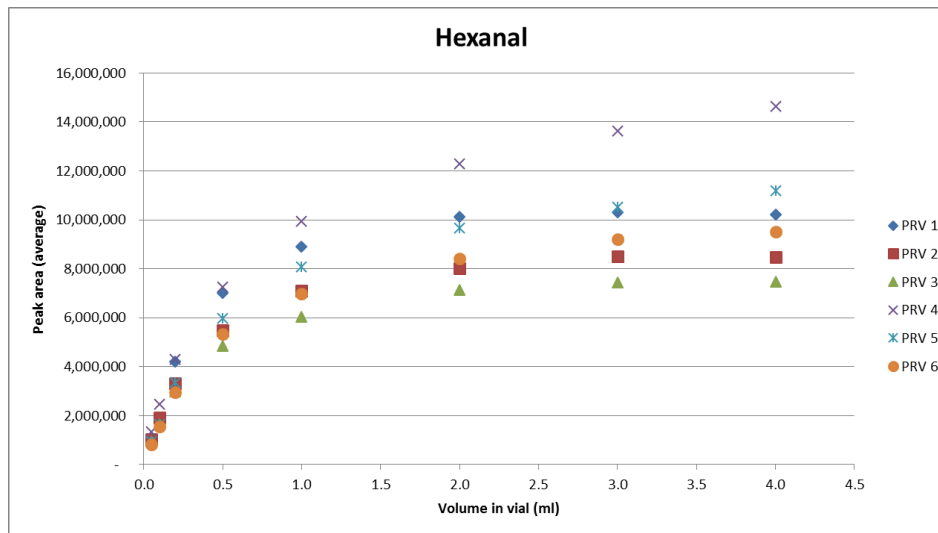
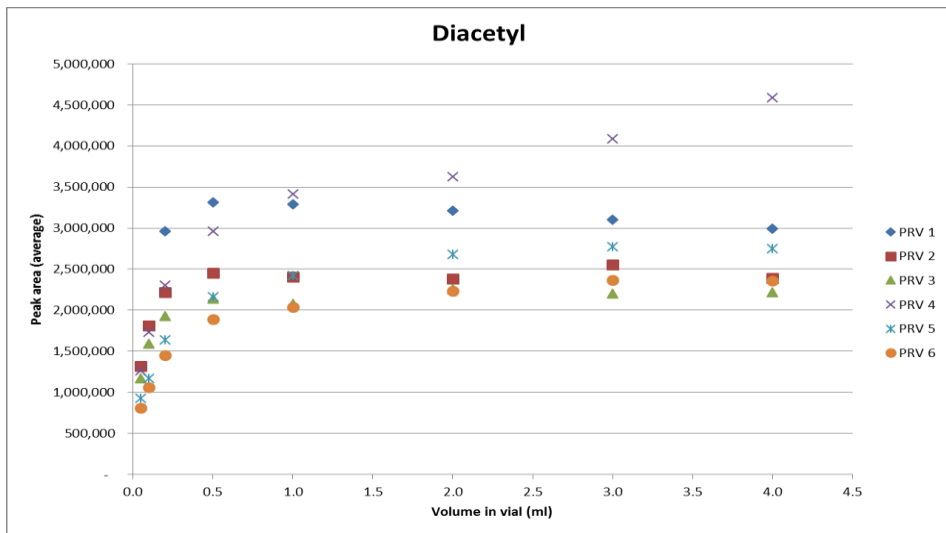
# Appendix 3 PRV calculation summary for hexanal

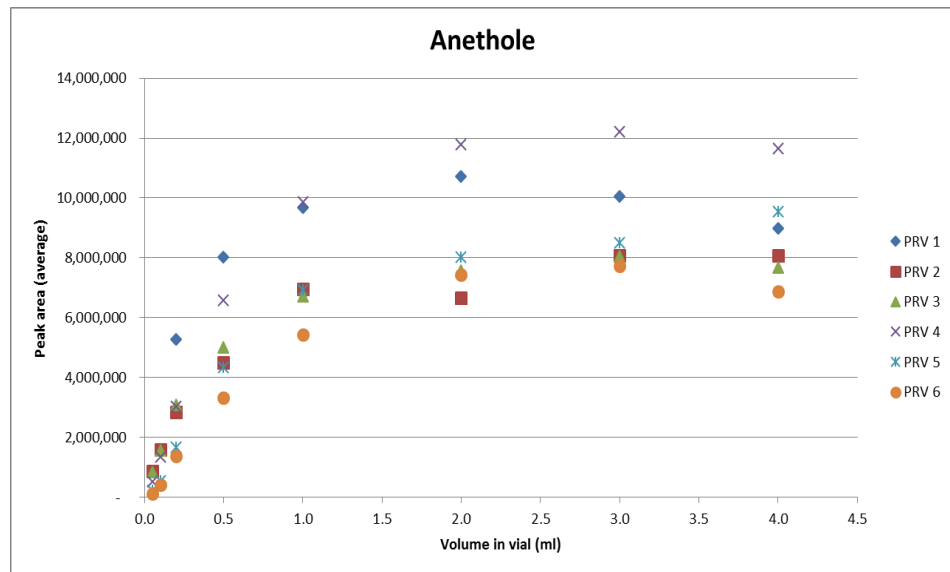
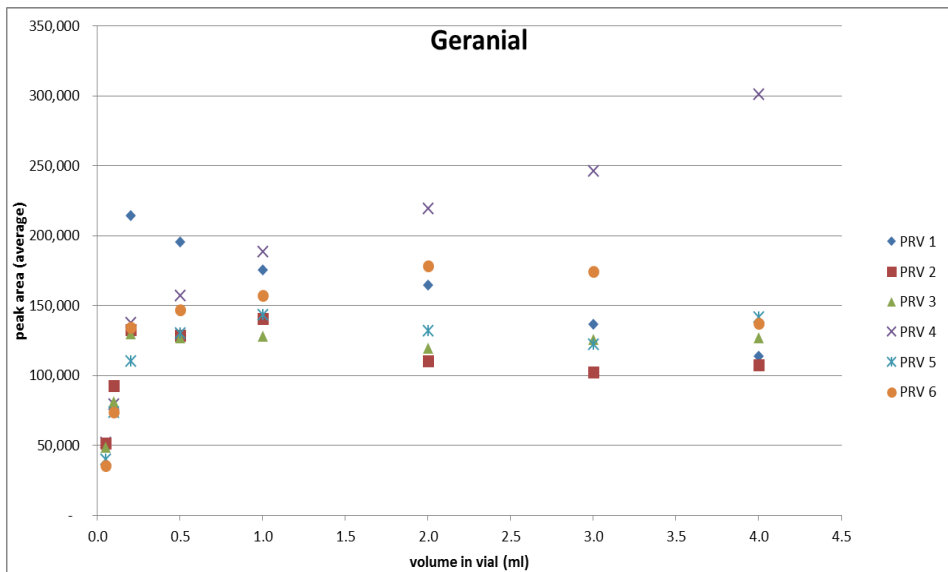
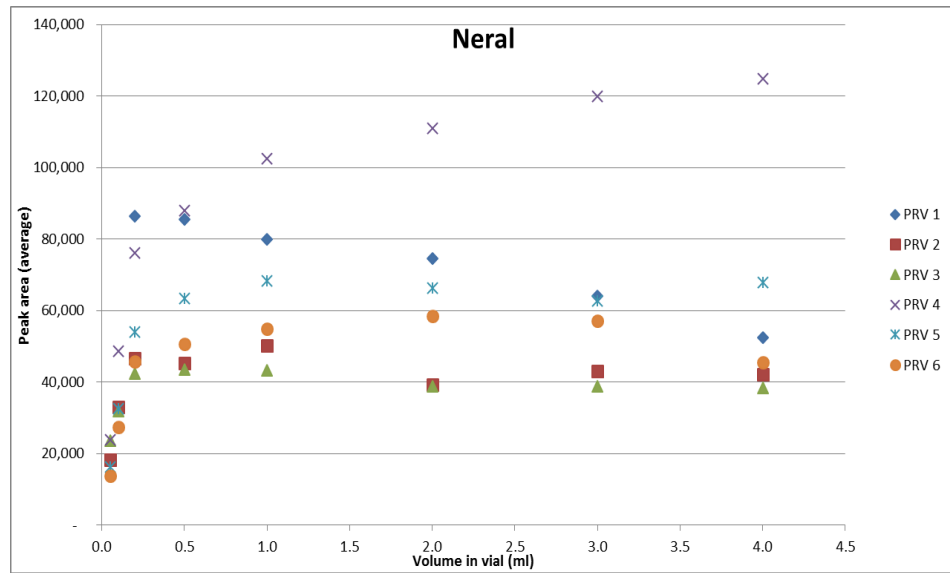
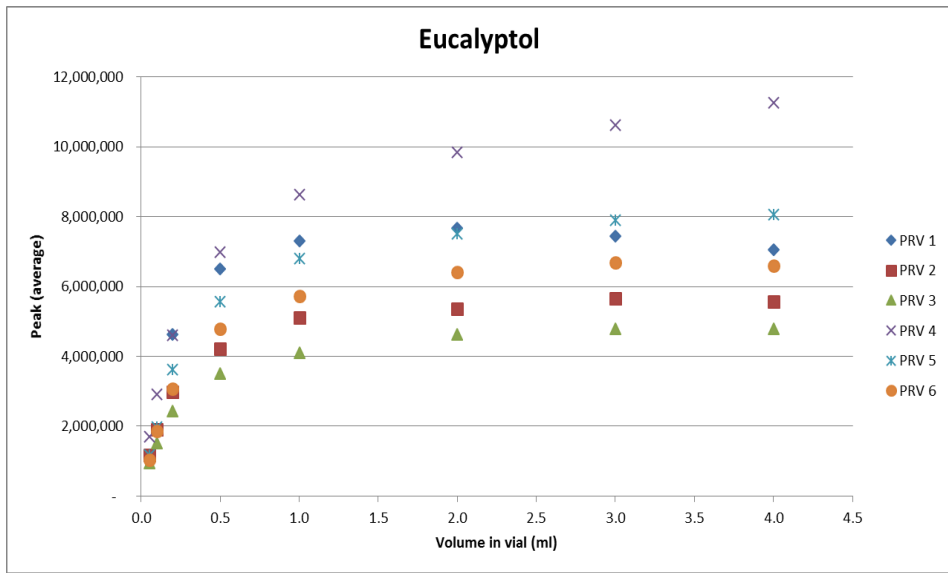


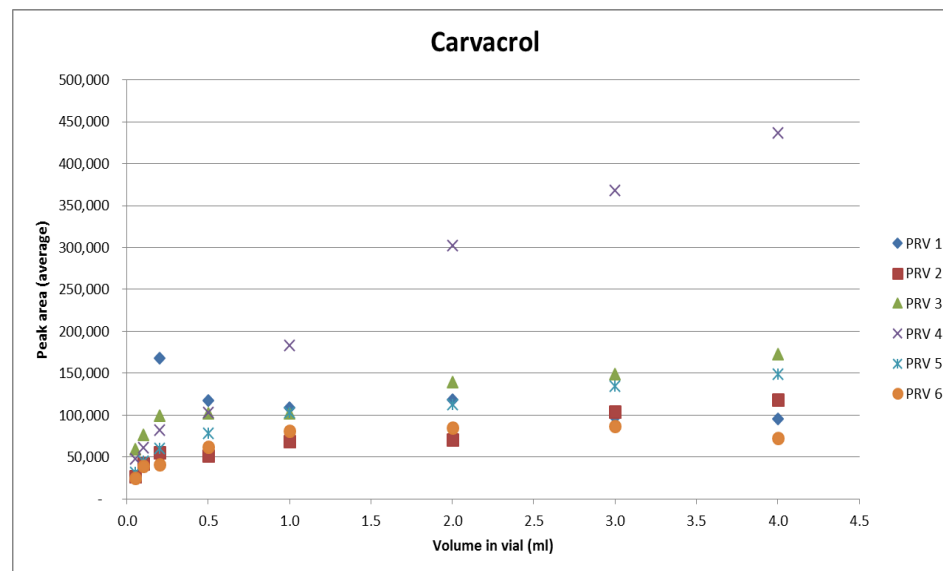
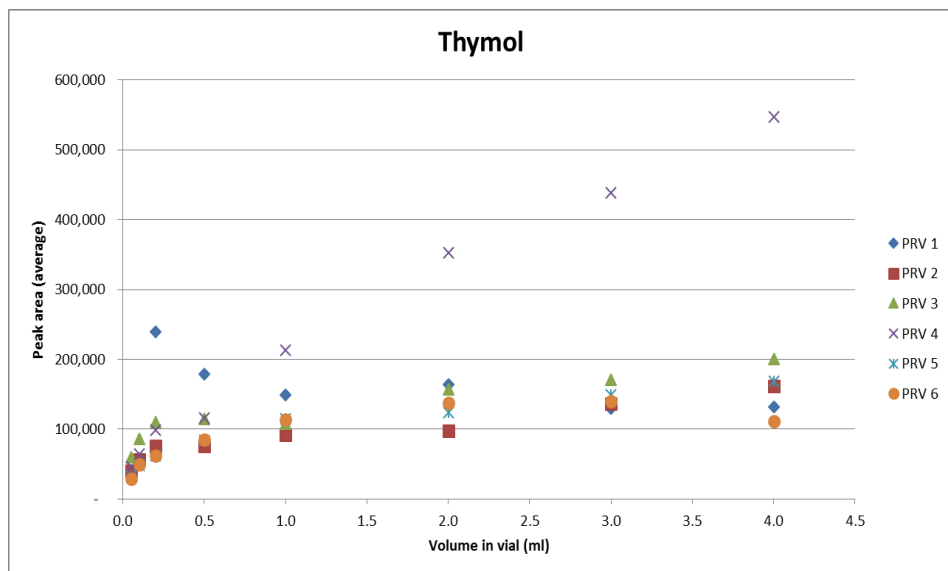
HEXANAL												
		all data					averages				A2/A1	
hexanal (m/z= 44.10)		peak areas	mean	stdev	COV	$\beta$	1/A	$\beta$	peak area (A)	1/A		
0.05	RT 4.89	a	958765			399	1.04301E-06					
0.05		b	935589	935,909.67	22696.7	2.43%	399	1.06885E-06	935909.6667	1.06848E-06		
0.05	Vial (mL)	c	913375			399	1.09484E-06					
0.1		a	1666280			199	6.00139E-07					
0.1		b	1649185	1,646,746.67	20859.66	1.27%	199	6.0636E-07	1646746.667	6.07258E-07		
0.1		c	1624775			199	6.1547E-07					
0.2		a	3004778			99	3.32803E-07					
0.2		b	2984943	2,995,155.00	9930.609	0.33%	99	3.35015E-07	2995155	3.33873E-07		
0.2		c	2995744			99	3.33807E-07					
0.5		a	4885242			39	2.04698E-07					
0.5		b	4878334	4,860,553.67	36940.77	0.76%	39	2.04988E-07	4860553.667	2.05738E-07	1.622805	
0.5		c	4818085			39	2.07551E-07					
1		a	6103026			19	1.63853E-07					
1		b	6133129	6,027,292.33	157963.2	2.62%	19	1.63049E-07	6027292.333	1.65912E-07	1.240042	
1		c	5845722			19	1.71065E-07					
2		a	7166968			9.0	1.39529E-07					
2		b	7135967	7,144,936.33	19189.42	0.27%	9.0	1.40135E-07	7144936.333	1.39959E-07	1.185431	
2		c	7131874			9.0	1.40216E-07					
3		a	7432402			5.7	1.34546E-07					
3		b	7404152	7,432,646.33	28617.28	0.39%	5.7	1.35059E-07	5.667	7432646.333	1.34542E-07	1.040268
3		c	7461385			5.7	1.34023E-07					
4		a	7546028			4.0	1.3252E-07					
4		b	7423446	7,483,814.00	61311.85	0.82%	4.0	1.34708E-07	4	7483814	1.33622E-07	1.006884
4		c	7481968			4.0	1.33655E-07					
partitioning cc		slope		2.39E-09								
		y-intercept		1.18E-07								
K g/m =		0.0203		at 35oC		$r^2 = 0.999$						

## Appendix 4 Reduction in peak areas post MSD maintenance

Graphical representation of peak area decrease for initial PRV trials 1-3 and 4-6 post electron ionisation source clean







## References

1. Clark, J. E. Taste and flavour: their importance in food choice and acceptance. *Proceedings of the Nutrition Society* **1998**, *57*, 639-643.
2. Guichard, E. Interactions between flavor compounds and food ingredients and their influence on flavor perception. *Food Reviews International* **2002**, *18*, 49.
3. Guth, H.; Rusu, M. Food matrices - determination of odorant partition coefficients and application of models for their prediction. *Food Chemistry* **2008**, *108*, 1208-1216.
4. Taylor, A. J.; Roozen, J. P. Volatile flavor release from foods during eating. *Critical Reviews in Food Science and Nutrition* **1996**, *36*, 765-784.
5. Druaux, C.; Voilley, A. Effect of food composition and microstructure on volatile flavour release. *Trends in Food Science & Technology* **1997**, *8*, 364-368.
6. Guyot, C.; Bonnafont, C.; Lesschaeve, I.; Voilley, A.; Spinnler, H. E. Relationships between odorous intensity and partition coefficients of delta-decalactone, diacetyl and butyric acid in model emulsions. In *Flavour Science: Recent Developments*, Taylor, A. J.; Mottram, D. S., Eds. The Royal Society of Chemistry: Cambridge, 1996; pp 380-385.
7. Taylor, A. J. Physical chemistry of flavour. *International Journal of Food Science & Technology* **1998**, *33*, 53-62.
8. Taylor, A. J.; Linforth, R. S. T. Flavour release in the mouth. *Trends in Food Science & Technology* **1996**, *7*, 444-448.
9. Le Thanh, M.; Thibeaudeau, P.; Thibaut, M. A.; Voilley, A. Interactions between volatile and non-volatile compounds in the presence of water. *Food Chemistry* **1992**, *43*, 129-135.
10. Ulrich, D.; Hoberg, E.; Rapp, A.; Kecke, S. Analysis of strawberry flavour – discrimination of aroma types by quantification of volatile compounds. *Zeitschrift für Lebensmitteluntersuchung und -Forschung A* **1997**, *205*, 218-223.
11. Reineccius, G. *Flavor chemistry and technology*. 2nd ed.; CRC Press: Boca Raton, 2006.
12. Reineccius, G. Instrumental methods of analysis. In *Food Flavour Technology*, Taylor, A. J., Ed. Sheffield Academic Press: Sheffield, 2002; pp 210-251.
13. Plug, H.; Haring, P. The influence of flavour-ingredient interactions on flavour perception. *Food Quality and Preference* **1994**, *5*, 95-102.
14. Laing, D. G.; Jinks, A. Flavour perception mechanisms. *Trends in Food Science & Technology* **1996**, *7*, 387-389.

15. Salles, C. Odour-taste interactions in flavour perception. In *Flavour in Food*, Voilley, A.; Etievant, P., Eds. Woodhead Publishing Limited: Cambridge, 2006; pp 345-368.
16. Keast, R. S. J.; Dalton, P. H.; Breslin, P. A. S. Flavour interactions at the sensory level. In *Flavour Perception*, Taylor, A. J.; Roberts, D. D., Eds. Blackwell Publishing Ltd: Cornwall, 2004; pp 228-255.
17. Van Ruth, S. M.; Roozen, J. P. Delivery of flavours from food matrices. In *Food flavour technology*, Sheffield Academic Press: Sheffield, 2002; pp 167-184.
18. Taylor, A. J. Release and transport of flavors in vivo: physicochemical, physiological, and perceptual considerations. *Comprehensive Reviews in Food Science and Food Safety* **2002**, *1*, 45-57.
19. Juteau, A.; Cayot, N.; Chabanet, C.; Doublier, J. L.; Guichard, E. Flavour release from polysaccharide gels: different approaches for the determination of kinetic parameters. *Trends in Food Science & Technology* **2004**, *15*, 394-402.
20. Roberts, D. D.; Taylor, A. J. Flavor release: a rationale for its study. In *Flavor Release*, Roberts, D. D.; Taylor, A. J., Eds. American Chemical Society: Washington DC, 2000; pp 1-6.
21. González-Tomás, L.; Bayarri, S.; Taylor, A. J.; Costell, E. Flavour release and perception from model dairy custards. *Food Research International* **2007**, *40*, 520-528.
22. Hewson, L.; Hollowood, T.; Chandra, S.; Hort, J. Taste-aroma interactions in a citrus flavoured model beverage system: Similarities and differences between acid and sugar type. *Food Quality and Preference* **2008**, *19*, 323-334.
23. Widder, S.; Fischer, N. Measurement of the influence of food ingredients on flavour release by headspace gas chromatography-olfactometry. In *Flavour Science: Recent Developments*, Taylor, A. J.; Mottram, D. S., Eds. The Royal Society of Chemistry: Cambridge, 1996; pp 405-412.
24. Lauerjat, C.; Loubens, C. d.; Déléris, I.; Tréléa, I. C.; Souchon, I. Rapid determination of partition and diffusion properties for salt and aroma compounds in complex food matrices. *Journal of Food Engineering* **2009**, *93*, 407-415.
25. Tarrega, A.; Yven, C.; Sémon, E.; Salles, C. Aroma release and chewing activity during eating different model cheeses. *International Dairy Journal* **2008**, *18*, 849-857.
26. Martuscelli, M.; Savary, G.; Pittia, P.; Cayot, N. Vapour partition of aroma compounds in strawberry flavoured custard cream and effect of fat content. *Food Chemistry* **2008**, *108*, 1200-1207.
27. Kersiene, M.; Adams, A.; Dubra, A.; Kimpe, N. D.; Leskauskaite, D. Interactions between flavour release and rheological properties in model custard desserts: effect of starch concentration and milk fat. *Food Chemistry* **2008**, *108*, 1183-1191.

28. Salles, C.; Phan, V. A.; Yven, C.; Chabanet, C.; Reparet, J.-M.; Le Quéré, J.-L.; Lubbers, S.; Decourcelle, N.; Guichard, E.; Wender, L. P. B.; Mikael Agerlin, P. In vivo flavour release from dairy products: relationships between aroma and taste release, temporal perception, oral and matrix parameters. In *Developments in Food Science*, Elsevier: 2006; Vol. Volume 43, pp 385-390.
29. Nongonierma, A. B.; Colas, B.; Springett, M.; Quéré, J.-L. L.; Voilley, A. Influence of flavour transfer between different gel phases on perceived aroma. *Food Chemistry* **2007**, *100*, 297-305.
30. González-Tomás, L.; Bayarri, S.; Taylor, A. J.; Costell, E. Rheology, flavour release and perception of low-fat dairy desserts. *International Dairy Journal* **2008**, *18*, 858-866.
31. Carrapiso, A. I. Effect of fat content on flavour release from sausages. *Food Chemistry* **2007**, *103*, 396-403.
32. Déléris, I.; Andriot, I.; Gobet, M.; Moreau, C.; Souchon, I.; Guichard, E. Determination of aroma compound diffusion in model food systems: comparison of macroscopic and microscopic methodologies. *Journal of Food Engineering* **2010**, *100*, 557-566.
33. de Roos, K. B. Effect of texture and microstructure on flavour retention and release. *International Dairy Journal* **2003**, *13*, 593-605.
34. Buettner, A.; Schieberle, P. Influence of mastication on the concentrations of aroma volatiles: some aspects of flavour release and flavour perception. *Food Chemistry* **2000**, *71*, 347-354.
35. Bakker, J.; Brown, W.; Hills, B.; Boudaud, N.; Wilson, C.; Harrison, M. Effect of the food matrix on flavour release and perception. *Flavour Science. Recent Developments* **1996**, 369-374.
36. Guichard, E. COST Action 96: interaction of food matrix with small ligands influencing flavour and texture. *Food Research International* **2000**, *33*, 187-190.
37. Seuvre, A. M.; Diaz, M. A. E.; Voilley, A. Influence of the food matrix structure on the retention of aroma compounds. *Journal of Agricultural and Food Chemistry* **2000**, *48*, 4296-4300.
38. Seuvre, A.-M.; Philippe, E.; Rochard, S.; Voilley, A. Kinetic study of the release of aroma compounds in different model food systems. *Food Research International* **2007**, *40*, 480-492.
39. Friel, E. N.; Linforth, R. S. T.; Taylor, A. J. An empirical model to predict the headspace concentration of volatile compounds above solutions containing sucrose. *Food Chemistry* **2000**, *71*, 309-317.
40. Heng, L.; van Koningsveld, G. A.; Gruppen, H.; van Boekel, M. A. J. S.; Vincken, J. P.; Roozen, J. P.; Voragen, A. G. J. Protein-flavour interactions in relation to

development of novel protein foods. *Trends in Food Science & Technology* **2004**, *15*, 217-224.

41. Boland, A. B.; Buhr, K.; Giannouli, P.; van Ruth, S. M. Influence of gelatin, starch, pectin and artificial saliva on the release of 11 flavour compounds from model gel systems. *Food Chemistry* **2004**, *86*, 401-411.
42. Linforth, R. S. T.; Baek, I.; Taylor, A. J. Simultaneous instrumental and sensory analysis of volatile release from gelatine and pectin/gelatine gels. *Food Chemistry* **1999**, *65*, 77-83.
43. Tromelin, A.; Andriot, I.; Guichard, E. Protein-flavour interactions. In *Flavour in food*, Woodhead Publishing Limited: Cambridge, 2006; pp 172-207.
44. Boelrijk, A. E. M.; Smit, G.; Weel, K. G. C. Flavour release from liquid food products. In *Flavour in Food*, Voilley, A.; Etievant, P., Eds. Woodhead Publishing Limited: Cambridge, 2006; pp 260-284.
45. Guichard, E. Flavour retention and release from protein solutions. *Biotechnology Advances* **2005**, *24*, 226-229.
46. Guichard, E.; Langourieux, S. Interactions between [beta]-lactoglobulin and flavour compounds. *Food Chemistry* **2000**, *71*, 301-308.
47. Pérez-Juan, M.; Flores, M.; Toldrá, F. Effect of ionic strength of different salts on the binding of volatile compounds to porcine soluble protein extracts in model systems. *Food Research International* **2007**, *40*, 687-693.
48. Pérez-Juan, M.; Flores, M.; Toldrá, F. Binding of aroma compounds by isolated myofibrillar proteins: Effect of protein concentration and conformation. *Food Chemistry* **2007**, *105*, 932-939.
49. Lawrie, R. A.; Ledward, D. A. Chemical and biochemical constituents of muscle. In *Lawrie's meat science*, 7th ed.; Woodhead Publishing Limited: Cambridge, 2006; pp 75-127.
50. Rayment, I.; Rypniewski, W.; Schmidt-Base, K.; Smith, R.; Tomchick, D.; Benning, M.; Winkelmann, D.; Wesenberg, G.; Holden, H. Three-dimensional structure of myosin subfragment-1: A molecular motor. *Science* **1993**, *261*, 50-58.
51. Xiong, Y. L. Myofibrillar protein from different muscle fiber types: Implications of biochemical and functional properties in meat processing. *Critical Reviews in Food Science and Nutrition* **1994**, *34*, 293 - 320.
52. Pérez-Juan, M.; Flores, M.; Toldrá, F. Effect of pork meat proteins on the binding of volatile compounds. *Food Chemistry* **2008**, *108*, 1226-1233.
53. Damodaran, S.; Kinsella, J. E. Binding of carbonyls to fish actomyosin. *Journal of Agricultural and Food Chemistry* **1983**, *31*, 856-859.

54. Tietz, M.; Buettner, A.; Conde-Petit, B. Interaction between starch and aroma compounds as measured by proton transfer reaction mass spectrometry (PTR-MS). *Food Chemistry* **2008**, *108*, 1192-1199.
55. Moon, S.-Y.; Li-Chan, E. C. Y. Assessment of added ingredient effect on interaction of simulated beef flavour and soy protein isolate by gas chromatography, spectroscopy and descriptive sensory analysis. *Food Research International* **2007**, *40*, 1227-1238.
56. Kühn, J.; Delahunty, C. M.; Considine, T.; Singh, H. In-mouth flavour release from milk proteins. *International Dairy Journal* **2009**, *19*, 307-313.
57. Voilley, A.; Souchon, I. Flavour retention and release from the food matrix: an overview. In *Flavour in Food*, Voilley, A.; Etievant, P., Eds. Woodhead Publishing Limited: Cambridge, 2006; pp 117-132.
58. Benjamin, O.; Leus, M.; Everett, D. W. Static headspace analysis of volatile compounds released from  $\beta$ -lactoglobulin-stabilized emulsions determined by the phase ratio variation method. *Food Research International* **2011**, *44*, 417-424.
59. Land, D. G. Perspectives on the effects of interactions on flavor perception: an overview. In *Flavor-Food Interactions*, McGorin, R. J.; Leland, J. V., Eds. American Chemical Society: Washington DC, 1996; pp 2-11.
60. Kolb, B.; Ettre, L. S. *Static headspace-gas chromatography: theory and practice*. John Wiley & Sons: New Jersey, 2006.
61. Tromelin, A.; Ayed, C.; Lubbers, S.; Pagès-Hélary, S.; Andriot, I.; Guichard, E. Proposed alternative phase ratio variation method for the calculation of liquid–vapour partition coefficients of volatiles. *Journal of Chromatography A* **2012**, *1263*, 158-168.
62. Savary, G.; Doublier, J.-L.; Cayot, N. Phase ratio variation method as an efficient way to determine the partition coefficients of various aroma compounds in mixture. In *Developments in Food Science*, Wender, L. P. B.; Mikael Agerlin, P., Eds. Elsevier: 2006; Vol. Volume 43, pp 461-464.
63. Ettre, L. S.; Welter, C.; Kolb, B. Determination of gas-liquid partition coefficients by automatic equilibrium headspace-gas chromatography utilizing the phase ratio variation method. *Chromatographia* **1993**, *35*, 73-84.
64. Tehrany, E. A.; Mouawad, C.; Desobry, S. Determination of partition coefficient of migrants in food simulants by the PRV method. *Food Chemistry* **2007**, *105*, 1571-1577.
65. Hu, H.-C.; Chai, X.-S.; Barnes, D. Determination of solid–liquid partition coefficient of volatile compounds by solid phase ratio variation based headspace analysis. *Fluid Phase Equilibria* **2014**, *380*, 76-81.
66. Kechagia, Z.; Kiparissides, C.; Economou, I. G. Determination of liquid–gas partition coefficients of BuA and MMA by headspace-gas chromatography utilizing the phase ratio variation method. *Fluid Phase Equilibria* **2008**, *266*, 21-30.

67. Van Durme, J.; Werbrouck, B. Phase ratio variation approach for the study of partitioning behavior of volatile organic compounds in polymer sample bags: Nalophan case study. *Environmental Science and Pollution Research* **2015**, *22*, 11067-11075.
68. Savary, G.; Guichard, E.; Doublier, J.-L.; Cayot, N. Mixture of aroma compounds: determination of partition coefficients in complex semi-solid matrices. *Food Research International* **2006**, *39*, 372-379.
69. Athès, V.; Peña y Lillo, M.; Bernard, C.; Pérez-Correa, R.; Souchon, I. Comparison of experimental methods for measuring infinite dilution volatilities of aroma compounds in water/ethanol mixtures. *Journal of Agricultural and Food Chemistry* **2004**, *52*, 2021-2027.
70. Ettre, L. S.; Kolb, B. Headspace-gas chromatography: the influence of sample volume on analytical results. *Chromatographia* **1991**, *32*, 5-12.
71. Nongonierma, A. B.; Springett, M.; Le Quéré, J.-L.; Cayot, P.; Voilley, A. Flavour release at gas/matrix interfaces of stirred yoghurt models. *International Dairy Journal* **2006**, *16*, 102-110.
72. Taylor, A.; Linforth, R. Understanding flavour release: the key to better food flavour? *Nutrition & Food Science* **1998**, *98*, 202-206.
73. Linforth, R., S. T.; Ingham, K. E.; Taylor A, J. Time course profiling of volatile release from foods during the eating process. In *Flavour Science: Recent Developments*, Taylor A, J.; Mottram, D. S., Eds. The Royal Society of Chemistry: 1996; pp 361-368.
74. Taylor, A. J.; Hort, J. Measuring proximal stimuli involved in flavour perception. In *Flavour Perception*, Taylor, A. J.; Roberts, D. D., Eds. Blackwell Publishing Ltd: Cornwall, 2004; pp 1-38.
75. Saint-Eve, A.; Martin, N.; Levy, C.; Souchon, I.; Wender, L. P. B.; Mikael Agerlin, P. How can protein ratio affect aroma release, physical properties and perceptions of yoghurt? In *Developments in Food Science*, Elsevier: 2006; Vol. Volume 43, pp 391-394.
76. Piggott, J. R. Dynamism in flavour science and sensory methodology. *Food Research International* **2000**, *33*, 191-197.
77. Guinard, J. X.; Marty, C. Time-intensity measurement of flavor release from a model gel system: effect of gelling agent type and concentration. *Journal of Food Science* **1995**, *60*, 727-730.
78. Xiong, Y. L.; Mikel, W. B. Meat and meat products. In *Meat Science and Applications*, Marcel Dekker: New York, 2001; pp 351-369.
79. Feiner, G. Additives: phosphates, salts (sodium chloride and potassium chloride, citrate, lactate) and hydrocolloids. In *Meat products handbook: Practical science and technology*, Elsevier: 2006; pp 72-83.

80. Moreau, C.; Tavel, L.; Le Quéré, J.-L.; Guichard, E.; Wender, L. P. B.; Mikael Agerlin, P. NMR spectroscopy study of interactions between [beta]-lactoglobulin and aroma compounds. In *Developments in Food Science*, Elsevier: 2006; Vol. Volume 43, pp 425-428.
81. Sostmann, K.; Guichard, E. Immobilized [beta]-lactoglobulin on a HPLC-column: a rapid way to determine protein--flavour interactions. *Food Chemistry* **1998**, *62*, 509-513.
82. Asghar, A.; Samejima, K.; Yasui, T.; Henrickson, R. L. Functionality of muscle proteins in gelation mechanisms of structured meat products. *CRC Critical Reviews in Food Science and Nutrition* **1985**, *22*, 27 - 106.
83. Perez-Juan, M.; Flores, M.; Toldra, F. Simultaneous process to isolate actomyosin and actin from post-rigor porcine skeletal muscle. *Food Chemistry* **2007**, *101*, 1005-1011.
84. Feiner, G. Burgers, patties and crumbed products. In *Meat Products Handbook: Practical Science and Technology*, Elsevier: 2006; pp 481-498.
85. Mohan, C. *Buffers: A guide for the preparation and use of buffers in biological systems*; EMD Biosciences Inc: California, 2006.
86. Russo, I.; Del Mese, P.; Viretto, M.; Doronzo, G.; Mattiello, L.; Trovati, M.; Anfossi, G. Sodium azide, a bacteriostatic preservative contained in commercially available laboratory reagents, influences the responses of human platelets via the cGMP/PKG/VASP pathway. *Clinical Biochemistry* **2008**, *41*, 343-349.
87. Fares, K.; Landy, P.; Guillard, R.; Voilley, A. Physicochemical interactions between aroma compounds and milk proteins: effect of water and protein modification. *Journal of Dairy Science* **1998**, *81*, 82-91.
88. Tornberg, E. Effects of heat on meat proteins – implications on structure and quality of meat products. *Meat Science* **2005**, *70*, 493-508.
89. Sun, L.-C.; Yoshida, A.; Cai, Q.-F.; Liu, G.-M.; Weng, L.; Tachibana, K.; Su, W.-J.; Cao, M.-J. Mung bean trypsin inhibitor is effective in suppressing the degradation of myofibrillar proteins in the skeletal muscle of blue scad (*decaapterus maruadsi*). *Journal of Agricultural and Food Chemistry* **2010**, *58*, 12986-12992.
90. Smith, P. K.; Krohn, R. I.; Hermanson, G. T.; Mallia, A. K.; Gartner, F. H.; Provenzano, M. D.; Fujimoto, E. K.; Goeke, N. M.; Olson, B. J.; Klenk, D. C. Measurement of protein using bicinchoninic acid. *Analytical Biochemistry* **1985**, *150*, 76-85.
91. Kralj, J. G.; Munson, M. S.; Ross, D. Total protein quantitation using the bicinchoninic acid assay and gradient elution moving boundary electrophoresis. *Electrophoresis* **2014**, *35*, 1887-1892.
92. Scientific, T. F., Thermo Scientific Pierce Protein Assay Technical Handbook. In 2nd ed.; USA, 2010; p 41.

93. Walker, J. M. The bicinchoninic acid (BCA) assay for protein quantitation. In *The protein protocols handbook*, Springer: 2009; pp 11-15.
94. Molina, I.; Toldra, F. Detection of proteolytic activity in microorganisms isolated from dry-cured ham. *Journal of Food Science* **1992**, *57*, 1308-1310.
95. Doerscher, D. R.; Briggs, J. L.; Lonergan, S. M. Effects of pork collagen on thermal and viscoelastic properties of purified porcine myofibrillar protein gels. *Meat Science* **2004**, *66*, 181-188.
96. Veldhuizen, E. J.; Tjeerdsma-van Bokhoven, J. L.; Zweijtzer, C.; Burt, S. A.; Haagsman, H. P. Structural requirements for the antimicrobial activity of carvacrol. *Journal of Agricultural and Food Chemistry* **2006**, *54*, 1874-1879.
97. Burt, S. Essential oils: their antibacterial properties and potential applications in foods-a review. *International Journal of Food Microbiology* **2004**, *94*, 223-253.
98. Sanla-Ead, N.; Jangchud, A.; Chonhenchob, V.; Suppakul, P. Antimicrobial activity of cinnamaldehyde and eugenol and their activity after incorporation into cellulose-based packaging films. *Packaging Technology and Science* **2012**, *25*, 7-17.
99. Konczak, I.; Zabaras, D.; Dunstan, M.; Aguas, P. Antioxidant capacity and phenolic compounds in commercially grown native Australian herbs and spices. *Food Chemistry* **2010**, *122*, 260-266.
100. Lis-Balchin, M.; Deans, S. G.; Eaglesham, E. Relationship between bioactivity and chemical composition of commercial essential oils. *Flavour and Fragrance Journal* **1998**, *13*, 98-104.
101. Plug, H.; Haring, P. The role of ingredient-flavour interactions in the development of fat-free foods. *Trends in Food Science & Technology* **1993**, *4*, 150-152.
102. Reineccius, G. Flavour Analysis. In *Flavour Chemistry and Technology*, CRC Press: Boca Raton, 2006; pp 33-67.
103. Griffin, S.; Wyllie, S. G.; Markham, J. Determination of octanol-water partition coefficient for terpenoids using reversed-phase high-performance liquid chromatography. *Journal of Chromatography A* **1999**, *864*, 221-228.
104. Mirhosseini, H.; Tan, C. P. Response surface methodology and multivariate analysis of equilibrium headspace concentration of orange beverage emulsion as function of emulsion composition and structure. *Food Chemistry* **2009**, *115*, 324-333.
105. Griffin, S. G.; Wyllie, S. G.; Markham, J. L.; Leach, D. N. The role of structure and molecular properties of terpenoids in determining their antimicrobial activity. *Flavour and Fragrance Journal* **1999**, *14*, 322-332.

106. Ben Arfa, A.; Combes, S.; Preziosi-Belloy, L.; Gontard, N.; Chalier, P. Antimicrobial activity of carvacrol related to its chemical structure. *Letters in Applied Microbiology* **2006**, *43*, 149-154.
107. *A Technical Guide for Static Headspace using GC*; Restek Corporation: USA, 2000; p 20.
108. Sithersinch, M., J.; Snow, N., H. Headspace-gas chromatography. In *Gas Chromatography*, Elsevier: 2012; pp 221 - 235.
109. Perreault, V.; Britten, M.; Turgeon, S. L.; Seuvre, A. M.; Cayot, P.; Voilley, A. Effects of heat treatment and acid-induced gelation on aroma release from flavoured skim milk. *Food Chemistry* **2010** *118*, 90-95.
110. Jouquand, C.; Ducruet, V.; Giampaoli, P. Partition coefficients of aroma compounds in polysaccharide solutions by the phase ratio variation method. *Food Chemistry* **2004**, *85*, 467-474.
111. Klee, M., S. Detectors. In *Gas Chromatography*, Elsevier: USA, 2012; pp 307-348.
112. Tromelin, A.; Lubbers, S.; Andriot, I.; Guichard, E. Improvement of partition coefficients determination of aroma compounds in food matrices by the phase ratio variation method. In *Flavour Science*, Academic Press: San Diego, 2014; pp 401-406.
113. Atlan, S.; Trelea, I. C.; Saint-Eve, A.; Souchon, I.; Latrille, E. Processing gas chromatographic data and confidence interval calculation for partition coefficients determined by the phase ratio variation method. *Journal of Chromatography A* **2006**, *1110*, 146-155.